DNA 6187F

HIGH-EXPLOSIVE FIELD TESTS

Explosion Phenomena and Environmental Impacts

Kenneth E. Gould
Kaman Tempo
816 State Street (P.O. Drawer QQ)
Santa Barbara, California 93102

1 October 1981

Final Report for Period 1 October 1980—1 October 1981

CONTRACT No. DNA 001-79-C-0053

APPROVED FOR PUBLIC RELEASE;
DISTRIBUTION UNLIMITED.

THIS WORK WAS SPONSORED BY THE DEFENSE NUCLEAR AGENCY
UNDER RDT&E RMSS CODE B344079464 Y99QAXSX36705 H2590D.

Prepared for
Director
DEFENSE NUCLEAR AGENCY
Washington, DC 20305

Destroy this report when it is no longer needed. Do not return to sender.

PLEASE NOTIFY THE DEFENSE NUCLEAR AGENCY, ATTN: STTI, WASHINGTON, D.C. 20305, IF YOUR ADDRESS IS INCORRECT, IF YOU WISH TO BE DELETED FROM THE DISTRIBUTION LIST, OR IF THE ADDRESSEE IS NO LONGER EMPLOYED BY YOUR ORGANIZATION.

UNCLASSIFIED

SECURITY CLASSIFICATION OF THIS PAGE (When Data Entered)

REPORT DOCUMENTATION PAGE	READ INSTRUCTIONS BEFORE COMPLETING FORM
1. REPORT NUMBER: DNA 6187F	2. GOVT ACCESSION NO.: AD-A135737
3. RECIPIENT'S CATALOG NUMBER:	
4. TITLE (and Subtitle): HIGH-EXPLOSIVE FIELD TESTS Explosion Phenomena and Environmental Impacts	5. TYPE OF REPORT & PERIOD COVERED: Final Report for Period 1 October 1980—1 October 1981
	6. PERFORMING ORG. REPORT NUMBER: KT-81-004(R)
7. AUTHOR(s): Kenneth E. Gould	8. CONTRACT OR GRANT NUMBER(s): DNA 001-79-C-0053
9. PERFORMING ORGANIZATION NAME AND ADDRESS: Kaman Tempo 816 State Street (P.O. Drawer QQ) Santa Barbara, California 93102	10. PROGRAM ELEMENT, PROJECT, TASK AREA & WORK UNIT NUMBERS: Subtask Y99QAXSX367-05
11. CONTROLLING OFFICE NAME AND ADDRESS: Director Defense Nuclear Agency Washington, D.C. 20305	12. REPORT DATE: 1 October 1981 13. NUMBER OF PAGES: 90
14. MONITORING AGENCY NAME & ADDRESS(if different from Controlling Office)	15. SECURITY CLASS. (of this report): UNCLASSIFIED 15a. DECLASSIFICATION/DOWNGRADING SCHEDULE: NA since UNCLASSIFIED

16. DISTRIBUTION STATEMENT (of this Report)

Approved for public release; distribution unlimited.

17. DISTRIBUTION STATEMENT (of the abstract entered in Block 20, if different from Report)

18. SUPPLEMENTARY NOTES

This work was sponsored by the Defense Nuclear Agency under RDT&E RMSS Code B344079464 Y99QAXSX36705 H2590D.

19. KEY WORDS (Continue on reverse side if necessary and identify by block number)

High Explosives
Explosions
Airblast
Ground Shock
Environmental Impact

20. ABSTRACT (Continue on reverse side if necessary and identify by block number)

Methodologies are formulated to predict the magnitudes of high-explosive explosions phenomena for various high-explosive charge sizes and configurations and to relate these magnitudes to impacts on the natural physical and biological environment and on humans and the socioeconomic environment. The methodologies apply for the explosives normally used in land-based military high-explosive field tests, i.e., 0.5 to 500 tons of TNT-equivalent weight. The phenomena addressed include airblast and noise; craters and ejecta and missiles; ground shock; and explosion clouds of chemical products and dust.

DD FORM 1 JAN 73 1473 EDITION OF 1 NOV 65 IS OBSOLETE

UNCLASSIFIED

SECURITY CLASSIFICATION OF THIS PAGE (When Data Entered)

TABLE OF CONTENTS

LIST OF ILLUSTRATIONS

LIST OF ILLUSTRATIONS (Continued)

LIST OF TABLES

SECTION 1

INTRODUCTION

Since 1972, Tempo has been preparing environmental assessments (EAs) and environmental impact statements (EISs) for high-explosive (HE) field tests sponsored by the Defense Nuclear Agency (DNA). Although some of these field tests involved substantial construction activities, the major concern of military reviewers and the public has been regarding the effects of the explosion phenomena. Accordingly, considerable effort has gone into the analysis of explosion phenomena and their effects on the physical, biological, and socioeconomic environments. This report documents the expertise that has been gained and can serve as:

1. A tool to be used during site-selection to determine if environmental damage criteria are likely to be exceeded, and the magnitude of any such damage
2. A reference document for use in preparing future EAs for HE field tests
3. A background document for use in scoping meetings to determine the impacts to be assessed in EISs for HE field tests and a reference document for preparing EISs.

This report addresses only the explosion phenomena aspects of HE field tests; it does not address the construction and other aspects of such tests. The scope of this report is limited to solid or liquid HE in the range of interest for field tests, equivalent to from 1,000 pounds to 500 tons of TNT. The evaluation is limited to field tests conducted on land; gaseous explosives or underwater explosions are not covered in this analysis.

In general, conservative assumptions regarding the magnitude of explosion phenomena and their effects are used to avoid underestimating the environmental impact of the phenomena. If significant impact is indicated, less conservative assumptions can be used in a careful analysis to provide a more realistic assessment.

This report is organized as follows: Section 2 describes the explosion phenomena of airblast and noise, craters, ejecta and missiles, ground shock, explosive products, and a buoyant cloud which will carry dust and explosive products downwind. The phenomena are described in the form of parametric curves of magnitude versus distance for various explosive charge sizes and other conditions.

Section 3 describes the magnitudes of explosion phenomena that may have significant effects on the environment and combines these damage criteria with the explosion phenomena in Section 2 to obtain damage distances or conditions, i.e., distances within, or other conditions for, which the effects of explosion phenomena can be significant.

A variety of units of measurement is used in this report, depending on how particular types of data are customarily given. In general, however, information in output form for users of this manual is presented in metric units, except HE charge sizes are given in TNT-equivalent tons. Table 1-1 shows the factors to convert to other measurement systems.

Table 1-1. Unit conversion factors.

To Convert	Into	Multiply By
cubic feet (ft^3)	cubic meters (m^3)	2.832×10^{-2}
cubic meters (m^3)	cubic feet (ft^3)	35.31
grams (g)	pounds (lb)	2.205×10^{-3}
gravitational units of acceleration (g's)	centimeters per second^2 (cm/sec^2)	981
feet (ft)	meters (m)	0.3048
pounds (lb)	grams (g)	453.6
Pascals (Pa)	pounds per square inch (psi)	1.451×10^{-4}
pounds per square inch (psi)	Pascals (Pa)	6,894
square feet (ft^2)	square meters (m^2)	9.290×10^{-2}
meters (m)	feet (ft)	3.281

SECTION 2

EXPLOSION PHENOMENA

The detonation of a charge of high explosive (HE) near the earth's surface produces airblast and noise, a crater, ejecta and missiles, ground shock, explosive products, and a buoyant cloud that will carry dust and explosive products downwind. In this section, the magnitudes of each of these phenomena are estimated for explosive charge weights ranging from 1,000 pounds to 500 tons (typical for field tests) exploded on or near the ground surface. The variation of magnitude of phenomena for special situations (e.g., multiple charges and elevated or buried charges) is also discussed.

In this report, all weights of explosives are given in terms of their TNT-equivalent weight, i.e., the weight of TNT (with explosive energy of 10^9 calories/ton) that would produce approximately the same magnitude of a particular phenomenon as the specific explosive charge in question.

AIRBLAST AND NOISE

Airblast (the explosion shock wave in air) is usually of greatest concern in HE field tests because damage can occur at relatively long distances from the explosion. Damage can be caused by various airblast mechanisms but is usually related to the peak overpressure of the airblast wave. Table 2-1 shows TNT-equivalent weight factors for some explosives. The airblast phenomena discussed in this section include close-in airblast, long-distance airblast and noise, and refracted atmospheric propagation.

Close-In Airblast

Figure 2-1 shows measured values of airblast peak overpressure as functions of distance for four field tests in which large, spherical charges of TNT were detonated on the ground surface. The measurements have been adjusted to convert all results to 1 pound of TNT at sea level and standard atmospheric conditions. It can be seen that these results agree very well and were predictable.

Airblast measurements from a number of charges of various shapes (sphere, hemisphere, and capped cylinder), varying in TNT-equivalent weight from a few hundred pounds to 500 tons and employing different types of explosives, show results consistent with Figure 2-1 in the region of environmental interest, below 10 to 20 psi (References 3, 4, 5, and 6). Also, except for charges elevated significantly above the earth's surface (at least tens to hundreds of feet for charge sizes of interest), Figure 2-1 is a slightly conservative estimate of airblast overpressure. Field tests

Table 2-1. TNT-equivalent weights of explosives for airblast peak overpressure. (Source: Reference 1)

Explosive Type	TNT-Equivalent Weight Factor[a]	Explosive Type	TNT-Equivalent Weight Factor[a]
TNT	1.00	Pentolite	1.42
Tritonal	1.07	PETN	1.27
Composition B	1.11	Nitroglycerine	1.23
HBX-1	1.17	RDX-Cyclonite	1.17
HBX-3	1.14	Nitromethane	1.00
TNETB	1.36	Ammonium Nitrate	0.84
Composition C-4	1.37	Black Powder	0.46
H-6	1.38		

[a]To determine the TNT-equivalent weight of an explosive, multiply the weight of the explosive by the equivalent weight factor, e.g., at a given distance, 1 ton of ammonium nitrate is required to produce the peak overpressure equivalent to that from 0.84 ton of TNT.

conducted at higher altitudes result in peak overpressures somewhat less than those indicated in Figure 2-1. Burying a charge tends to also reduce the peak overpressures. Thus it can be assumed that except for significantly elevated charges (discussed later), the airblast overpressure will not be greater than indicated by Figure 2-1.

The distance at which any particular peak overpressure occurs varies proportional to the cube root of the charge weight, e.g., increasing a charge weight by a factor of 8 increases the ground distance for a given overpressure by a factor of $8^{1/3}$, i.e., 2. The curves shown in Figure 2-2 for typical weights of field test HE charges are obtained from Figure 2-1 by plotting overpressures of environmental concern (below 20 psi or 140 kPa) versus the product of ground distance and the cube root of the charge weight.

Long-Distance Airblast

As the peak overpressure decreases at increasing distances from the explosion, the airblast front slows down to a speed approaching the speed of sound. As the airblast approaches an acoustic wave, it is refracted by temperature and wind-speed gradients in the air. At distances where the airblast peak overpressure is less than approximately 2.5 kPa, meteorological conditions usually predominate to cause anomalous propagation; airblast

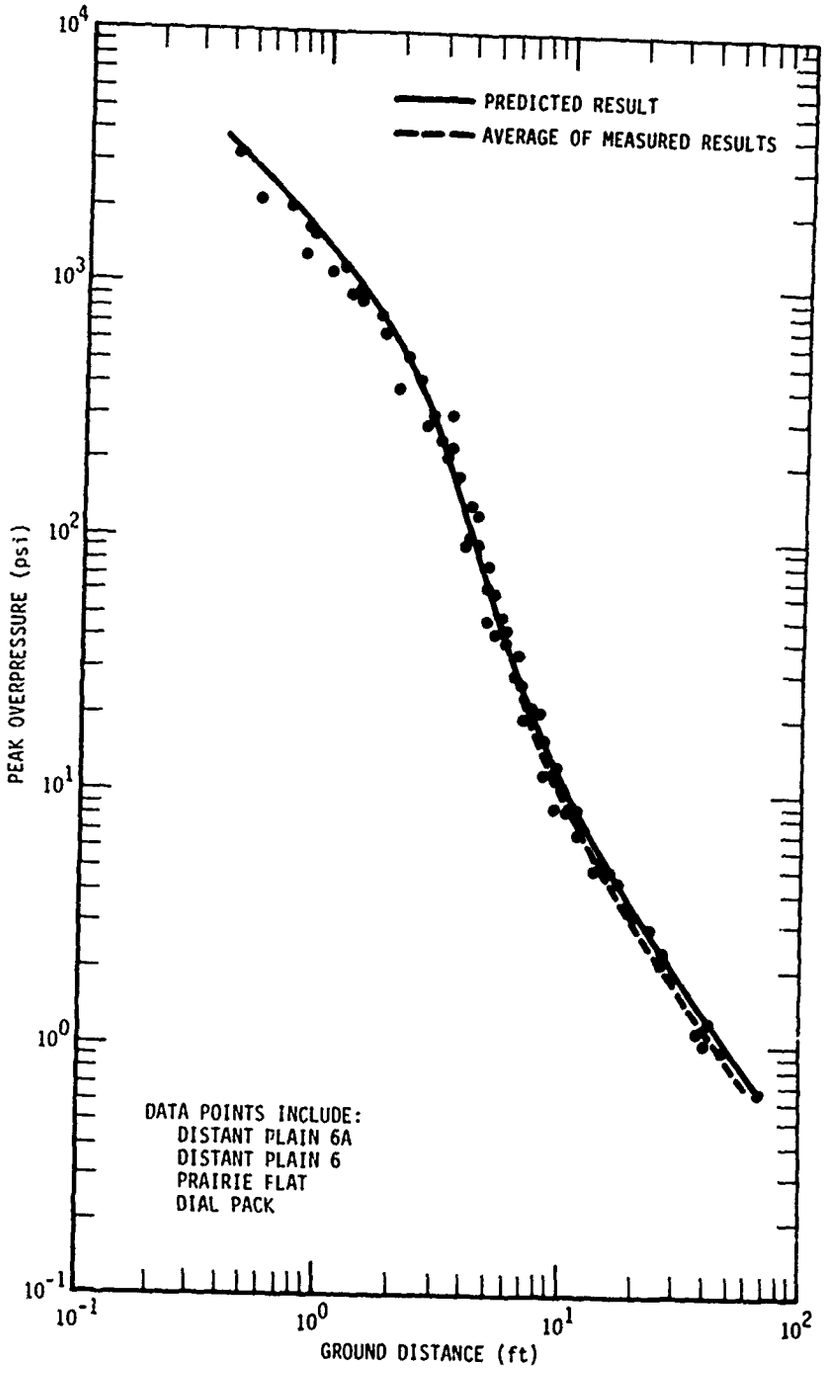

Figure 2-1. Peak airblast overpressure measurements from large TNT explosions (scaled to 1 pound of TNT at sea level and standard atmospheric conditions). (Source: Reference 2)

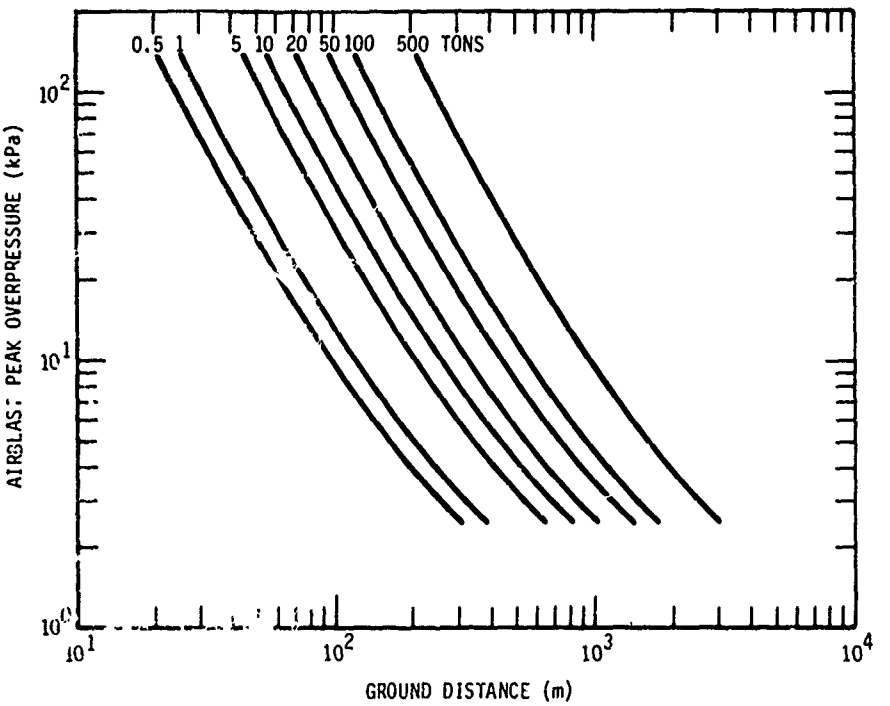

Figure 2-2. Airblast peak overpressures versus ground distance for charges exploded on or near the ground surface.

is refracted toward or away from the ground, resulting in peak overpressures either greater or less than would occur in a nonrefracting atmosphere. Peak overpressures at long distances may vary by an order of magnitude or more, depending upon whether the meteorological conditions are favorable or unfavorable. Long-distance airblast is of concern because very low peak overpressures can crack windows and cause excessive noise, as discussed in Section 3.

Based on a large amount of empirical data, Reed (Reference 1) has formulated relationships for estimating the overpressure at long distances from explosions. For a large chemical explosion on, or near, the ground surface with the airblast propagating through a homogeneous, nonrefracting atmosphere, the peak overpressure at long distances near the ground surface is approximately:

$$\Delta p = 668\ (2W)^{0.37}\ D^{-1.1}\ (P/P_o)^{0.63} \qquad (2\text{-}1)$$

where

Δp = incident peak overpressure (Pa)

W = TNT-equivalent weight of the explosive charge (tons) (the factor of 2 is to account for the fact that the ground surface produces distant blast pressures equivalent to those from a free-air burst about double in size)

D = distance from the explosion (km)

P = ambient atmospheric pressure at the test site

P_0 = standard sea-level atmospheric pressure.

Equation 2-1 is plotted in Figure 2-3 for explosive yields of interest at standard sea-level ambient atmospheric pressure. (For most situations of interest, P can be assumed equal to P_0 in Equation 2-1. Peak overpressure is reduced by only 1 percent for each 140 meters of elevation of the test site above sea level.)

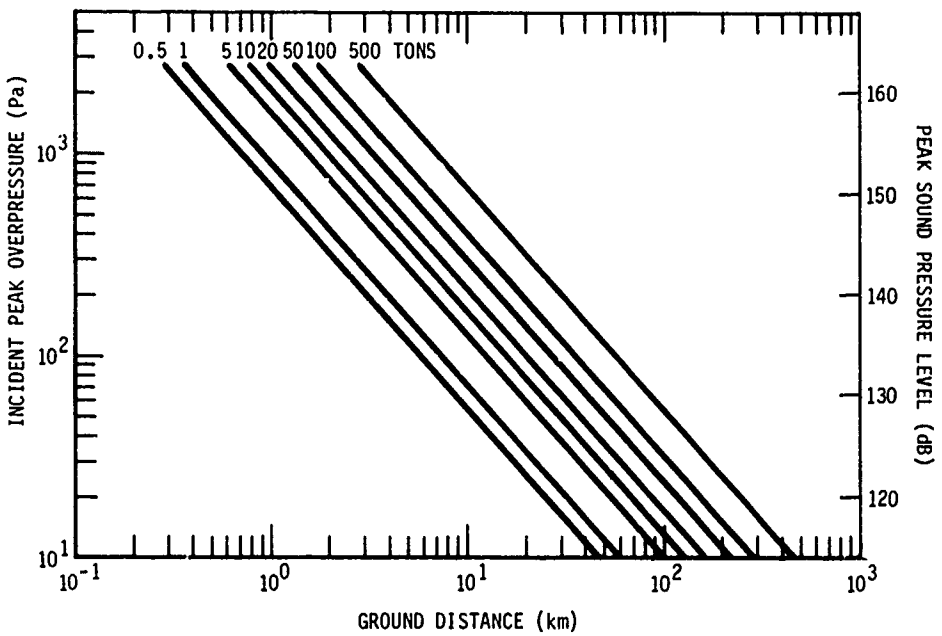

Figure 2-3. Long-distance airblast and noise (idealized, nonrefracting atmosphere).

Noise

An explosion produces impulsive, predominantly low-frequency sound of sufficient intensity to be heard at long distances. The measure of sound intensity is the unweighted sound pressure level (SPL) expressed in decibels (dB), which are dimensionless units proportional to the square of the pressure ratio (relative to a reference pressure of 2×10^{-5} Pa). The equation is:

$$SPL(dB) = 20 \log (\Delta p/0.00002) = 20 \log (\Delta p) + 94 \qquad (2\text{-}2)$$

where Δp = peak pressure change in Pa. The sound pressure levels in decibels are shown on the right-hand scale of Figure 2-3.

Explosive charges produce a sound energy spectrum that is predominantly low frequency at distances of interest, approximately 10 hertz (Hz) or less for large charges. The energy concentration is displaced toward the low end as explosive yield increases. Also at greater distances, the spectrum is displaced toward lower frequencies as higher frequencies undergo greater attenuation and the shock wave loses its impulsive characteristics. At long distances, the sound of an explosion is a rumble.

Refracted Atmospheric Propagation

Vertical wind and temperature gradients in the atmosphere will refract low-pressure airblast. A decrease in temperature with altitude (the usual daytime condition) refracts airblast away from the ground, so the overpressure at a given ground distance will be less than shown in Figure 2-3 for the case of no refraction. Conversely, an increase in temperature with altitude, or an inversion, refracts airblast toward the ground, thus increasing the overpressure that would be expected at a given ground distance. An increase in wind speed with altitude (the usual condition) refracts upwind airblast away from the ground and downwind airblast toward the ground, thus tending to increase downwind overpressures and decrease upwind overpressures. Conversely, decreasing wind speeds with altitude tend to refract upwind airblast toward the ground and downwind airblast away from the ground, which tend to increase upwind overpressures and decrease downwind overpressures. The combined effects of wind and temperature variations with altitude must be considered when analyzing long-range propagation of airblast and noise.

The "standard atmosphere" (temperature decreasing with altitude) and no wind corresponds to a "weak gradient" condition, i.e., overpressures will be somewhat less than indicated by Figure 2-3. With a "strong gradient," overpressures vary approximately inversely with the square of the distance, resulting in strong refraction away from the ground and greatly reduced distant blast pressures. To reduce the possibility of window breakage by airblast, gradient conditions are usually sought and obtained when detonating a large explosive charge in a field test.

The meteorological conditions that lead to amplification of long-distance airblast and the relative location and magnitude of such amplification are summarized by Reed from a large amount of data (Reference 1). The three conditions of concern are boundary layer ducting, jet stream ducting and focusing, and downwind ozonosphere propagation.

In a temperature inversion, warm air overlies cooler air near the ground surface with the result that acoustic waves are trapped and ducted to propagate along the ground. The magnification of overpressure at distances is further enhanced in the downwind direction because of normal downward refraction due to the usual condition of increasing wind speed with altitude. Based on the available data, it appears inversion or downwind conditions may produce boundary layer ducting that enhances the unrefracted overpressures shown in Figure 2-3 at any given distance by a factor of 2 to 3.

The jet streams, high-speed winds at several tens of thousands feet altitude, can strongly refract acoustic waves back to the earth. Amplification of the peak overpressure by somewhat less than an order of magnitude can be expected where such refracted waves are focused back to the earth's surface. Typically, such focusing occurs approximately 40 to 50 miles away, in the direction of the jet stream flow.

In northern temperate climates, winds at altitudes of about 30 miles usually blow from east to west in summer and west to east in winter. Since temperature and sound speed at 30 miles altitude are near their values at ground surface, the result is enhanced blast pressures approximately 125 miles downwind from these high-altitude winds and reduced blast pressures upwind. There is a rather low probability of overpressure enhancement downwind by a factor of 2 to 3.

As indicated by the above discussion, the long-distance airblast magnitude at any particular point can vary by more than an order of magnitude, depending on the particular meteorological conditions. Under enhancing meteorological conditions, a relatively small explosive charge can produce airblast at long distances, in excess of that from a large charge exploded under gradient conditions. The prediction of the pattern of long-distance airblast and noise magnitudes on the ground requires specialized skills and meteorological measurements that are normally part of field tests. The scheduling of field tests to reduce the possibility of window breakage is based on such measurements and predictions, with the result that little damage has occurred from previous large field tests.

Special Test Configurations

The preceeding discussion applies for most test configurations, where the charge is exploded relatively near the ground surface. A significantly elevated or buried charge can produce different magnitudes of airblast than shown in Figures 2-2 and 2-3.

Even a moderate amount of dirt cover will significantly reduce overpressure in the relatively high-overpressure region shown in Figure 2-2. However, there is little if any reduction in overpressures at long distances, shown in Figure 2-3, unless the depth-of-burst is relatively deep (Reference 7). In fact, exploding a charge at a shallow depth-of-burst may increase airblast magnitude at long distances because of more efficient conversion of explosive energy to shock energy when an explosion is confined (Reference 8). The assumption of no reduction in airblast or noise from burying a charge is usually warranted for environmental assessment. If this assumption indicates that significant environmental damage may occur from close-in airblast and if the depth-of-burst is deeper than about one charge radius, it may be desirable to have the airblast phenomena calculated by a specialist who can include depth-of-burst effects.

When a charge is exploded above the ground surface, shock waves reflected from the ground surface merge with the direct shock wave to enhance the magnitude of the peak overpressure at any given distance. As shown in Figure 2-4, the effect of elevating a charge is to make it appear that the charge is increased in weight. At the optimum height-of-burst for airblast enhancement, a charge appears to be increased in weight approximately 3.5 times so that the distance to a given overpressure (by cube root scaling) is about 1.5 times that from a charge of the same weight exploded on the ground surface.*

Figure 2-4 can be used to estimate the increase in airblast magnitude for an elevated charge. The product of the TNT-equivalent charge weight and the multiplying factor should be used in Figures 2-2 and 2-3 to estimate the airblast magnitude as a function of distance. Substantial elevation is required to significantly extend the distance of a given peak overpressure, e.g., a 1-ton charge would have to be elevated approximately 60 feet above ground level to extend a given overpressure 10 percent farther.

If more than one charge is exploded at nearly the same location and time so that the shock waves interact, the airblast environment is complex. Outside the array of charges and depending on the distance, as was shown with the MISERS BLUFF multicharge event, the airblast may appear as a series of explosions or as a single explosion of larger size than any of the individual explosions. The conservative assumption for distant blast is that the individual shocks will merge to produce a single shock equivalent to that from a single charge with a weight equal to the sum of the weights of the individual charges and located at the center of the array.

---

* Height-of-burst is measured from the center of gravity of the explosive charge to the ground surface. Therefore, zero height of burst means the charge is half buried in the ground.

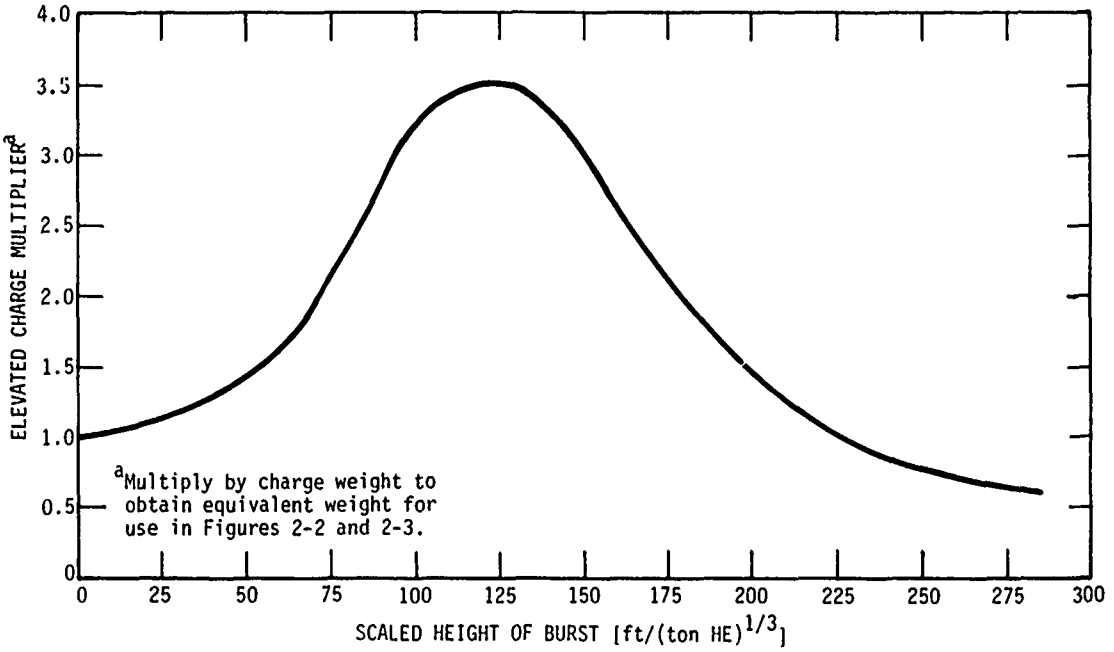

Figure 2-4. Height-of-burst multiplying factor. (Adapted from Reference 1)

CRATERS

The dimensions of an explosion-produced ground crater depend on a number of factors but are most strongly influenced by the TNT-equivalent weight of the charge, the placement of the charge relative to the ground surface, and the type of soil or rock and its water content. Crater dimensions are best predicted based on any previous explosions at the same test site, but even in this case crater dimensions can vary considerably under seemingly identical conditions. For example, PRE-DICE THROW I and II were both 100-ton TNT-equivalent HE charges at virtually the same location; yet, one crater was considerably shallower and wider than the other.

Figure 2-5 shows data for crater volumes from 256-pound spheres of TNT exploded on and below the ground surface in alluvium soils at two different sites.* As can be seen, crater volume increases with depth of charge burial to a maximum volume at the optimum depth for cratering, which is proportional to the charge weight and is about 10 feet for these 256-pound charges. Below the optimum cratering depth, the explosion becomes more

---

* Negative values of height-of-burst are used here for explosive charges whose center of gravity is below the ground surface. The absolute values of these numbers are often referred to as depths-of-burst.

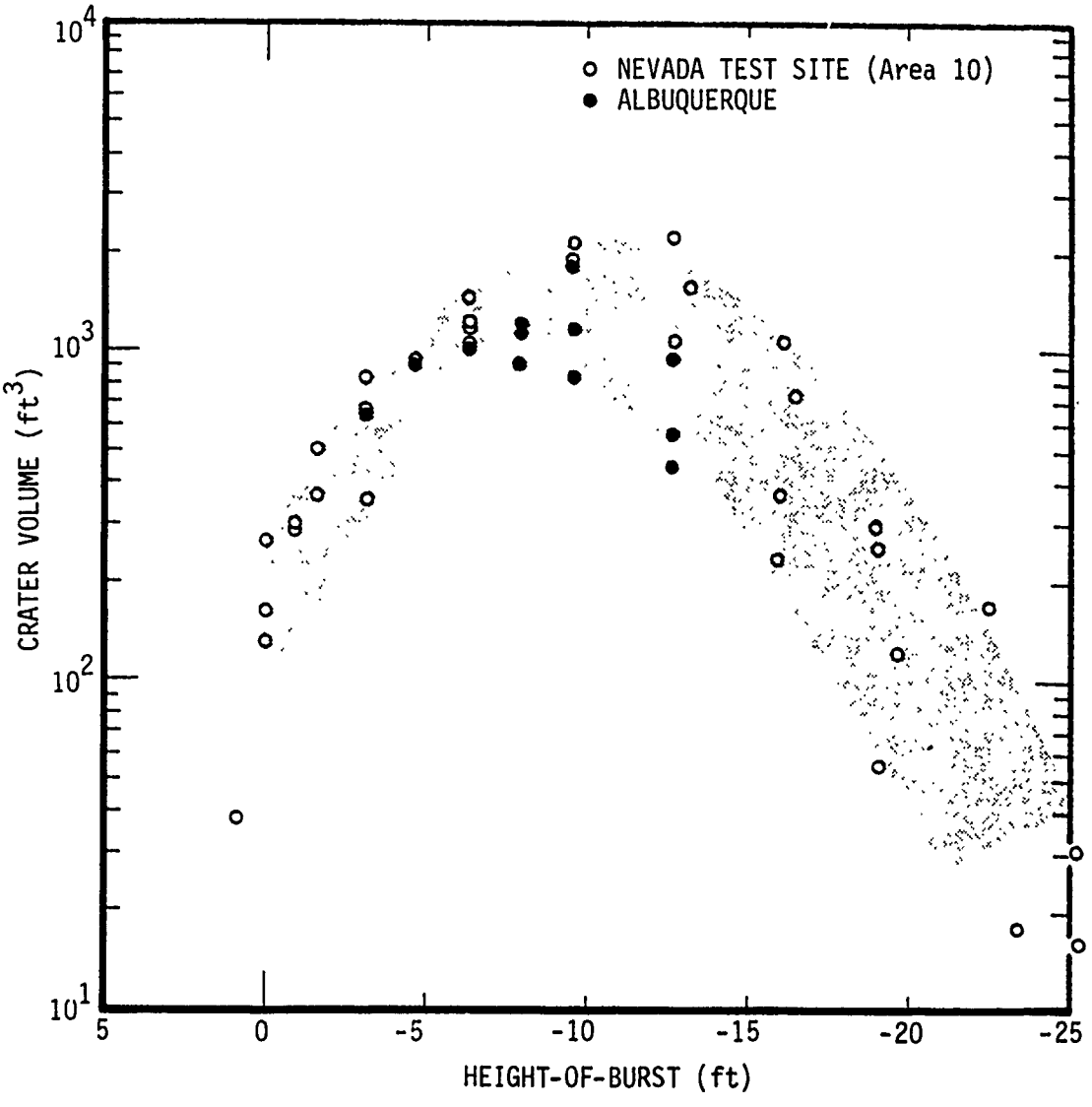

Figure 2-5. Crater volumes from 256-pound spheres of TNT in dry alluvium. (Source: Reference 9)

contained and crater volume decreases. If the charge is buried deep enough, it will be fully contained and no crater will be visible. Note that for relatively shallow-buried charges (those above the optimum cratering depth), the scatter of data indicates that crater volumes may differ by a factor of 2 or 3 for this specific situation, primarily from geological uncertainties. A different geological condition would result in a different set of data.

Table 2-2 lists TNT-equivalency cratering factors for some of the more common explosives, e.g., from a cratering standpoint 1.23 tons of TNT are equivalent to 1 ton of Pentolite. It must be stressed that the factors in Table 2-2 are based on very little data and data trends can be obscured by geological influences.

Table 2-2. TNT-equivalent weights of explosives for ground cratering. (Source: Reference 10)

Explosive Type	TNT-Equivalent Weight Factor[a]
TNT	1.00
Amatol	0.94
Dynamite (40%)	0.68
Pentolite	1.23
C-4, C-3	1.34
Ammonium Nitrate	1.00
Nitromethane	1.10

[a]To determine the TNT-equivalent weight of an explosive, multiply the weight of the explosive by the equivalent weight factor, e.g., 1 ton of Pentolite will produce a crater approximately equivalent to one that would result from 1.23 tons of TNT.

The shape of the explosive charge also has some influence on crater size for explosions on the ground surface. In general, hemispherical, or similar shaped, charges produce somewhat larger craters than do spherical charges of the same weight resting on the ground surface; however, at least part of this difference is because a hemisphere has a lower center of gravity than a sphere on the ground surface and thus has a lower height-of-burst.

Charge type and shape, however, have relatively small influence on crater dimensions compared to the dominance of the geology and depth-of-burst. Figure 2-5 shows that for a given explosive charge and test site, crater volume can vary by more than an order of magnitude, depending only on the depth-of-burst. Other parameters being equal, crater volumes can also vary by more than an order of magnitude depending on the particular type of soil

or rock and its moisture content. The geological influences are the major uncertainty in predicting crater dimensions for a particular field test. Great efforts have been devoted to analyzing cratering of various soils and rocks and the influence of height-of-burst and other explosive charge parameters. Of the numerous reports on the subject of cratering, the results from Reference 9 will be used. The author of Reference 9 is a noted authority on the subject, his report is concise but comprehensive, and his results are in a form that is most useful and understandable for the purposes of this study.

Interpretation of the data indicates that for surface bursts on a given "uniform" medium, the apparent crater volume is approximately proportional to the explosive yield. The apparent volume of a crater is the product of the yield and the "cratering efficiency," which is a function of the geologic medium, the explosive charge, and the height-of-burst. Also, evaluation of cratering data from different geologies suggests that height-of-burst effects can be separated from geological effects if height-of-burst dimensions are scaled inversely by the cube root of the apparent crater volume. Furthermore, for a given height-of-burst, cratering efficiency appears to be basically a function only of geology.

Figure 2-6 illustrates the best estimates of near-surface (within a few charge radii of the ground surface) cratering efficiency in various geologies. The tabular data (V_0) are crater volume per ton of explosive at a zero height-of-burst for various types of geologies. This figure illustrates the importance of the type of geology. Crater size increases as the geology is changed from hard rock to soft rock to dry soil to wet soil. A given charge size and depth-of-burst will produce a crater in wet clay that can be expected to be approximately 20 times the volume of a crater in hard rock. Figure 2-7 illustrates the data when all crater volumes are normalized by the cratering efficiency of the medium.

The summary of all this is that the apparent crater volume from a field test explosion within a few charge radii of the ground surface can be approximated by the following equation:

$$V_a = V_0 W \exp\left\{-5.2\, H(V_0 W)^{-1/3}\right\} \qquad (2\text{-}3)$$

where

V_a = expected apparent crater volume (ft^3)

V_0 = cratering efficiency of explosive for a zero height-of-burst (ft^3/ton)

W = TNT-equivalent explosive weight (tons)

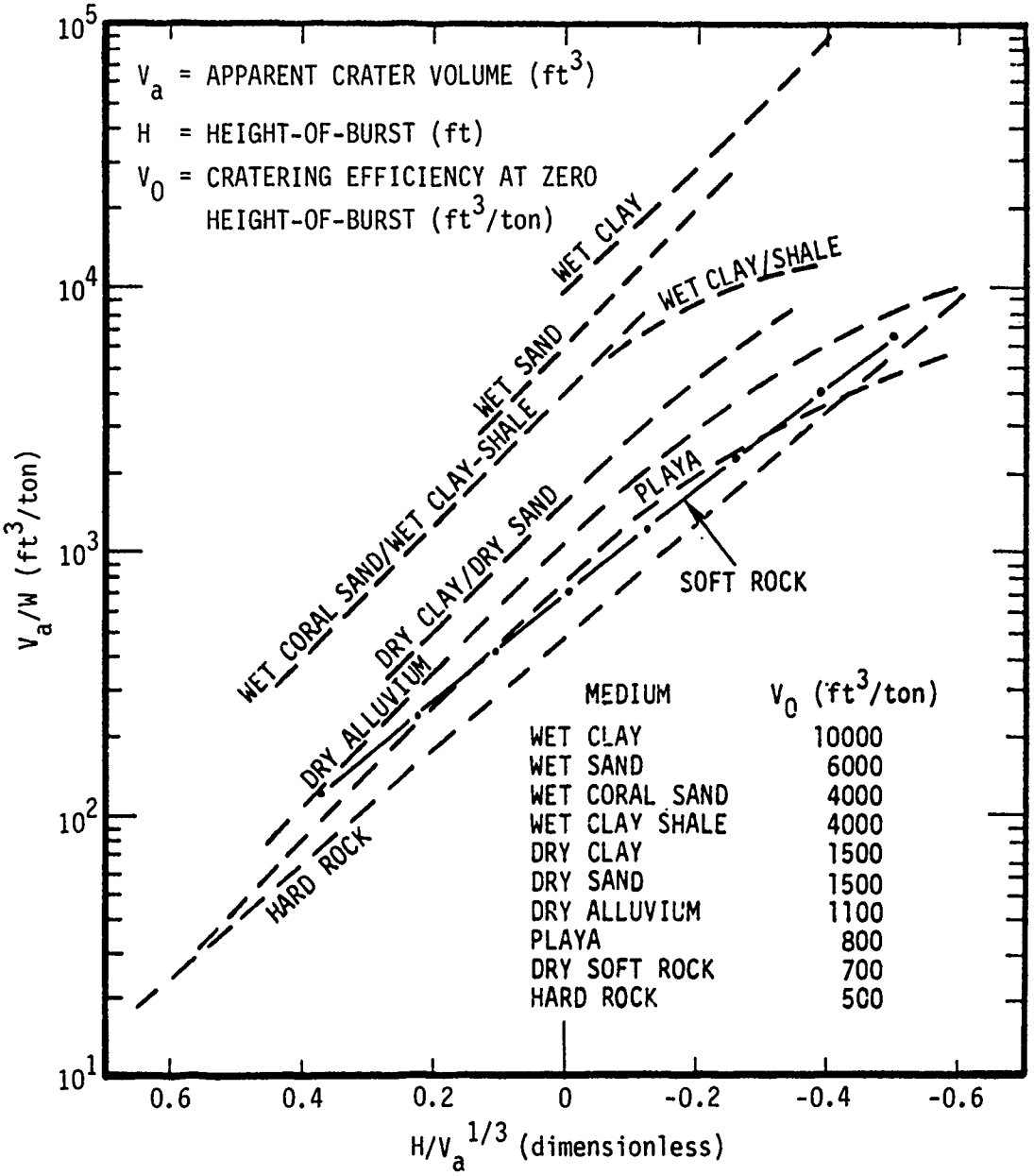

Figure 2-6. Near-surface HE cratering efficiencies. (Adapted from Reference 9)

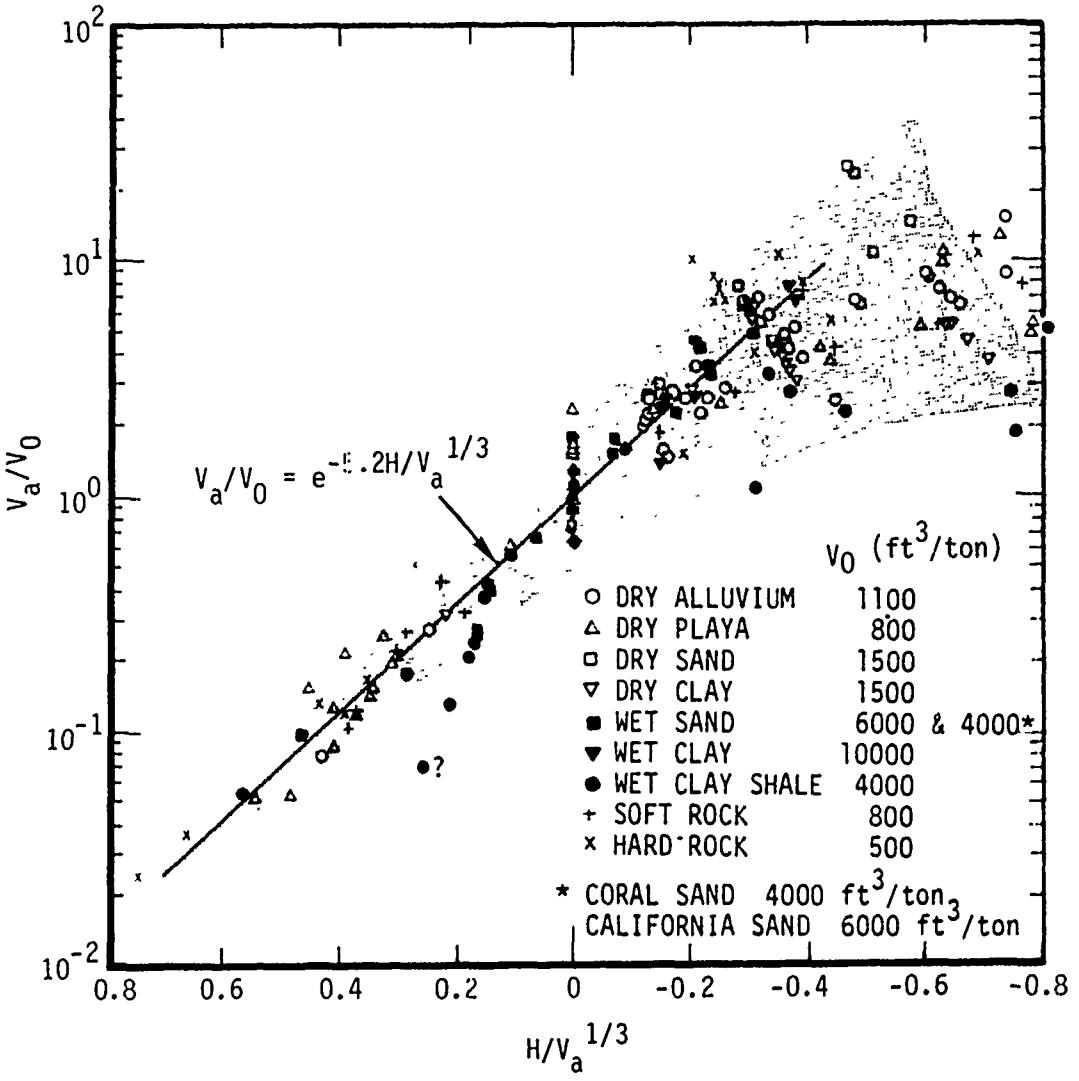

Figure 2-7. Normalized cratering efficiency for various geologies. (Adapted from Reference 9)

H = height-of-burst of the explosive charge (ft) (negative for buried charges).

(Since we are attempting to predict crater volumes rather than normalize known volumes into a data fit, the term V_0W is used in Equation 2-3 as the best estimate of the apparent crater volume.) Equation 2-3 is shown on Figure 2-7 where it can be seen that it is a reasonable fit to the data for near-surface heights-of-burst.

Cooper has gone further and has combined the various types of geologies into four basic categories of wet geologies (including soils and clay shales), dry soil, dry soft rocks, and dry hard rocks. The data organized into these categories are shown in Figures 2-8 through 2-11, from which he estimates the values of V_0 shown in Table 2-3. Using these values of V_0, Equation 2-3 has been plotted on the figures. Thus, to roughly predict a crater volume, either the values shown in Table 2-3 or the values tabulated in Figure 2-7 can be used for V_0 and either applied directly into Equation 2-3 or used in the appropriate figure (2-7 through 2-11). If the figures are used, a range of crater volumes that considers the data scatter can be estimated.

Figure 2-12 illustrates how crater depth and crater radius vary with crater volume. Thus, the following equations can be used to estimate crater depth and radius after the crater volume has been estimated as discussed previously:

$$R_a \simeq 1.2\ V_a^{1/3} \tag{2-4}$$

$$D_a \simeq 0.5\ V_a^{1/3} \tag{2-5}$$

where

R_a = apparent crater radius (ft)

D_a = apparent crater depth (ft)

V_a = apparent crater volume (ft^3).

For large HE craters (between 10^5 and 10^6 ft^3) in wet soil, however, the data points indicate shallower craters than predicted by Equation 2-5. This is consistent with results from large HE tests at a site with a shallow water table. Such sites tend to produce wider, but shallower, craters than those in dry geologies.

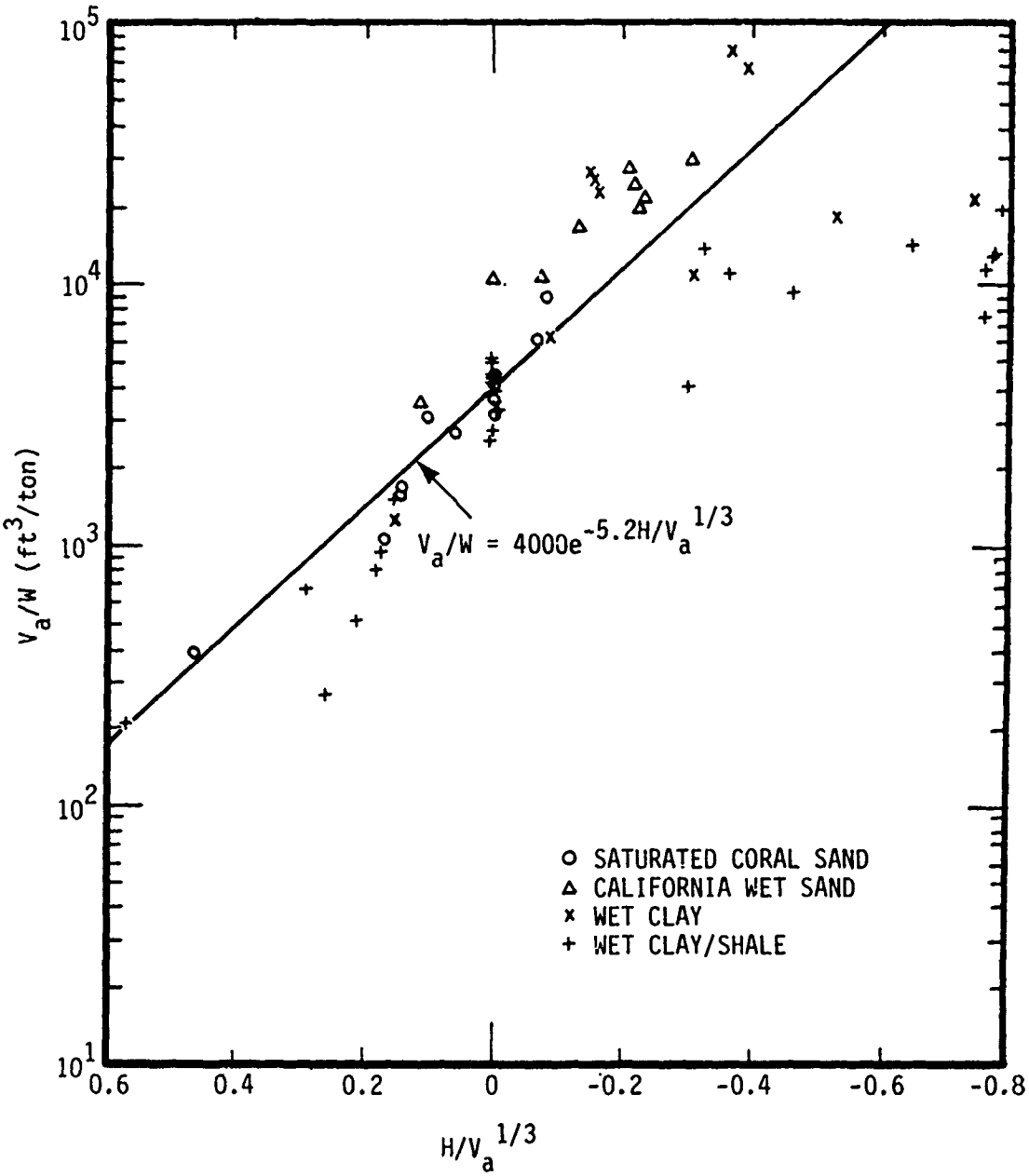

Figure 2-8. Near-surface HE cratering efficiency in wet geologies. (Adapted from Reference 9)

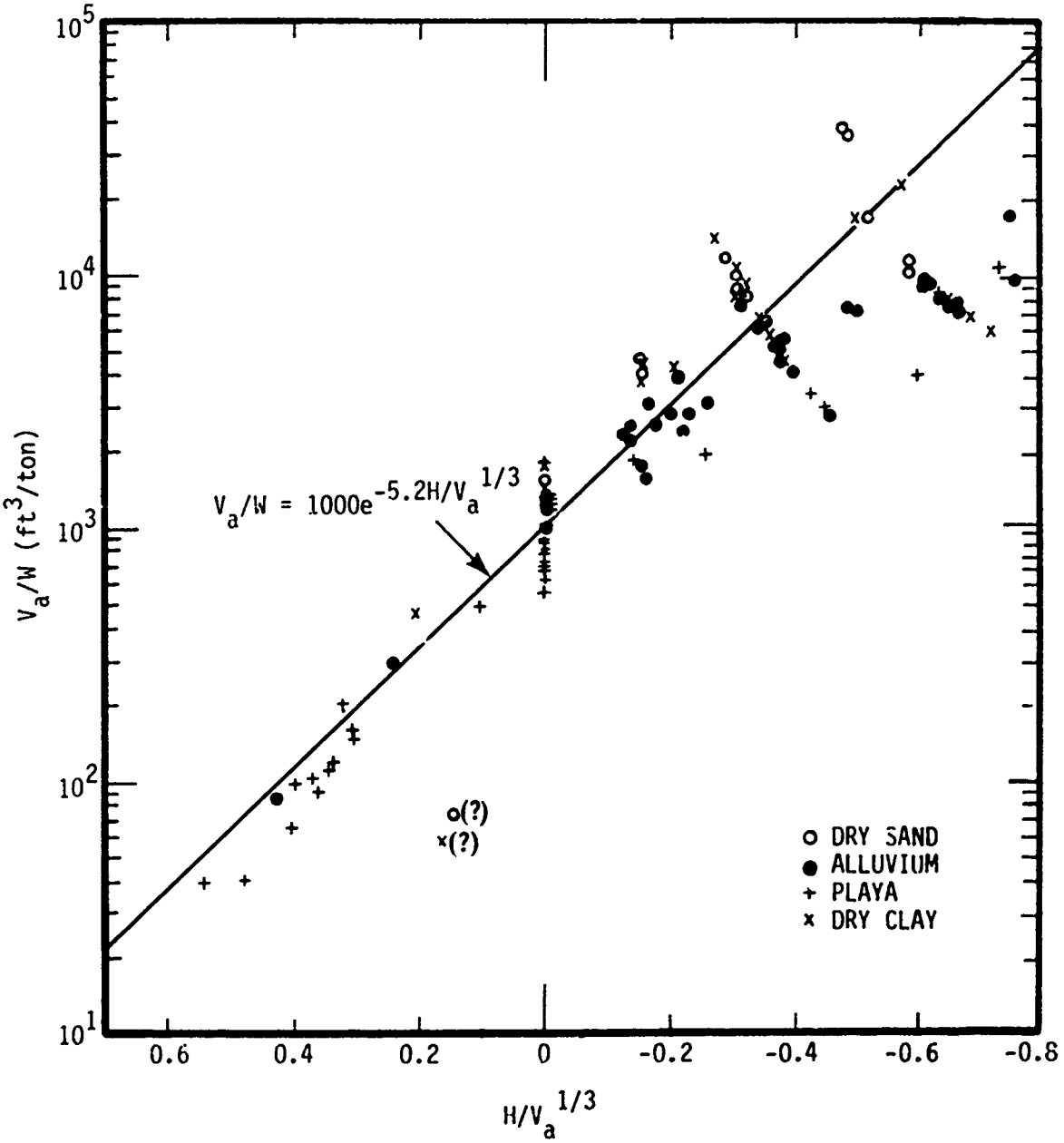

Figure 2-9. Near-surface HE cratering efficiency in dry soil. (Adapted from Reference 9)

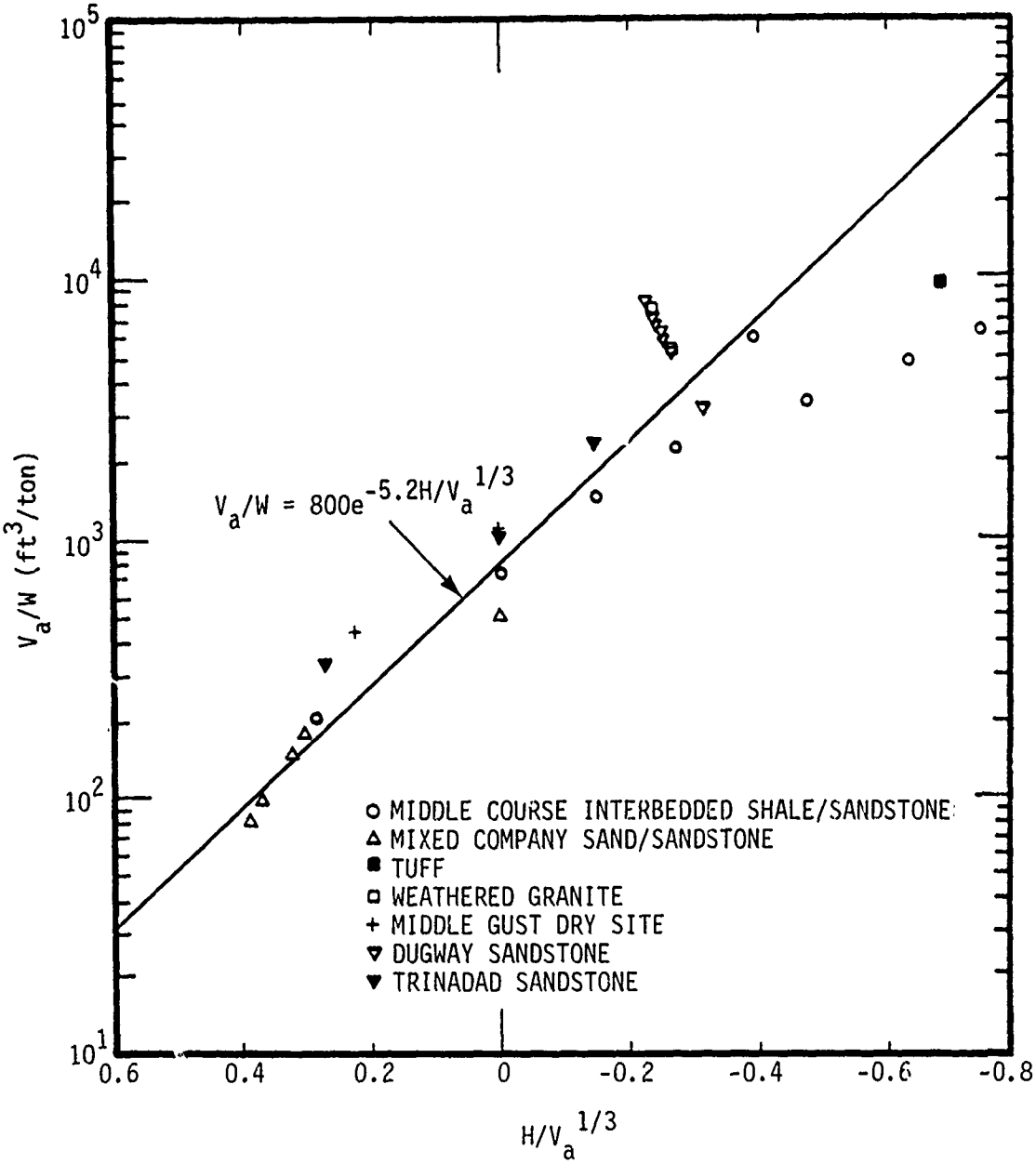

Figure 2-10. Near-surface HE cratering efficiency in dry soft rock. (Adapted from Reference 9)

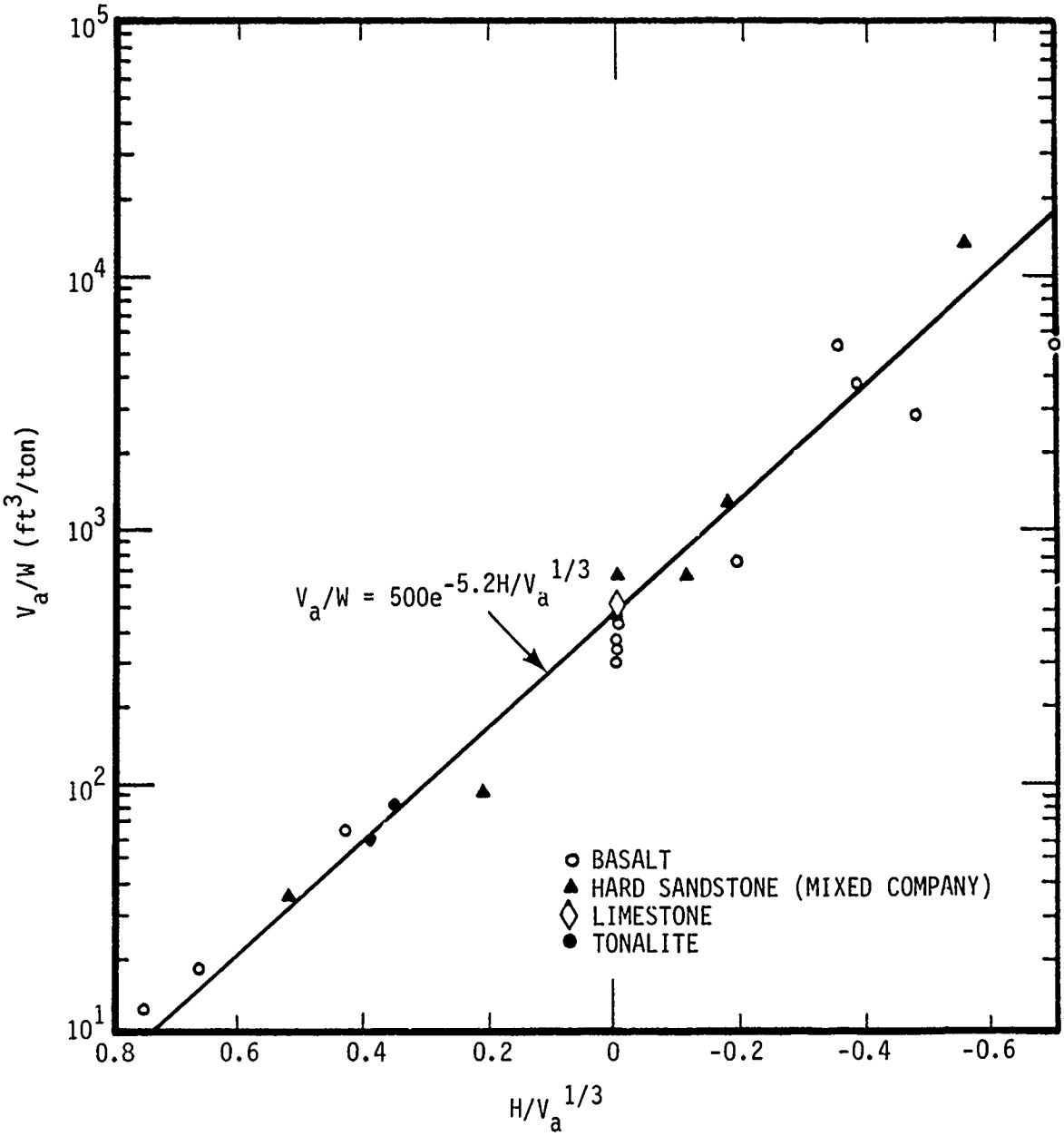

Figure 2-11. Near-surface HE cratering efficiency in dry hard rock. (Adapted from Reference 9)

Table 2-3. HE cratering efficiency for generic geologic materials. (Adapted from Reference 9)

Medium	V_0 (ft^3/ton) Range	Best Estimate
Wet Geology (including soils and clay shales)	2,000 to 8,000	4,000
Dry Soil	600 to 1,800	1,000
Dry Soft Rock	500 to 1,200	800
Dry Hard Rock	300 to 700	500

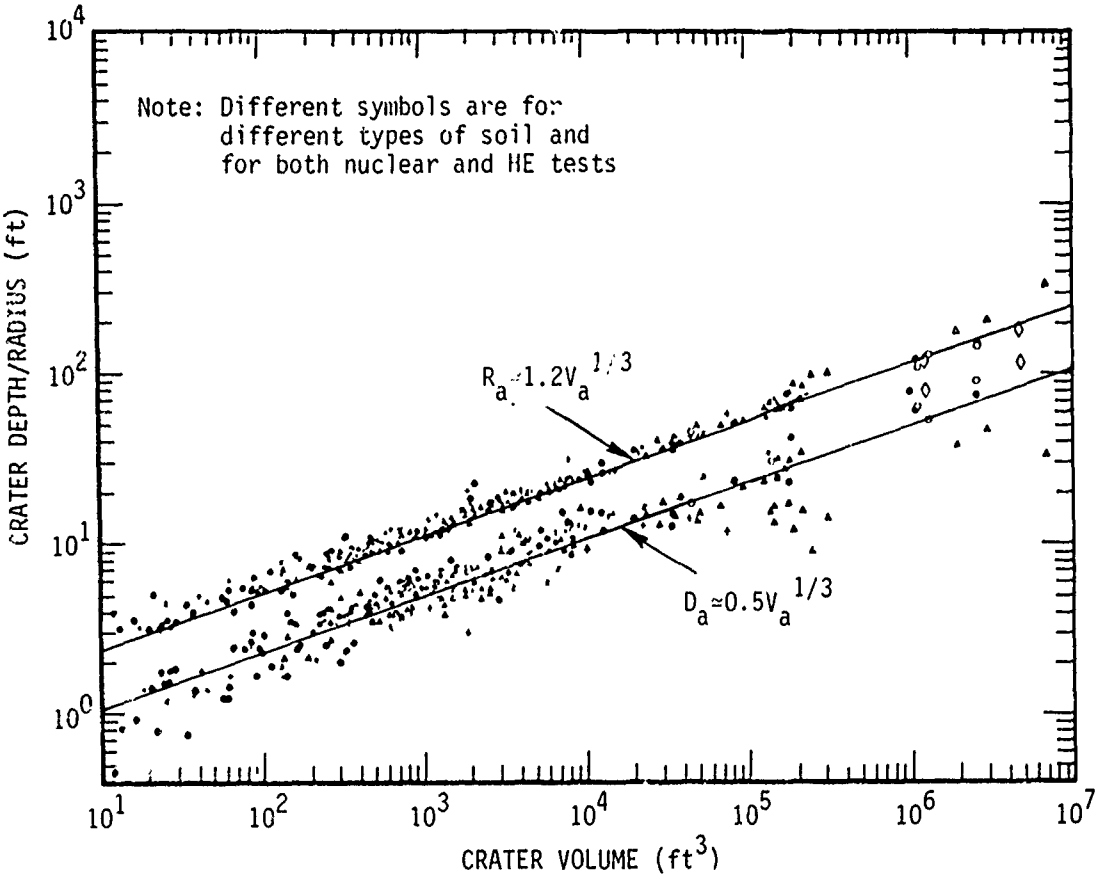

Figure 2-12. Crater radii and depths as functions of crater volume. (Adapted from Reference 9)

EJECTA AND MISSILES

Most of the ejecta, the earth materials from the apparent crater, from a large HE explosion are deposited within about 3 to 5 crater radii of ground zero (GZ), i.e., within a few hundred feet of a 500-ton charge. Beyond this distance, the ejecta do not completely cover the ground surface and the areal density decreases rapidly with increased distance from GZ.

The ground coverage of the ejecta can be estimated from Figure 2-13 as a function of crater dimensions and the density of earth materials. The unit weight of dry earth materials in-place varies, but reasonable values to use are 80 lb/ft^3 for porous earth, 90 lb/ft^3 for clay, 100 lb/ft^3 for sand, 120 lb/ft^3 for desert alluvium, 140 lb/ft^3 for soft rock, and 160 lb/ft^3 for hard rock.

Theoretically, some ejecta (missiles) can be propelled very long distances; in fact, however, very few missiles have been found beyond 3,000 feet from large HE explosions.

GROUND SHOCK

There are relatively few data on ground motion measurements from large HE field tests at distances of interest for environmental analysis, i.e., where the peak particle velocity is less than a few centimeters per second. Figure 2-14 shows the peak particle velocities from five HE field tests that had ground motion measurements at the magnitudes of interest. (All distances have been scaled to 1 ton of TNT by the cube root of the TNT-equivalent weight.) The three charges exploded either on the ground surface or, at most, just buried with the top of the charge flush with the ground surface (MIXED COMPANY III, JANGLE HE-2, AFWL 1-5) produced reasonably consistent ground motions, with the MIXED COMPANY III ground shock having the greatest magnitude. The more deeply buried charges in the ESSEX I--Phase 2 and PRE-GONDOLA--Shot B tests produced somewhat stronger ground shocks, as would be expected. In this study, the MIXED COMPANY III data will be assumed as the worst-case ground shock for near-surface explosions. Assuming that the maximum vertical, radial, and tangential peak particle velocities add vectorially,* the equation of the resultant peak ground motions can be expressed as follows:

$$V_{max} = 2{,}700\ (D/W^{1/3})^{-1.4} \qquad (2\text{-}6)$$

---

* The combined data are not given in the references, but adding the peak vectors results in the largest possible magnitudes of ground motion and therefore is a conservative assumption.

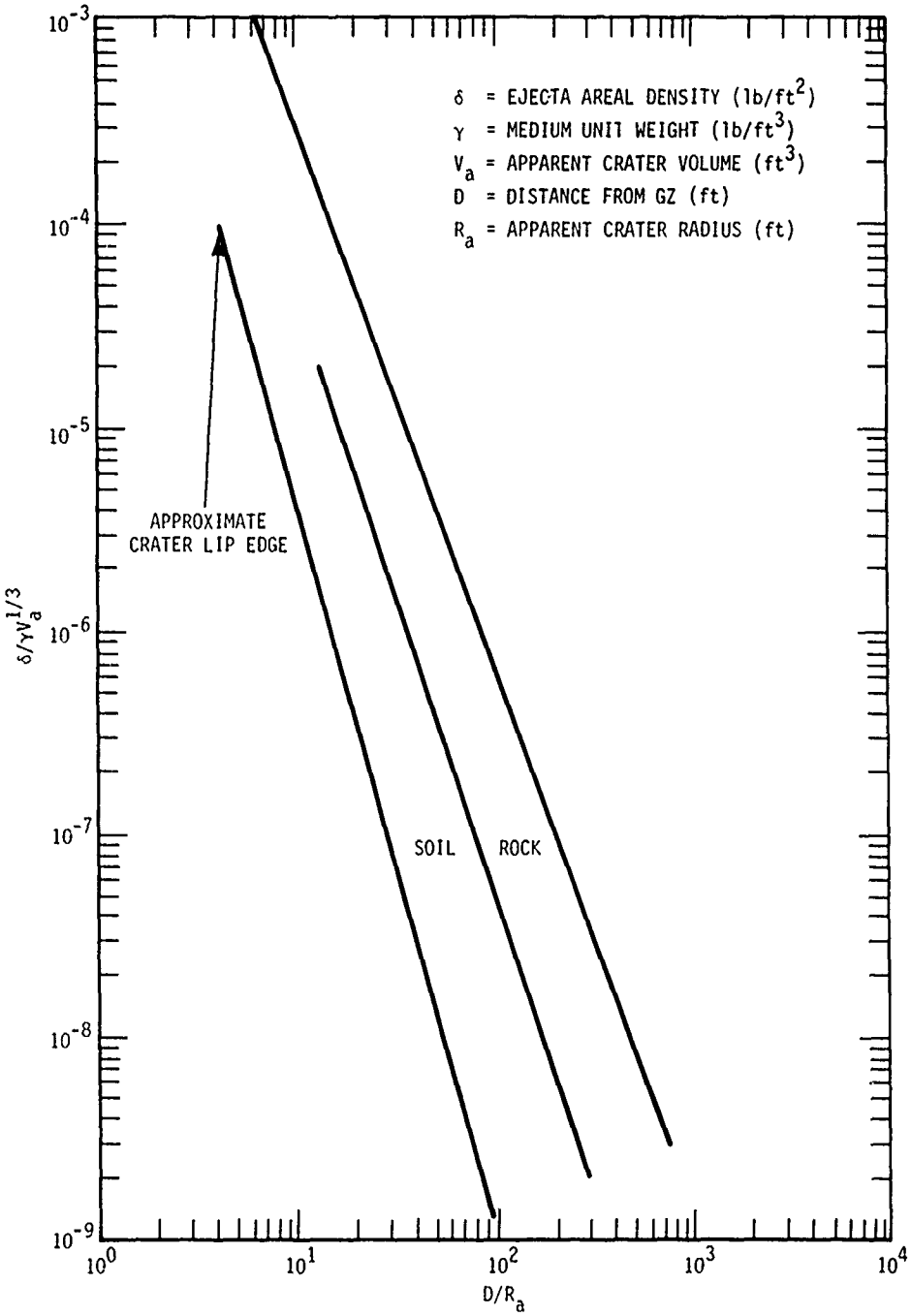

Figure 2-13. Dimensionless plot of ejecta mass density as a function of range (expressed as multiples of the apparent crater radius). (Source: Reference 10)

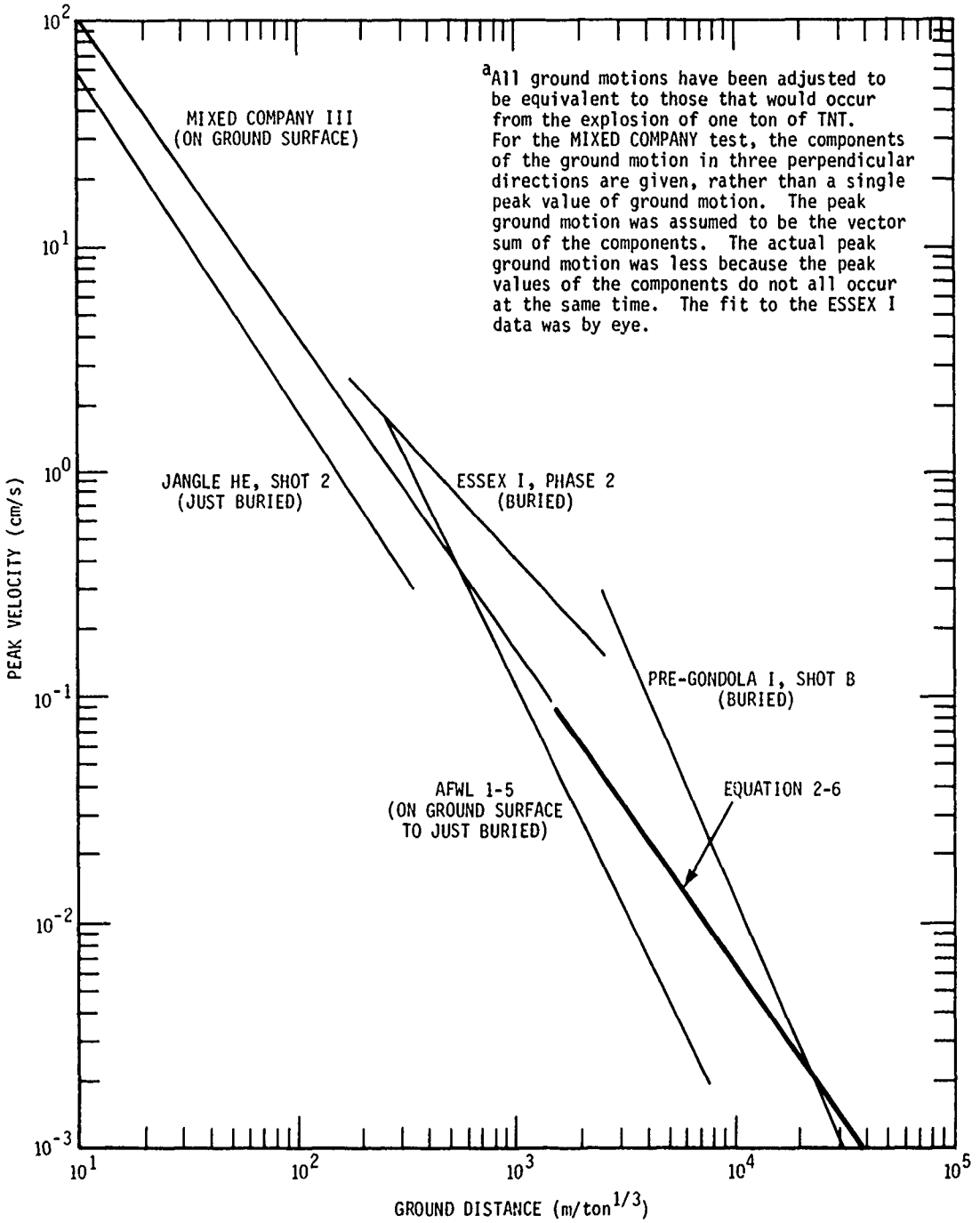

Figure 2-14. Ground motions from previous large HE field tests. (Source: References 11 through 15)

where

V_{max} = resultant peak particle velocity (cm/sec)

D = distance (m)

W = TNT-equivalent weight (tons).

Equation 2-6 is shown on Figure 2-14 for comparison with the data. Recent large field test explosions tend to confirm that Equation 2-6 is a reasonably conservative assumption for distant ground motion from near-surface explosions. Ground motions at two dams and a large tunnel were measured during the execution of Event I of MISERS BLUFF, a 120-ton charge of ANFO. The peak ground motion at one of the dams was about an order of magnitude below that predicted by Equation 2-6 and ground motions at the other dam and the tunnel were not measurable (Reference 16). Ground motion measurements for PRE-DICE THROW I, PRE-DICE THROW II, and DICE THROW generally appear to be about equivalent to, or less than, the values that would be obtained from Equation 2-6 (Reference 17).

Scaling ground motions by crater volume and comparing buried explosions with those at zero height-of-burst indicates that buried explosions produce ground shocks of approximately 4 times the magnitude determined from Equation 2-6 (Reference 18), although that analysis is only for relatively large ground motions. Since this would be a conservative estimate of the buried explosions shown in Figure 2-14, it will be assumed in this study that Equation 2-6 multiplied by 4 applies to deeply buried explosions.

Ground motion damage criteria are usually given as functions of accelerations rather than velocities. Based on MIXED COMPANY III results (Reference 11), velocities correspond to simple harmonic motion of a fundamental Raleigh wave frequency of 6 hertz, i.e., multiply V_{max} by 37.7 to obtain the value of peak acceleration. Accelerations based on Equation 2-6 are plotted on Figure 2-15 for TNT-equivalent explosive weights of interest.

EXPLOSIVE PRODUCTS

The explosion of a charge of HE results in a hot fireball of numerous chemical elements and compounds that are mostly in the gaseous state. Because of oxidation of the initial chemical products, the total weight of the final products is greater than the weight of the explosive charge. For any particular explosive, the types and amounts of chemical species can be calculated by computer programs; the problem is in determining the best values for the input parameters to the particular equation of state. Comparing computer program theoretical calculations against empirical data is extremely difficult because laboratory tests are limited to very small amounts of explosives exploded in a relatively small chamber. Under such

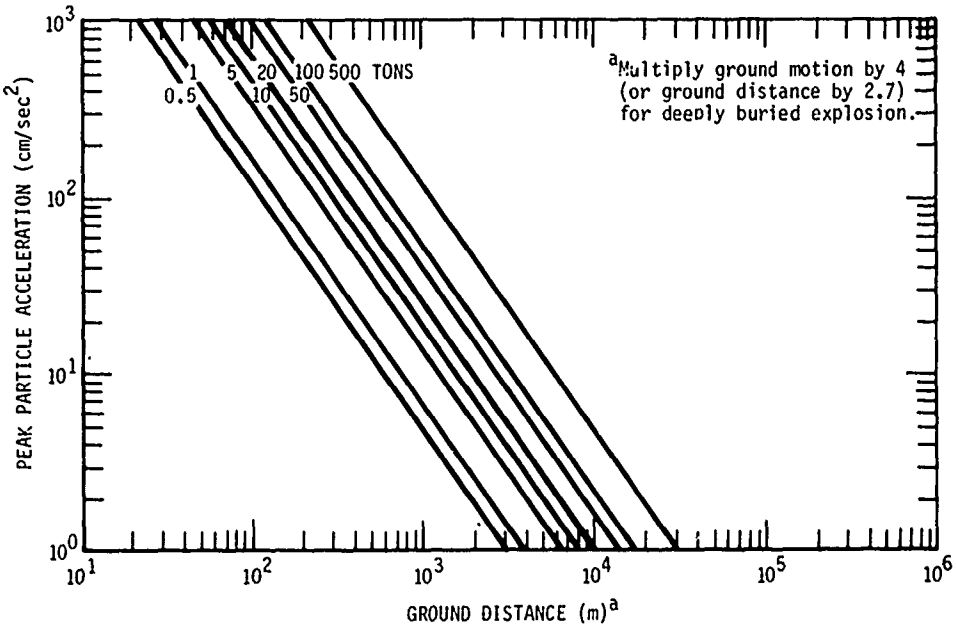

Figure 2-15. Maximum expected ground motions from near-surface explosions.[a]

conditions, the explosion products can be very different from those from a large charge exploded in the open air.

Table 2-4 lists the predicted ideal explosion products for the types of explosives commonly used in field tests. ANFO has essentially replaced TNT for large charge sizes, being much less expensive. TNT and the other types of explosives are used for smaller charges. The ANFO calculations are based on the virial equation of state, while the calculations for the other explosives are based on the Becker-Kistiakowsky-Wilson (BKW) equation of state. For types of explosives not shown here or in Reference 20, the author of Reference 20 or some other authority should be contacted for guidance.

Based on Table 2-4, explosives produce relatively small fractions of chemical species that are of environmental concern in the open air. For each of the explosive types shown; at least 90 percent of the compounds consist of innocuous water vapor, carbon dioxide, nitrogen gas, and solid carbon. However, it must again be stressed that the amounts of products that actually result from a field test may be significantly different from the theoretical amounts shown in Table 2-4. The calculations from References 20 and 21 have not been continued beyond the time when the pressure drops below about 100 atmospheres and any reaction with oxygen in the atmosphere is not included. Presumably, atmospheric oxygen has also not been

Table 2-4. Ideal explosion products, given in percent by weight.

Chemical Species		Explosive Type				
Formula	Name	ANFO[a] (Ammonium Nitrate and Fuel Oil)	TNT[b] (Trinitro-toluene)	PETN[c] (Pentaerythritol Tetranitrate)	Pentolite[c] (Equal Parts of TNT and PETN)	Nitromethane[b]
H_2O	Water	49.3	12.5	17.0	19.1	24.1
H_2	Hydrogen	0.1	0.4	0.26	0.055	0.792
O_2	Oxygen	1.1	-	-	-	-
CO_2	Carbon Dioxide	15.5	39.7	61.2	47.5	40.0
CO	Carbon Monoxide	2.1	3.9	1.92	0.00755	3.37
NH_3	Ammonia	0.085	0.02	0.0192	0.00150	0.0557
H	Hydrogen Radical	-	-	-	-	-
NO	Nitric Oxide	1.7	-	-	-	-
N_2	Nitrogen	32.8	18.5	17.7	18.1	22.9
OH	Hydroxide Radical	0.0289	-	-	-	-
CH_4	Methane	0.000032	1.62	1.52	0.760	5.74
NO_2	Nitrogen Dioxide	0.0322	-	-	-	-
N_2O	Nitrous Oxide	0.0132	-	-	-	-
O	Oxygen Radical	0.0032	-	-	-	-
HCN	Hydrogen Cyanide	0.0054	-	-	-	-
C	Solid Carbon	-	23.27	0.312	14.4	3.00

[a]Source: Reference 19. The calculations were performed for 5% and 6% and other even percentages of fuel oil. Between 5% and 6% fuel oil concentration, the oxygen balance of the charge shifts so that the concentrations of some of the minor products change considerably between these values. Past field tests have used a fuel oil concentration of 5.5%. Therefore, as a conservative assumption, the values shown in this column are for the highest concentration of each species, whether for 5% or for 6% fuel oil.

[b]Source: Reference 20.

[c]Source: Reference 21.

included in the calculations from Reference 19. There is disagreement on the significance of such conditions.

Because of the large ratio of volume to surface area for a multiton explosive charge, atmospheric oxygen may not be available to a large part of the explosive products until the temperature has decreased (because of expansion of the fireball) to where significant chemical reactions will not occur. Reference 19 states that reaction rates involving oxygen are sufficiently slow that the explosion products may be "frozen" at roughly their initial proportions as they expand and cool. In contrast, the informal opinion of Dr. Harold Ring, Assistant Director of Dupont De Nemours Research Section on explosives at Wilmington, Delaware, was that equation-of-state computations do not apply for large charges exploded in the open because virtually all of the explosion products will change to water, carbon dioxide, and nitrogen.

In either event, oxidation of the compounds shown in Table 2-4 will generally tend to change potentially hazardous compounds to less hazardous or innocuous products. Therefore, Table 2-4 can be assumed as a worst-case from the standpoint of hazardous explosion products.

CLOUD RISE AND DIFFUSION

The heat of explosion creates a buoyant fireball of hot gases and earth materials which rises rapidly until it loses buoyancy, continues to expand turbulently until it reaches stabilization dimensions, and then undergoes atmospheric diffusion as it drifts downwind. According to Church (Reference 22), explosion clouds cease to rise buoyantly within about 2 minutes after detonation, although cloud growth by turbulence may give the appearance that the cloud is still rising. Based on measurements of clouds from 22 HE charges exploded on the ground surface, Church recommends that the maximum height of the cloud at 2 minutes be calculated from the empirical relationship:

$$C_t = 508\ W^{0.25} \qquad (2\text{-}7)$$

where

C_t = cloud-top height at 2 minutes after detonation (m)

W = explosive charge TNT-equivalent weight (tons).

Based on Equation 2-7, a 500-ton event would have a cloud height of 2,400 meters. However, Equation 2-7 is based on few charges in excess of 1 ton and does not give information on the cloud dimensions after turbulence ceases. There is evidence that the top of the cloud produced from a large explosion continues to rise after 2 minutes, either from buoyancy or from turbulence, to reach a considerably greater height.

Figure 2-16 shows the cloud-top heights from four 500-ton explosions for which cloud measurements were made. The estimated height of a 100-ton explosion cloud is also shown. As can be seen, although Equation 2-7 adequately describes cloud height 2 minutes after an explosion, cloud heights continued to increase until about 5 minutes. From this data, it appears that the maximum cloud height for a 500-ton explosion is somewhat in excess of 3,000 meters and occurs about 5 minutes after the explosion.

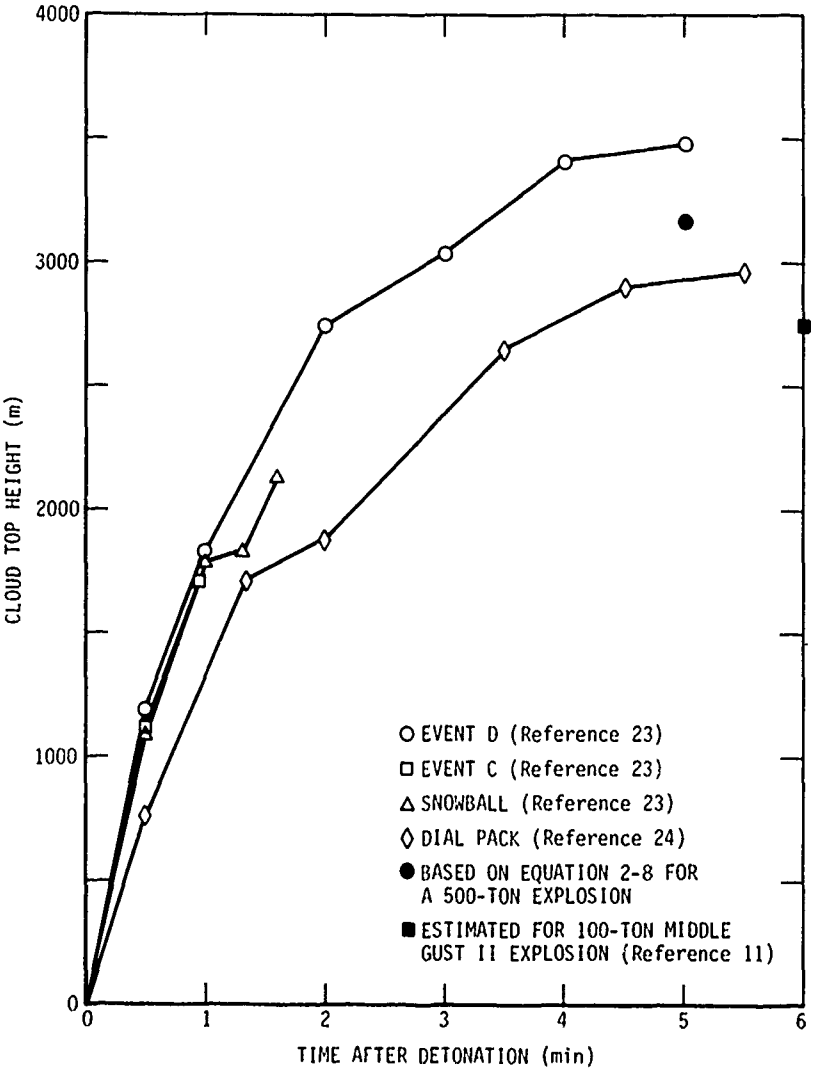

Figure 2-16. Height aboveground of large explosion clouds.

When a cloud reaches its maximum height, it has roughly a cylindrical shape. Most clouds appear to have a bottom that is about midway between the cloud top and the ground. For example, the DIAL PACK cloud bottom was calculated to be about 1,500 meters above the ground.

Figure 2-17 shows the data for diameters of large-explosion clouds. As can be seen, the DIAL PACK cloud continued to expand, contrary to most observations in which clouds appear to contract somewhat from turbulence before diffusing. Ignoring the DIAL PACK data, the other data seem to indicate a cloud diameter of approximately 1,500 meters from a 500-ton explosion.

Based on these limited data and assuming that cloud dimensions scale by the 0.25 power of the charge weight, cloud dimensions can be estimated by the following equations:

$$C_t = \text{height to top of cloud (m)} = 670\ W^{0.25} \quad (2\text{-}8)$$

$$C_b = \text{height to bottom of cloud (m)} = 335\ W^{0.25} \quad (2\text{-}9)$$

$$C_c = \text{height to center of cloud (m)} = 500\ W^{0.25} \quad (2\text{-}10)$$

$$C_d = \text{diameter of cloud (m)} = 335\ W^{0.25} \quad (2\text{-}11)$$

$$C_v = \text{volume of cloud } (m^3) = 3 \times 10^7\ W^{0.75} \quad (2\text{-}12)$$

The cloud-top height and diameter based on Equations 2-8 and 2-11 for a 500-ton explosion are plotted on Figures 2-16 and 2-17, respectively, for comparison with the data. For 1-ton explosions, Equations 2-8 and 2-11 give a cloud-top height of 670 meters and a cloud diameter of 335 meters, which is roughly compatible with data on charges of this size from References 25 and 26. These references also indicate that charges must be considerably buried before cloud sizes are significantly affected.

Cloud measurements have also been reported for MISERS BLUFF II-1, a 100-ton event, and II-2, six 100-ton closely-spaced charges that were detonated simultaneously (Reference 27). These data, shown in Figures 2-18 and 2-19, are of considerable interest. The MISERS BLUFF II-1 cloud shows the classic behavior of a cloud during its stabilization phase when the cloud size is relatively unchanged until turbulence ceases and the cloud diffuses with the winds. The MISERS BLUFF II-2 cloud shows vertical stabilization but continual growth in width, which may be due to the interaction of multiple clouds or to strong winds. (The cloud tracking data indicate the cloud was moving downwind at 25 to 30 mph during the observation period.)

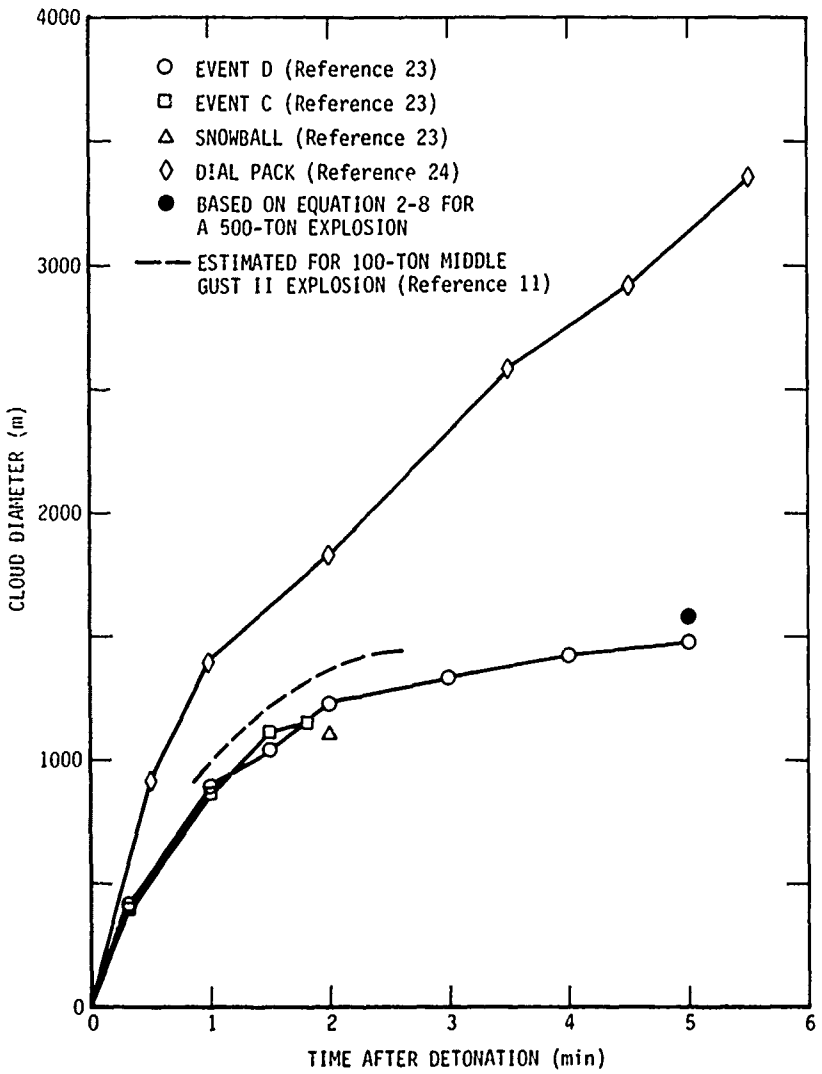

Figure 2-17. Diameters of large-explosion clouds.

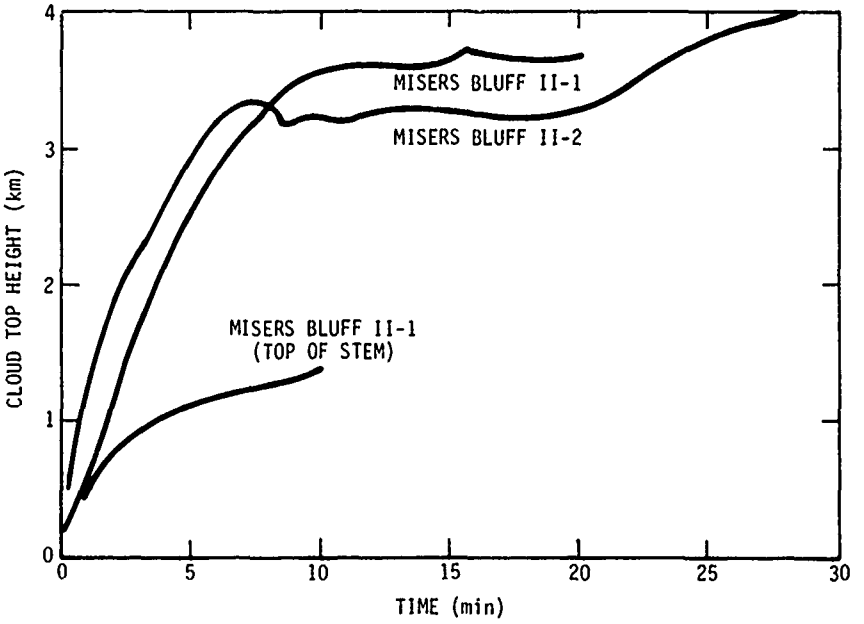

Figure 2-18. Top of MISERS BLUFF clouds. (Source: Reference 27)

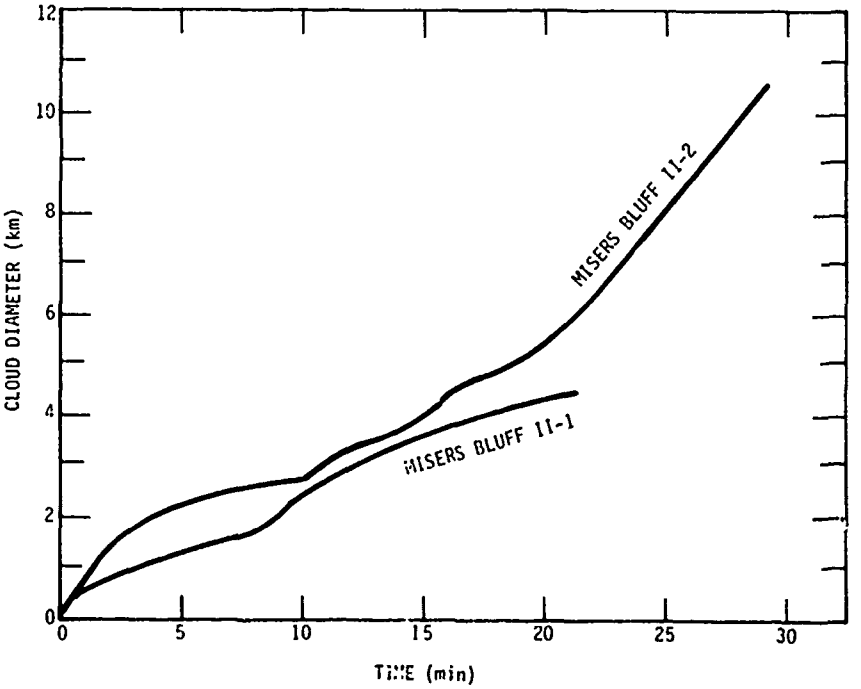

Figure 2-19. Diameter of MISERS BLUFF clouds. (Source: Reference 27)

The cloud dimensions during the first 6 minutes are in good agreement with the other data clouds in Figures 2-16 and 2-17 and with Equations 2-8 through 2-12. The measurements of the bottom of the MISERS BLUFF II-2 cloud (the stem height) support the previous observations that the bottom of a cloud is about midway between the top of the cloud and the ground. Note, however, that the MISERS BLUFF observations were carried out over a longer time period than for the previous field tests, and they indicate that maximum cloud size at stabilization occurs later than 5 minutes after the explosion. This indicates that Equations 2-8 through 2-12 may underestimate the size of an explosion cloud at stabilization. For the purposes of environmental analysis, however, underestimation of an explosion cloud is conservative because a larger cloud is necessarily more diffuse and the concentrations of gaseous detonation products and dust at ground level downwind would be less than for a smaller cloud size at stabilization. Therefore, Equations 2-8 through 2-12 are still recommended for the purposes of environmental analysis, until more cloud measurements from other large-scale field tests are available to better estimate stabilized cloud dimensions.

Most of the earth materials from a crater fall back to earth in the vicinity of the crater. The earth materials in a stabilized cloud are relatively fine particles that can be transported downwind with the gaseous detonation products. Dust samples taken from the DIAL PACK cloud by aircraft fly-throughs showed that the average dust concentration at the time the cloud stabilized (approximately 15 minutes after the explosion) was approximately 4 mg/m^3 and the concentration decreased inversely with time to the 1.4 power over the measurement period of from 10 to 60 minutes following the explosion; that is, for each ten-fold increase in time, the dust concentration decreased by a factor of 25 (Reference 28). Based on the approximate cloud dimensions at 5 minutes of a vertical thickness of 1,500 meters and a horizontal diameter of about 3,100 meters and the apparent crater volume of 7,400 m^3, approximately 2 percent of the crater volume was in the DIAL PACK explosion cloud at the time of cloud stabilization.

The more extensive sampling and analysis of the dust clouds from MISERS BLUFF II-1 and II-2 events (Reference 29) indicate much higher concentrations than the data from DIAL PACK. Figures 2-20 and 2-21 show the cloud dimensions and concentrations from the MISERS BLUFF events at 10 and 20 minutes after the detonations, as reconstructed from the extensive data. These dust concentrations are one to two orders of magnitude greater than the concentration of the DIAL PACK cloud. The total mass of dust in the II-1 cloud 10 to 20 minutes after detonation is reconstructed to be approximately 8×10^8 grams (880 tons), which indicates approximately one-third of the crater volume of 150 m^3 was in the stabilized explosion cloud. The total mass in the multiburst II-2 cloud 10 to 20 minutes after detonation was reconstructed to be approximately 5×10^9 grams, which also indicates approximately one-third of the crater volume of 10,600 m^3 was in the stabilized explosion cloud.

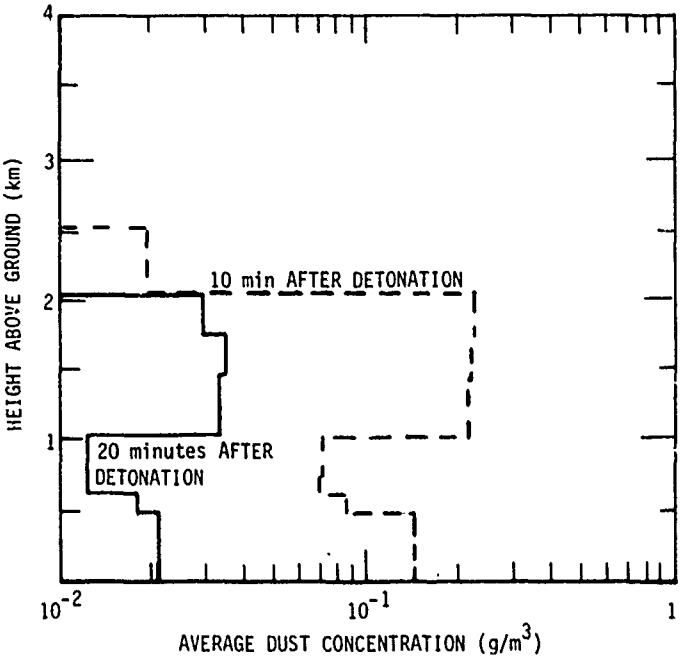

Figure 2-20. Reconstructed MISERS BLUFF II-1 dust cloud. (Source: Reference 29)

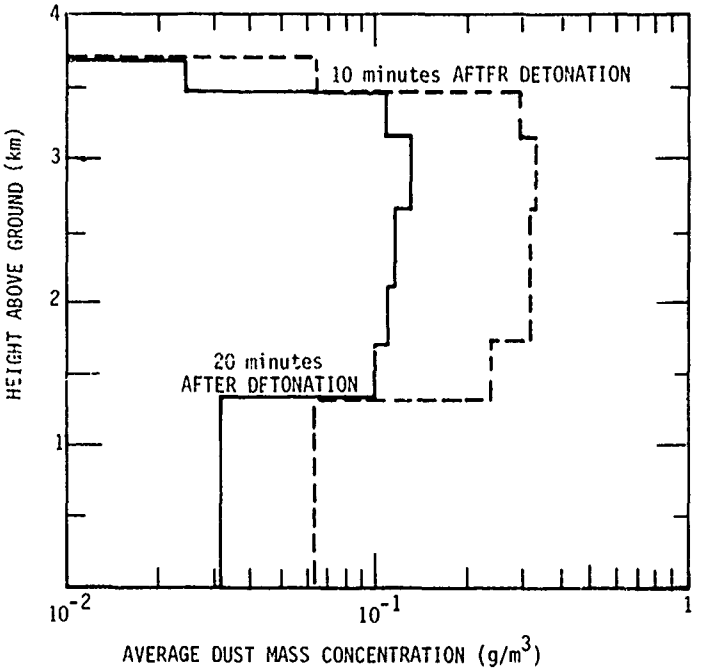

Figure 2-21. Reconstructed MISERS BLUFF II-2 (multiburst) dust cloud. (Source: Reference 29)

The sampling data from the individual aircraft sampling passes through the cloud and the cloud reconstruction indicate that, although the concentrations varied at different points in the cloud, there was no indication of the concentrations being greater at the center of the cloud. It can be assumed that the dust mass is distributed evenly throughout the cloud at the time of stabilization.

Since the recent MISERS BLUFF data are based on an extensive experimental program and are more conservative from an environmental impact standpoint than the DIAL PACK results, the results from MISERS BLUFF will be assumed in this analysis, i.e., it is assumed that one-third of the apparent crater contents will be distributed evenly throughout an explosion cloud and available for distant transport downwind as the cloud diffuses. Cloud sampling in future field tests may clarify the considerable disparity between the MISERS BLUFF and DIAL PACK data.

As an explosion cloud drifts downwind, it diffuses and the concentrations of dust and explosive products decrease while the edge of the cloud approaches ground level. At a certain distance downwind, which is a function of the initial height and dimensions of the cloud, the rates of diffusion in the horizontal and vertical directions, and wind speed, the exposure at ground level from this cloud will reach a maximum; at closer distances, the cloud has not diffused to ground level and at greater distances, the horizontal diffusion dominates to reduce the exposure below the maximum. The estimated exposure at ground level directly downwind from an explosion cloud can be calculated from Equation 2-13 which has been adapted from Reference 30:

$$E = \frac{\sigma_{XI}\,\sigma_{YI}\,\sigma_{ZI}}{\sigma_{XI}\,\sigma_{YI}\,\sigma_{ZI} + V_I} \times \frac{Q}{\pi\,\sigma_{YI}\,\sigma_{ZI}\,\bar{u}} \exp\left\{\frac{-h^2}{2\,\sigma_{ZI}^2}\right\} \qquad (2\text{-}13)$$

where

E = exposure ($g \cdot sec/m^3$)

σ_{XI} = standard deviation of the distribution of material in the cloud in the horizontal downwind direction (m)

σ_{YI} = standard deviation of the distribution of material in the cloud in the horizontal crosswind direction (m)

σ_{ZI} = standard deviation of the distribution of material in the cloud in the vertical direction (m)

V_I = volume of the initial cloud, i.e., at stabilization (m^3)

Q = total mass of the material of concern in the cloud (gm)

$\bar{u}$ = average wind speed (m/sec)

h = height of point of release, i.e., height to center of the initial cloud (m).

The standard deviations in Equation 2-13 are functions of the meteorological conditions and the distance of travel of the cloud. An unstable atmosphere has a relatively large amount of vertical mixing. Such a condition results in relatively high ground level concentrations downwind and also is less likely to duct airblast. Therefore, an unstable atmosphere is not only a conservative assumption from an air pollution standpoint but is also the most likely condition when detonating a large charge of explosive.

Figure 2-22 shows recommended values of the standard deviations for cloud diffusion in an unstable atmosphere for instantaneous puffs, such as explosion clouds. Based on these values and the values for cloud height

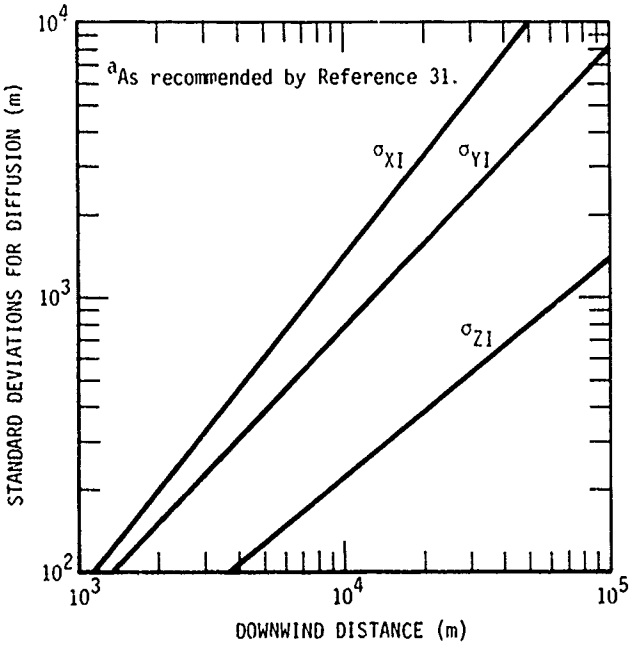

Figure 2-22. Standard deviations for diffusion parameters of instantaneous puff in unstable atmosphere.[a]

(from Equation 2-10) and for initial cloud volume (Equation 2-12), normalized calculations of exposure are shown in Figure 2-23 for some charge sizes of interest.

When the maximum values from Figure 2-23 are plotted against the TNT-equivalent weight of the explosive charge on log-log graph paper, they form straight lines, as shown in Figure 2-24. As this useful figure indicates, the maximum normalized ground level exposure (i.e., the ground level exposure for a unit mass of material in the cloud and a 1-m/sec wind) decreases with increasing charge size and occurs further downwind. The actual maximum exposure depends on the initial amount of material of interest in the cloud, the wind speed assumed, and the exposure time interval chosen.

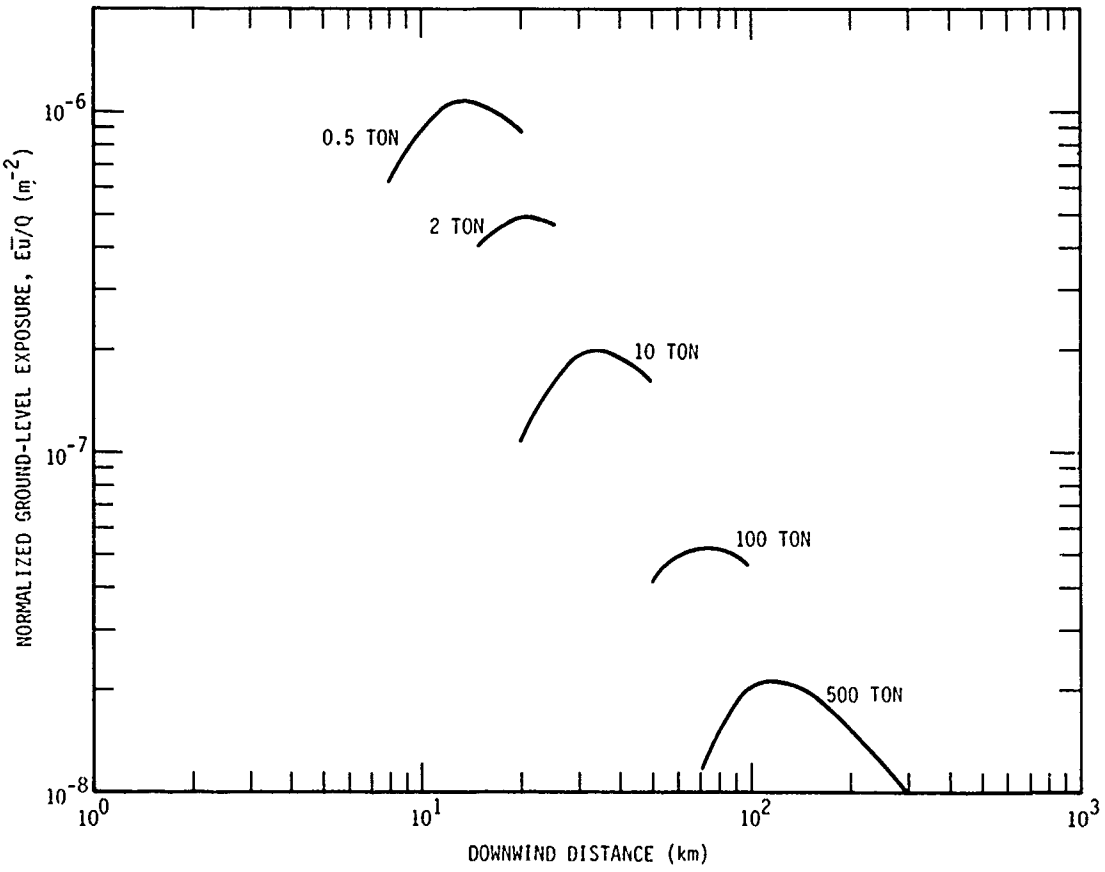

Figure 2-23. Normalized ground level cloud concentrations for unstable atmosphere.

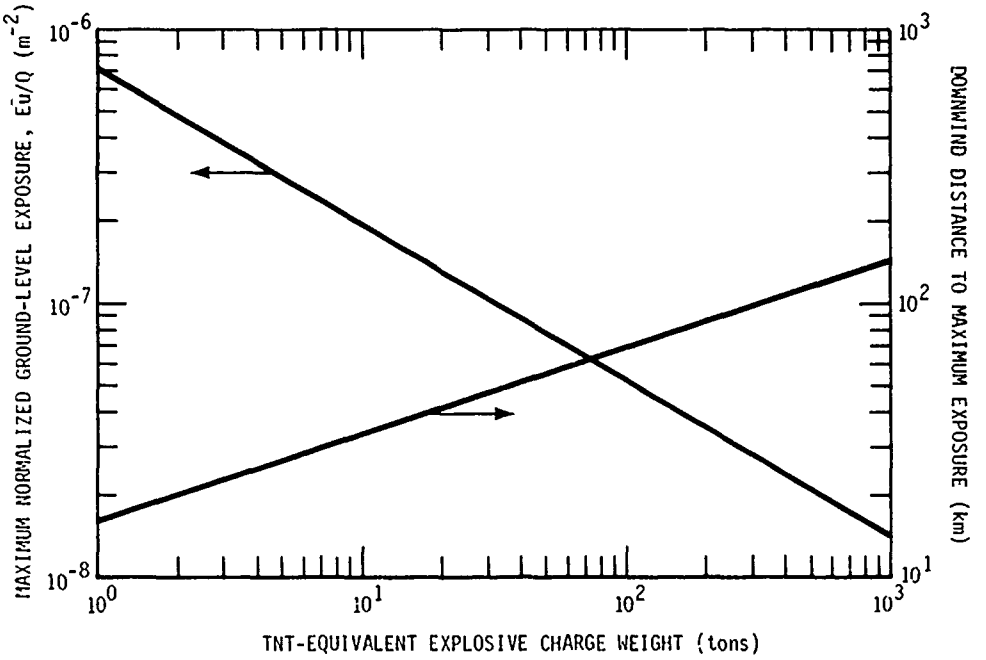

Figure 2-24. Maximum normalized ground level exposure (magnitude and distance) for unstable atmosphere.

SECTION 3

ENVIRONMENTAL EFFECTS OF EXPLOSIONS

This section describes in detail the effects of explosions phenomena on the natural physical and biological environments and on humans and the socioeconomic environment. The environmental effects are discussed in the same order as the discussion of phenomena in Section 2, viz., airblast and noise; craters, ejecta, and missiles; ground shock; and explosive products and dust. Damage distances or criteria are summarized as appropriate.

AIRBLAST AND NOISE

Although many of the phenomena from a large explosion are spectacular, airblast typically determines the limits of the environmental damage. Not only can strong airblast cause environmental damage at distances where the effects of the other phenomena are not significant, but low-pressure airblast can break windows and cause excessive noise at great distances from the explosion. The environmental effects of airblast and noise are discussed in detail in this subsection.

Close-In Effects on Animals and Humans

Most studies of airblast effects on animals (and humans) have been concerned with lethality rather than threshold damage. Consequently, it is difficult to draw firm conclusions as to the levels of airblast that might injure wild animals to the extent that they might die from inability to obtain food and water or to avoid predators. Animals can be injured directly by airblast (primarily eardrum and lung injuries), or indirectly from tumbling and impact or being struck by objects propelled by the airblast.

DIRECT AIRBLAST EFFECTS. Reference 32 summarizes the results of numerous experiments conducted on "large" and "small" mammals to determine lethality levels from direct effects of airblast. The surprisingly simple conclusion from these experiments (for the relatively long-duration blast waves from a large charge of HE) is that the "small" animals (all rodents or rodent-like animals such as mice, rats, hamsters, guinea pigs, and rabbits), that have a relatively low ratio of lung capacity to body weight, suffered 50-percent lethality at an average peak overpressure of 33 psi (227 kPa). The "large" animals (none of which were rodents), or those with a relatively high ratio of lung capacity to body weight (which would include man), suffered 50-percent lethality at an average peak overpressure of 61 psi (420 kPa). From the statistical standard deviations in the table on Figure 3-1, 2-percent lethality corresponds to overpressures of 46 psi (317 kPa) for the "large" animals and 28 psi (193 kPa) for the "small" animals. Animals exposed to lower overpressures will not be immediately

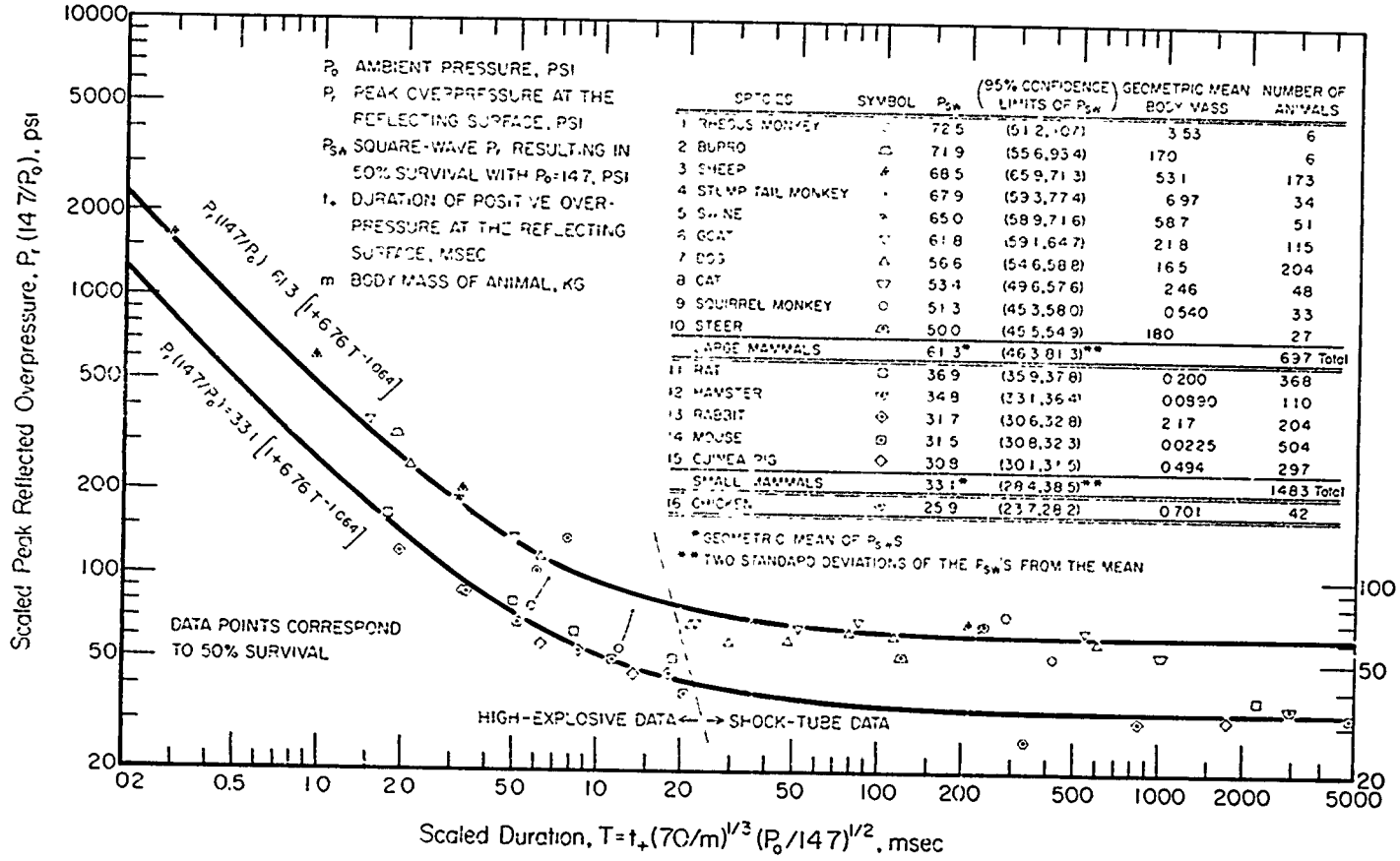

	SPECIES	SYMBOL	P_{SW}	(95% CONFIDENCE) LIMITS OF P_{SW}	GEOMETRIC MEAN BODY MASS	NUMBER OF ANIMALS
1	RHESUS MONKEY		72.5	(51.2, 103)	3.53	6
2	BURRO		71.9	(55.6, 95.4)	170	6
3	SHEEP		68.5	(65.9, 71.3)	53.1	173
4	STUMP TAIL MONKEY		67.9	(59.3, 77.4)	6.97	34
5	SWINE		65.0	(58.9, 71.6)	58.7	51
6	GOAT		61.8	(59.1, 64.7)	21.8	115
7	DOG		56.6	(54.6, 58.8)	16.5	204
8	CAT		53.4	(49.6, 57.6)	2.46	48
9	SQUIRREL MONKEY		51.3	(45.3, 58.0)	0.540	33
10	STEER		50.0	(45.5, 54.9)	180	27
	LARGE MAMMALS		61.3*	(46.3, 81.3)**		697 Total
11	RAT		36.9	(35.9, 37.8)	0.200	368
12	HAMSTER		34.8	(33.1, 36.4)	0.0990	110
13	RABBIT		31.7	(30.6, 32.8)	2.17	204
14	MOUSE		31.5	(30.8, 32.3)	0.0225	504
15	GUINEA PIG		30.8	(30.1, 31.5)	0.494	297
	SMALL MAMMALS		33.1*	(28.4, 38.5)**		1483 Total
16	CHICKEN		25.9	(23.7, 28.2)	0.701	42

*GEOMETRIC MEAN OF P_{SW}S
**TWO STANDARD DEVIATIONS OF THE P_{SW}'S FROM THE MEAN

Figure 3-1. Scaled peak reflected overpressures and scaled durations for "sharp-rising" blast waves which result in 50-percent mortality. (The curves are computed for a hypothetical average large and small mammal.) (Source: Reference 32)

killed by the direct effects of airblast, but may be injured to the extent that they subsequently die of other causes. The threshold for lung damage is roughly a factor of 5 less than the 50-percent lethality level (Reference 32), i.e., 45 kPa for rodents and 85 kPa for "large" animals.

The above statistics correlate with experiments on birds (Reference 33) where pigeons in flight were not injured by peak overpressures of less than 12 psi (83 kPa). Figure 3-2 summarizes the experiments of Reference 33, from which it can be shown that the threshold of injuries to birds in flight is estimated to be between 35 and 70 kPa, with 50-percent mortality at 140-kPa overpressure levels.

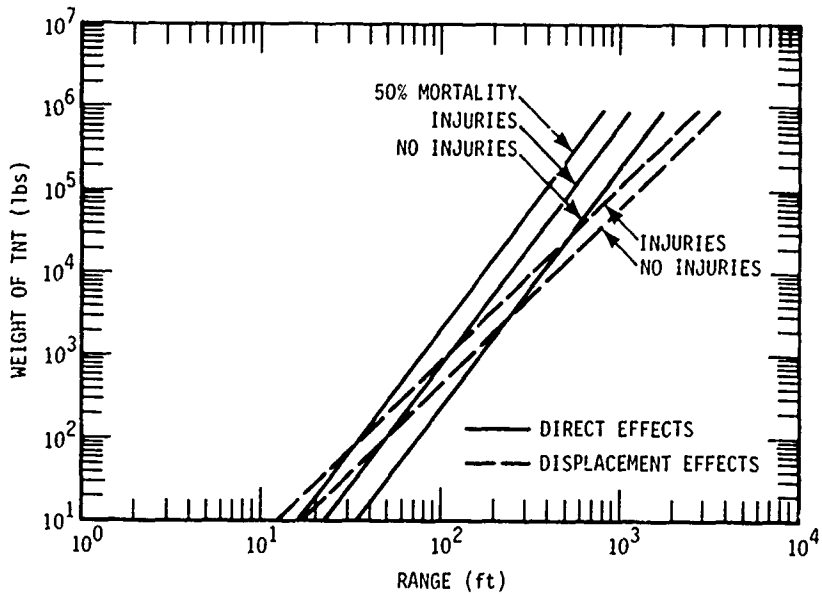

Figure 3-2. Biological criteria for birds exposed to airblast (surface burst at sea level). (Source: Reference 33)

The threshold for rupture of the human eardrum (and eardrums of dogs) is approximately 20 to 35 kPa, and an overpressure of approximately 100 kPa can be expected to rupture 50 percent of the exposed human eardrums (References 34 and 35). However, tolerance within and among species varies widely. Experiments with sheep and goats showed no eardrum ruptures for sheep at overpressures of 70 kPa, while goats suffered 55-percent eardrum ruptures at that level (Reference 35).

INDIRECT AIRBLAST EFFECTS. The ranges of injury or lethality due to direct effects of airblast are applicable for evaluating safe distances for birds in flight or animals in burrows. However for animals on the ground,

the primary mechanism of airblast damage is by tumbling or by being impacted with missiles propelled by the blast.

The 50-percent probability of lethality to small animals occurs with impacts on hard surfaces at velocities of approximately 30 to 45 ft/sec (Reference 36). (The 50-percent lethality values for these experiments were 39.4 ft/sec for mice, 43.5 ft/sec for rats, 31 ft/sec for guinea pigs, and 31.7 ft/sec for rabbits.) Statistical analysis indicated the 1-percent mortality level from impact occurs at velocities of 25 to 32 ft/sec. Based on analysis of suicide attempts by humans jumping from heights, the 50-percent lethality for humans is estimated to occur at impact velocities of approximately 54 ft/sec, and the 1-percent mortality is estimated to occur at impact velocities of roughly 20 ft/sec, with the mortalities of large animals, such as pigs and dogs, occurring at higher impact velocities (Reference 37). Experiments with dogs indicated 50-percent lethality at impact velocities of 64 ft/sec (Reference 37).

Potentially lethal velocities can be related to airblast overpressure through the acceleration coefficient of the animal. The acceleration coefficient is related to the total weight of the animal, with heavier animals having lower acceleration coefficients. References 38 and 39 give broadside acceleration coefficients for mice, rats, guinea pigs, and rabbits of approximately 0.4, 0.2, 0.15, and 0.08 ft^2/lb, respectively. For a 50-pound, four-legged animal, extrapolation of the small animal data indicates an acceleration coefficient of approximately 0.04 ft^2/lb when facing the blast and approximately 0.02 ft^2/lb when sideways to the blast.

Reference 40 relates acceleration coefficients and maximum velocities to peak overpressures from a 500-ton HE burst on the ground surface. Table 3-1 summarizes the above information and indicates that 1-percent lethality due to impact against hard surfaces can be expected for overpressures varying from about 20 kPa for a small animal such as a mouse to greater than 55 kPa for a 50-pound animal, and 50-percent lethality can be expected for overpressures varying from 28 kPa for a mouse to greater than 140 kPa for a 50-pound animal. For a man facing the blast, 1-percent and 50-percent lethality occur at peak overpressures of 50 and 110 kPa, respectively. The experimental results for birds, summarized in Figure 3-2, indicate that the threshold of injury for birds impacting against a hard surface occurs for weights of TNT that correspond to peak overpressures of approximately 14 kPa.

Summarizing Table 3-1, at distances where peak overpressure is less than 20 kPa (3 psi), few--if any--animals should be killed by translation and impact due to airblast. At distances where peak overpressures vary from 20 to 40 kPa (3 to 6 psi), some of the small animals in the open can be expected to be killed by translation and impact. At closer distances, fatalities of any larger animals can occur, with the probability of fatality increasing rapidly at distances where the peak overpressure is greater than 70 kPa (10 psi).

Table 3-1. Summary of estimates of lethality due to translation by airblast and impact against a hard surface (at peak velocity).

Species	Acceleration Coefficient (ft^2/lb)	1% Lethality			50% Lethality		
		Peak Velocity (ft/sec)	Peak Overpressure (kPa)[a]	Distance from 500-ton Yield (m)	Peak Velocity (ft/sec)	Peak Overpressure (kPa)[a]	Distance from 500-ton Yield (m)
Mouse	0.4	27	20	610	40	28	520
Rat	0.2	32	28	520	43	35-40	425
Guinea Pig	0.15	25	28	520	31	35	460
Rabbit	0.08	27	40	400	32	50	365
50-pound Animal	0.04	>20	>55	<335	>54	>140	<215
Man (side facing blast)	0.02	20	100	240	54	350	140
Man (facing blast)	0.05	20	50	365	54	110	240

[a]For 500-ton yield. Somewhat higher overpressures are required for smaller explosive yields.

Small stones and other objects that are picked up by the airblast can be propelled at sufficient velocities to injure or kill animals they strike. However, the range at which injuries due to airblast-translated missiles (not missiles propelled from the crater, which are discussed elsewhere) can occur is generally within the lethal range of translation and impact by airblast. For example, a 4-ounce stone with a typical acceleration coefficient of 0.07 ft/sec^2 (Reference 38) can be picked up and achieve a peak velocity of 25 to 30 ft/sec during translation (which is the threshold of lethality due to tumbling and impact) at distances where the airblast peak overpressure is roughly 50 kPa. However, it is likely that a higher velocity would be required to produce a lethal wound; for example, Reference 40 indicates that momentums greater than 100 ft-lb/sec are required to produce skull fracture in humans (e.g., 400 ft/sec for 1/4-pound objects). Reference 41 predicts approximately one skin penetration to a human behind a window exposed to 7 kPa peak overpressure, but no penetrations of the body wall are predicted for overpressures less than about 40 kPa.

In summary, the primary damage mechanism to animals on the ground and in the open can be expected to be from translation by airblast and subsequent impact. Animals in burrows and birds in flight at close ranges can be injured by direct airblast effects. Serious injury or death from airblast-induced missiles is not likely to occur beyond the distances where translation and impact is the primary damage mechanism.

Close-In Effects on Vegetation

Reference 42 summarizes the predicted effects of airblast on trees, based on theoretical and empirical data. Damage to trees, expressed as the percent of trees downed, is a function of type and class of tree, height of tree (for conifers), and type of site. Figure 3-3 summarizes the information in Reference 42 for explosive yields of from 50 to 600 tons. Most HE tests are conducted at arid or semiarid sites where trees, if any, have sparse foliage and extensive root systems. Under such circumstances, few trees should be downed at peak overpressures less than 5 to 10 psi (35 to 70 kPa) from a 500-ton burst, i.e., beyond about 300 to 400 meters.

Tree limbs and smaller vegetation can be expected to be broken at lower overpressures than indicated in Figure 3-3. The vegetation found in the semiarid areas usually selected for HE tests typically have few leaves and extensive root systems and are adapted to high desert winds, and thus are quite resistant to damage by airblast. The winds accompanying an ideal airblast wave of 1-, 2-, and 3-psi peak overpressure correspond to very short-duration wind gusts of approximately 35, 70, and 100 mph. Therefore, little damage to vegetation is expected for peak overpressures less than about 3 psi (20 kPa).

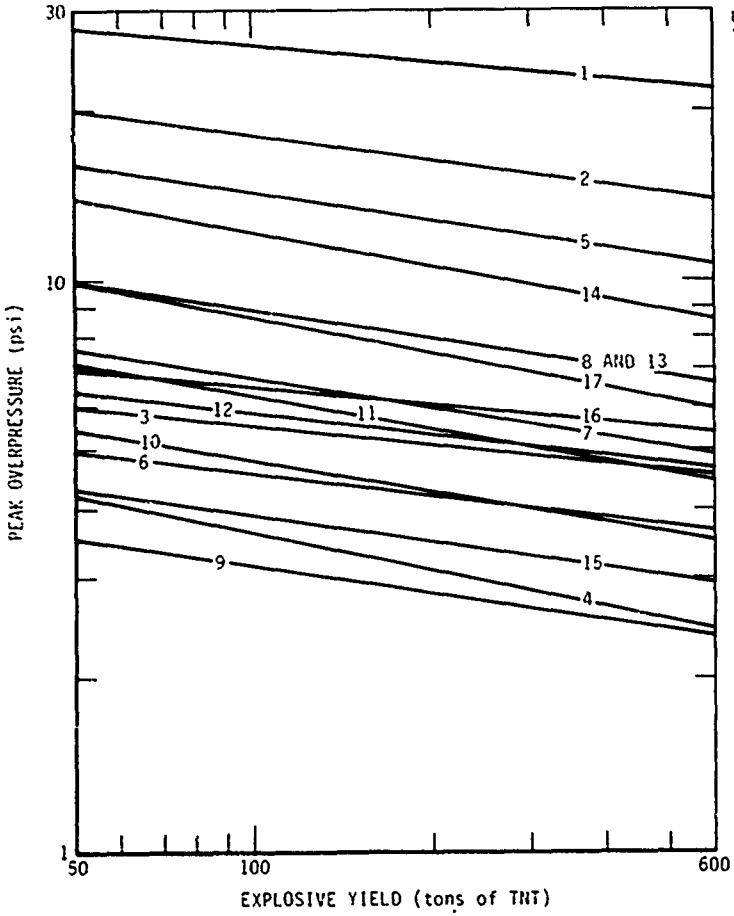

LEGEND.

	Type	Class	Height (feet)	Site*
1	Broadleaf	Small leaves or light crown (birch, poplar, scarlet oak)		Poor
2	Broadleaf	Small leaves or light crown (birch, poplar, scarlet oak)		Good
3	Broadleaf	Large leaves or heavy crown (beech, maple, hickory, sycamore)		Poor
4	Broadleaf	Large leaves or heavy crown (beech, maple, hickory, sycamore)		Good
5	Broadleaf	Defoliated		Average
6	Conifer	Light crown (spruce, cedar, hemlock, larch)	40	Poor
7	Conifer	Light crown (spruce, cedar, hemlock, larch)	80	Poor
8	Conifer	Light crown (spruce, cedar, hemlock, larch)	120	Poor
9	Conifer	Light crown (spruce, cedar, hemlock, larch)	40	Good
10	Conifer	Light crown (spruce, cedar, hemlock, larch)	80	Good
11	Conifer	Light crown (spruce, cedar, hemlock, larch)	120	Good
12	Conifer	Heavy crown (pine, fir)	40	Poor
13	Conifer	Heavy crown (pine, fir)	80	Poor
14	Conifer	Heavy crown (pine, fir)	120	Poor
15	Conifer	Heavy crown (pine, fir)	40	Good
16	Conifer	Heavy crown (pine, fir)	80	Good
17	Conifer	Heavy crown (pine, fir)	120	Good

*Good site has adequate rainfall, etc., which does not promote a deep root structure while poor site has lack of rain, rocks, etc., which promote a deep root structure with great holding power.

Figure 3-3. Ten-percent tree blowdown as function of explosive yield and overpressure. (Based on Reference 42)

Close-In Effects on Structures

Field tests are usually conducted in isolated areas with few, if any, manmade structures in the nearby vicinity, except those that pertain to the test. Also, many of the structures in field test areas (e.g., utility lines, fences) lack the broad surfaces that are most vulnerable at relatively low peak overpressures; such types of structures are typically not damaged by overpressures less than at least several tens of kPa from a large HE burst. Glasstone (Reference 43) shows damage/distance relationships for various types of structures exposed to nuclear explosions. These nomographs indicate that wood-frame buildings typically are badly damaged at lower overpressures than are bridges, vehicles, utility lines, or other types of buildings. A wood-frame house exposed to airblast peak overpressure of about 10 kPa will require major repairs. This conclusion is substantiated by References 44 and 45.

Reference 44 indicates that interior partitions of wood-frame buildings begin to fail at about 7 kPa and exterior walls begin to fail at about 10 kPa. Major reconstruction is required after exposure to overpressures greater than 10 kPa. Reference 44 also indicates that most light walls of other types of buildings will withstand peak overpressures less than about 7 kPa and damage will be primarily limited to windows, doors, shingles, etc.

Damage to houses exposed to nuclear and HE field tests is summarized in Reference 45. In these tests, 11 houses (mostly two-story, wood-frame) were exposed to peak overpressures between 1.1 and 2 psi (7.6 and 14 kPa). At 7.6 kPa, damage was cosmetic in nature, while above about 9 kPa most of the houses suffered damage to the frames of the walls and roofs. Damage could be expressed by the following relationship:

$$\text{percent damage} = 0.133\ (\text{peak overpressure in kPa})^{1.8}\ ; \qquad (3\text{-}1)$$

e.g., at 6.8, 10.3, and 13.8 kPa (1, 1.5, and 2 psi), a house will suffer about 4-, 9-, and 15-percent damage, respectively.*

As described by Glasstone (Reference 43), mobile homes in past field tests have suffered only light damage at 7-kPa overpressures. At 12-kPa overpressure, damage has been more significant but, on the whole, not of a serious nature.

---

* Unfortunately, Reference 45 relates damage to new construction costs, rather than repair costs; i.e., each component of the house was given a cost equivalent to its material and labor for original installation. Percent of damage is given as the sum of these incremental material and labor costs for each damaged item divided by the total cost for building the house. Labor for repair would be expected to be greater than labor for new construction.

In summary, the structural integrity of most structures is not threatened by overpressures less than 10 kPa. At higher overpressures, damage to most types of buildings increases rapidly. Seven kPa is about the threshold of failure for light exterior walls and interior partitions of buildings. Below 7 kPa, damage is limited to sensitive features of buildings such as windows and plaster.

Explosives Safety Standards

Department of Defense (DOD) Directive 5154.4S, DOD Ammunition and Explosives Safety Standards, establishes uniform safety standards and policy for ammunition and explosives. DOD HE field tests must be conducted in accordance with this directive. This directive requires certain separation distances between explosives and buildings, vehicles, and areas that might be inhabited. The regulations are detailed but can be summarized for the purposes of an environmental impact study as follows:

1. Military or nonmilitary buildings that might be inhabited must be separated from explosives at a distance that corresponds to an airblast peak overpressure of no more than 1.2 psi (8.3 kPa)
2. Areas that people might inhabit in the open or in ground vehicles must be separated from explosives at a distance that corresponds to an airblast peak overpressure of no more than 2.4 psi (16.5 kPa).

Greater separation distances are required where shrapnel might be the dominating hazard, but this is of concern only for smaller amounts of explosives than are generally used in HE field tests.

Distant Airblast and Noise

The preceding statistics show that damage to animals and vegetation is unlikely beyond about 600 meters from the explosion of 500 tons of TNT, and significant damage to structures is limited to buildings within about 1,300 meters of the explosion. Since most field tests are at remote and relatively barren sites, environmental impact from close-in effects of airblast is usually not significant. The primary concern in most HE field tests is the potential for causing "nuisance damage" to buildings (cracking of windows, plaster, and other brittle surfaces) and excessive noise in population centers at long distances from the field test site, particularly if meteorological conditions are not favorable. Even under normal meteorological conditions, a large-yield explosion can cause damage tens of miles distant. Even a charge as small as 1 pound exploded under a temperature inversion can cause nuisance damage in a population center more than a mile (1.6 kilometers) distant and cause noise complaints out to nearly 2 miles (3.2 kilometers) (Reference 46).

EFFECTS ON STRUCTURES. Window glass failure can occur at a lower overpressure level than any other type of structural material. An earlier Bureau of Mines report, based on small-charge data, recommended a "safe" airblast overpressure level of 0.5 psi (3.5 kPa) (Reference 47). Nuclear test experience indicates, however, that the approximate threshold of window glass breakage is 150 Pa (0.02 psi) peak incident overpressure. Sonic boom studies indicate that although windows can be broken at incident overpressures less than 150 Pa, the probability of breakage is very small (less than approximately one in a million) (Reference 48). Subsequent analysis indicates that windows can be broken at extremely low overpressures, but with a small probability, depending on such factors as the quality of the glass and the mounting of the panes. Although properly-mounted, good-quality glass is quite resistant to breakage, flawed or stressed window glass is easily broken. For example, laboratory tests with shock waves and field experiments with sonic booms required overpressure levels above 1 kPa to break windows (References 49 and 50). On the other hand, studies of sonic boom effects show that overpressure levels below 100 Pa can break significant numbers of glass panes of greenhouses, which are often of low strength and flawed or stressed (Reference 51).

Reed has continued to work extensively in the field of distant airblast phenomena and damage assessment and has developed a relationship between pressure and window damage that seems to fit the available data for both relatively high and low overpressures (Reference 1). The relationship is based on the assumption that the logarithms of the deviations from the mean value are normally distributed, i.e., the probability of damage can be determined from integration of a log-normal statistical distribution. Using the values recommended by Reed, a mean value of an incident peak overpressure value of 7.5 kPa (i.e., on the average, 7.5 kPa can be expected to break 50 percent of exposed windows) and a log-normal standard deviation of 2.5, the probability function takes the form of the expression:

$$\frac{1}{\sqrt{2\pi}} \exp - \frac{1}{2} \left[\frac{\ell n\ \Delta p - \ell n\ 7.5}{\ell n\ 2.5} \right]^2 \qquad (3\text{-}2)$$

where Δp is the incident peak overpressure in kPa. The term in brackets corresponds to the variable used to compute probabilities under a Gaussian statistical distribution. By applying Equation 3-2 to statistical tables for Gaussian distributions, the relationship between recorded peak overpressures and the probability of breaking a single randomly-chosen window is as shown in Figure 3-4. Figure 3-4 predicts about one window in 1,000 will be broken by an incident overpressure of 400 Pa and about one window in a million will be broken by an incident overpressure of 100 Pa.

These values are more conservative than some damage estimates for sonic booms; Reference 52 indicates that less than one window in 10 million can be expected to be broken by sonic boom overpressures of 125 kPa, and Reference 53 indicates that approximately one window in 100 million might be broken by an overpressure of 125 kPa.

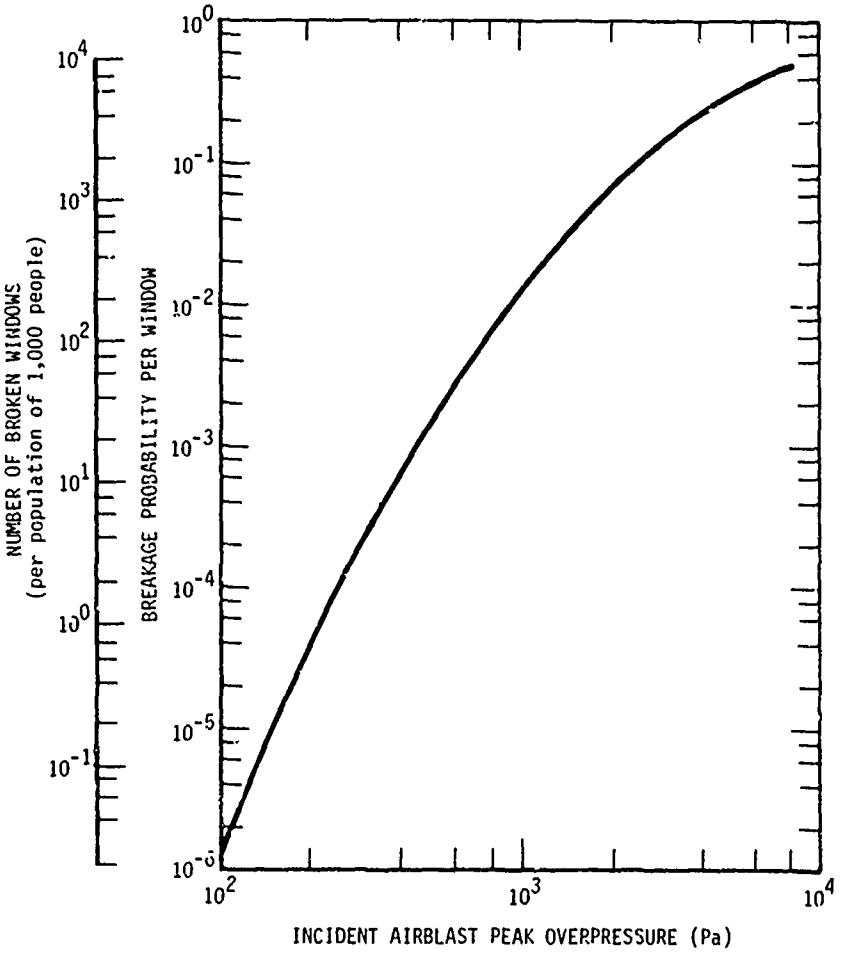

Figure 3-4. Window damage as a function of airblast overpressure. (Based on Reference 1)

The best estimate of the number of window panes per capita in an urban area is an average of 19 panes per person, based on a survey of San Antonio, Texas, in 1963 following an accidental explosion of 57 tons of HE at the Median Base which broke over 3,000 windows in the city. Based on this estimate, the extreme left-hand scale of Figure 3-4 estimates the number of broken windows (per human population of 1,000) that can be expected in a population center at any given magnitude of incident airblast peak overpressure. An overpressure of a few hundred Pa can cause a very large amount of window damage in urban and suburban areas, which may have population densities of thousands or tens of thousands of people per square mile.

Quantitative data on distant airblast magnitudes that can damage historic buildings, archaeological features, and significant natural physical

features or that could cause rock or snow slides are sparse. Most such information comes from sonic boom experiments and analyses and is summarized in References 51 and 54. The consensus is that the nominal sonic boom peak overpressure magnitude of 100 to 200 Pa is only one of the sources of vibration that contributes to the "ageing" of a structure (or a natural feature) to the point where damage might occur.

As shown in Section 2, airblast in excess of 100- to 200-Pa peak overpressure can occur over very large areas, hundreds or thousands of square miles of area in the case of a large-yield explosion. Lower overpressures are comparable with close thunder (135 dB or 100 Pa) (Reference 55). While it is very unlikely any significant natural or historical feature would be directly damaged by airblast peak overpressures of a few hundred Pa, the possibility cannot be ruled out. Following exposure to numerous sonic booms, overhanging cliffs fell at Canyon de Chelly National Monument, damaging cliff dwellings, and 10 to 15 tons of earth and rock fell near one of the main trails through the rock formations at Bryce Canyon National Park (Reference 54).

The threshold for possible flight hazard to light aircraft and helicopters is approximately 1.4 kPa (0.2 psi) (Reference 1).

EFFECTS ON HUMANS AND ANIMALS. Much of the information on the effects of impulsive noise on humans and other animals comes from studies of sonic booms, which typically have peak overpressure magnitudes of 100 to 200 Pa. Although there have been numerous claims of adverse effects on domesticated animals from sonic booms, no controlled study has indicated any significant lasting adverse effects on wild or domesticated animals exposed to occasional sonic booms of 100- to 200-Pa magnitude. References 56, 57, and 58 summarize the pertinent studies. (A case of extensive hatching failure of Dry Tortugas Sooty Tern eggs was attributed to sonic boom, but the conclusions were based on supposition. Sonic booms in subsequent years did not significantly disturb the same nesting colony. According to Reference 58, the researcher has since concluded that simple disturbance by sonic booms was not an adequate explanation for the hatching failure.)

Although humans can be annoyed and startled by a typical sonic boom, there is no evidence of any significant lasting adverse effects. A transient degeneration in hearing at conversational frequencies and tinnitus, or "ringing," can be produced by an impulse sound level of 160 dB (2 kPa) (Reference 55). Based on past experience, a recorded peak-to-peak pressure amplitude of about 100 Pa (about 36 Pa peak incident overpressure) correlates fairly well with the thresholds of complaints by the public exposed to blast noise (Reference 46).

Data regarding the effects on living organisms exposed to occasional impulses of magnitudes above a few hundred Pa are not plentiful. Eggs exposed repeatedly to impulse levels of 3 kPa (0.44 psi) hatched normally and the hatched chicks were normal (Reference 56). No significant lasting

adverse effects were observed in humans exposed to a series of extremely high-level sonic booms (3 to 7 kPa, or up to 1 psi) (Reference 59). Although hearing acuity was not physically measured, the subjects reported no indication of any observable symptoms of hearing loss or other ear involvement. In this same experiment, no significant adverse effects on livestock were observed.

In summary, there is no firm evidence to indicate that occasional impulse sounds below the level that will produce physical damage to living organisms produce any lasting significant adverse effects.

NOISE STANDARDS. The Environmental Protection Agency (EPA) has judged that exposure to less than 145-dB (0.05-psi or 350-Pa) impulse noise no more than once per day is "acceptable" in that hearing damage will not result (Reference 60). The occupational limit for industrial workers is 140 dB (0.03 psi or 200 Pa) (Reference 61). These noise levels can be exceeded many miles away from a large-yield explosion.

Technically, distant blast noise qualifies as impulse noise because neither References 60 nor 61 make any allowance for rise time or frequency spectrum of the impulse. However, noise from distant explosions is predominantly low frequency, mostly below 10 Hz, against which the ear strongly discriminates. On the A-weighted scale, which approximates the relative response of the human ear to frequencies, the ear discriminates against a frequency of 10 Hz by about 70 dB. In other words, a 10-Hz frequency having a sound pressure level of 145 dB would be perceived by a listener as having a magnitude of approximately 70 dB less, i.e., 75 dB. Distant airblast may therefore have an unweighted sound pressure level that exceeds recommended limits of 140 or 145 dB, but which is of such low frequency that the ear discriminates against it to the extent that the noise level is not greatly disturbing to the average person and may not be perceived by some people. (Annoyance from low-frequency shock waves is often related to rattling of windows and other building components, rather than hearing the shock wave directly.)

The recommended limit of 145 dB to the general public is not a law. The Occupational Safety and Health Administration (OSHA) limit of 140 dB presumably applies to personnel at test sites, but was designed for industrial conditions where hearing loss can occur to workers repeatedly exposed to impulsive noise. Carried to the extreme, many actions involve noise levels that exceed the OSHA limit. For perspective, the ear of a person firing a handgun is exposed to sound pressure levels of from 140 to 170 dB, or nearly 7 kPa (Reference 60).

Damage Distances

Table 3-2 summarizes threshold levels for damage from airblast. In Figures 3-5 and 3-6, levels are overlaid on the graphs of airblast peak overpressures versus distance that were developed in Section 2 to

Table 3-2. Summary of airblast damage threshold levels.

Effect	Corresponding Incident Peak Overpressure Level
Threshold of lethality	
Small animals in the open	20 - 40 kPa
50-pound animal in the open	>55 kPa
Small animals (rabbits or smaller) in burrows	190 kPa[a]
Larger animals in burrows	320 kPa[a]
Threshold of lung damage to animals in burrows	
Small animals	45 kPa[a]
Large animals	85 kPa[a]
Threshold of eardrum rupture to animals in the open	20 - 35 kPa
Threshold of injury to birds in flight	35 - 70 kPa
Toppling of trees (small leaves or defoliated or light crowned)	35 - 70 kPa
Damage to small vegetation or tree branches	20 kPa
Damage to building walls/roofs	7 kPa
Skin penetrations from broken windows	3.5 kPa
Flight hazard to light aircraft	1.4 kPa
Window breakage (one window for each 1,000 of human population)	200 Pa
Impulsive noise level limit for industrial workers by Occupational Safety and Health Administration (OSHA)	140 dB (0.2 kPa)
Tinnitus or "ringing" of ears	160 dB (2 kPa)

[a]The peak overpressure levels shown are the levels that occur without reflections. Airblast filling a burrow can produce pressures that are 2 to 3 times these values and are sufficient to result in the effect that is described.

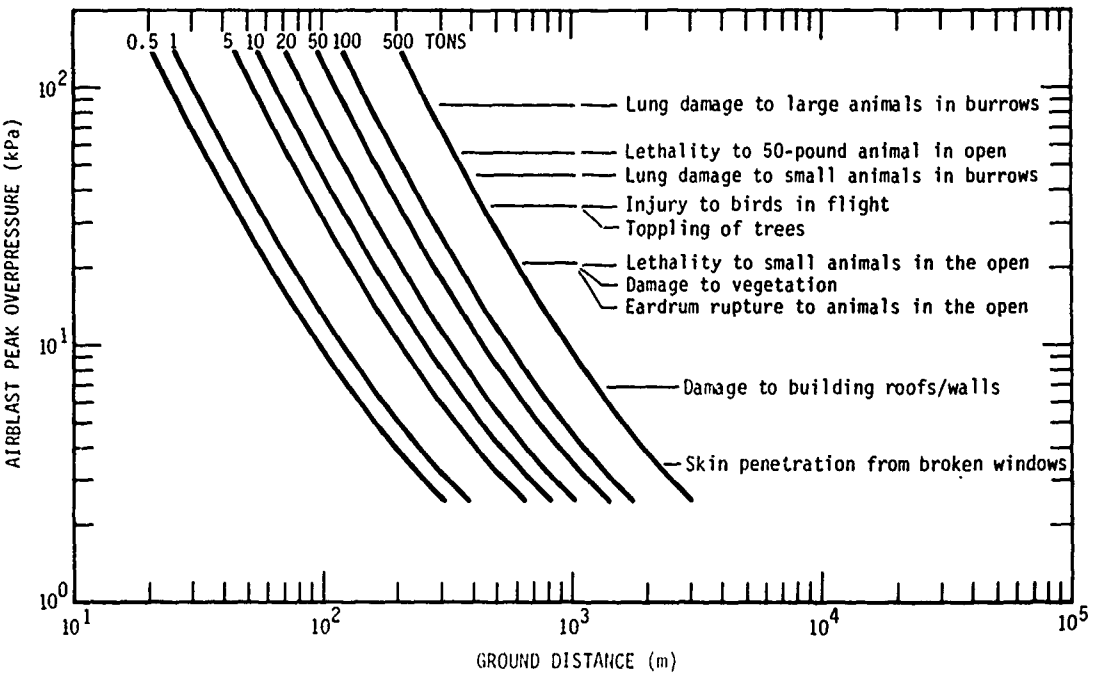

Figure 3-5. Threshold damage distances from close-in airblast.

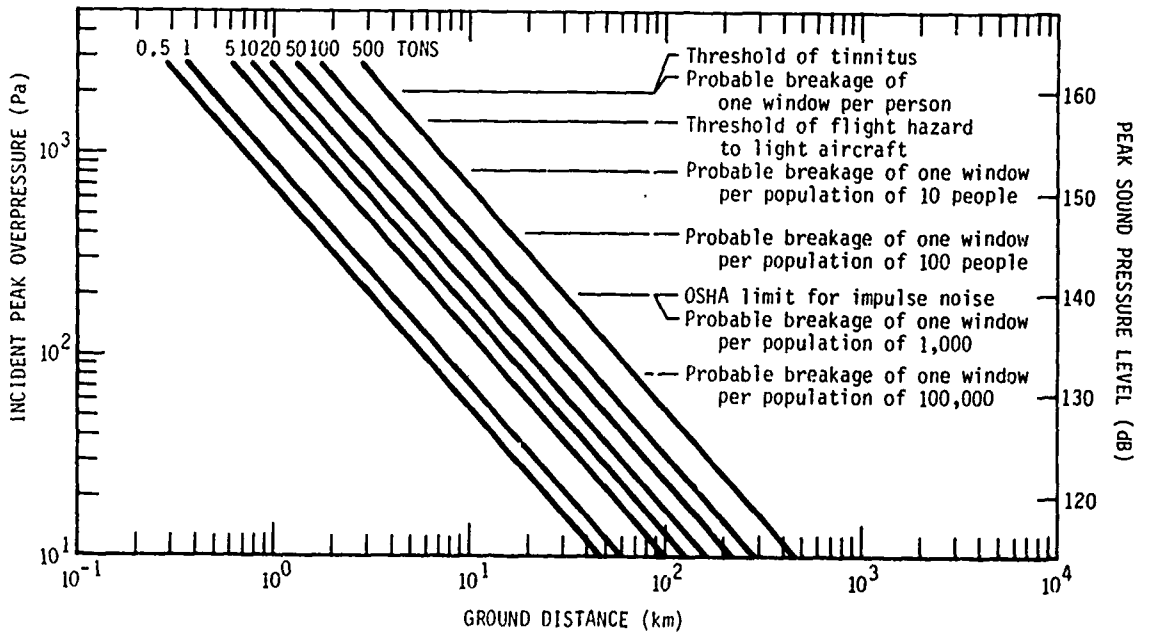

Figure 3-6. Damage distances from low-pressure airblast.

illustrate potentially significant damage distances. As can be seen in Figure 3-5, it is unlikely that animals will be killed or severely injured beyond about 600 meters from a 500-ton explosion. Damage to buildings (except architectural damage to windows, shingles, etc.) is unlikely beyond about 1,300 meters from such an explosion. Aircraft in flight, hearing of humans (and presumably animals), and windows can be adversely affected at great distances, as indicated in Figure 3-6 for a calm, nonrefracting atmosphere. For a charge exploded when gradient conditions exist, these criteria distances will be less than shown. If meteorological conditions that amplify airblast exist, however, criteria distances are increased approximately proportional to the increase in overpressure, e.g., if the overpressures should be double those shown in Figure 3-6 for nonrefracting conditions, criteria distances would also be approximately doubled.

CRATERS, EJECTA, AND MISSILES

The cleanup phase of an HE field test typically includes filling any explosive crater with the ejecta and other native earth materials. The final result is a small area of bare land that slowly returns to a natural state. Should the crater intersect the water table, it will cause some slight effect on the local hydrology, but such effects do not extend beyond a few crater radii.

For a 500-ton field test, the total land area covered by continuous ejecta from the crater typically amounts to approximately 10 acres. Since the airblast within this area is in excess of 100 psi (700 kPa), however, any damage that might have occurred from ejecta is dominated by destruction from the airblast. There is no environmental significance to the ejecta beyond the continuous range, except for the possibility of damage from missiles.

Missiles can be propelled very long distances, although, in fact, very few missiles have been found beyond 1 kilometer from GZ of previous field tests. Figure 3-7 can be used to estimate the hazard from missiles. As this figure indicates, a 500-ton HE charge could theoretically propel rock ejecta several kilometers. However, the odds are only 1 percent that a person standing in the open 600 meters from the charge would be struck by such a missile, and these odds would be even lower for striking an animal or other object smaller than a human. The corresponding airblast at 600 meters would be 20 kPa, which is the threshold of lethality to small animals and the threshold of eardrum rupture. Therefore, it can be assumed that airblast will again be the dominant damage mechanism.

GROUND SHOCK

Damage criteria for manmade structures, natural geological features, and animals and humans that are exposed to ground motions from explosions are developed in this subsection. The criteria are developed in considerable detail and in a conservative manner because of previous concern about

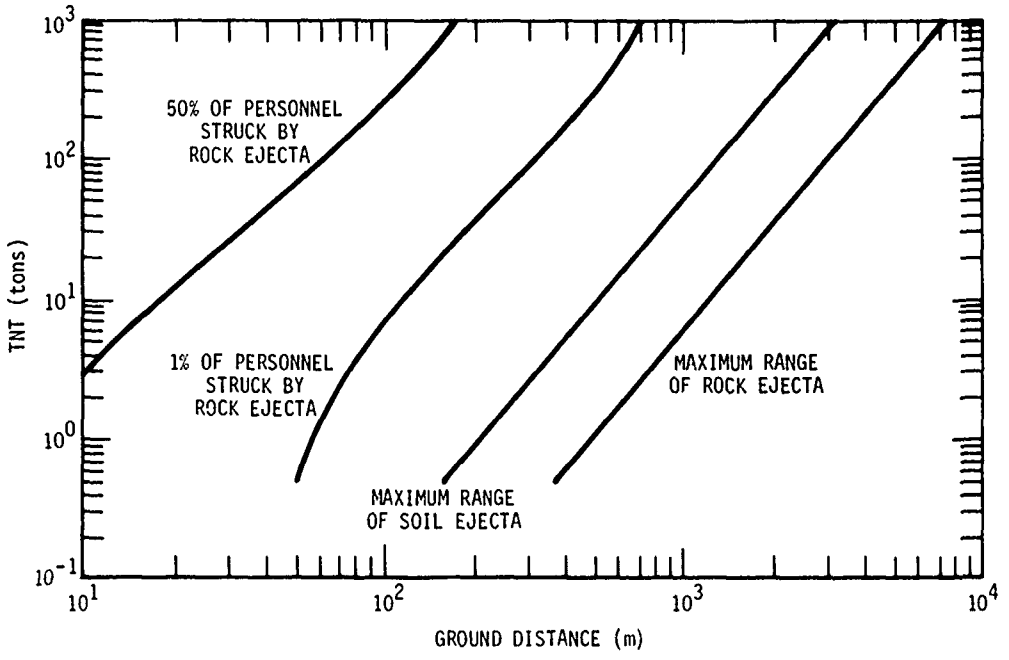

Figure 3-7. Damage-distance criteria for ejecta missiles. (Source: Reference 1)

effects of ground shock on such critical structures as dams and aqueducts. For situations where criteria have not been established, the potential for damage can be assessed by comparing the ground motions to those that commonly occur in the environment, such as ground motions from earthquakes or road traffic.

Earthquakes

GROUND MOTIONS FROM EARTHQUAKES. Intensity on the Modified Mercalli Scale (I_{MM}) is commonly used to describe the effects of an earthquake. On this scale of whole numbers from I to XII, the effects of earthquakes are described in narrative fashion. As can be seen from the abridged Modified Mercalli Scale in Table 3-3, slight damage to the most sensitive building elements occurs at an intensity of V and damage becomes more severe at greater intensities. (Intensity is a function of the distance from the earthquake epicenter, with intensity decreasing at greater distances.)

There have been various attempts to relate I_{MM} values to ground motion parameters. Three such relationships are given in Equations 3-3 through 3-5 below, from References 62 through 64, respectively:

$$\log a = I_{MM}/3 - 0.5 \qquad (3\text{-}3)$$

Table 3-3. Modified Mercalli Intensity Scale of 1931 (abridged).[a]

I.	Not felt except by a very few under especially favorable circumstances. (I Rossi-Forel Scale)
II.	Felt only by a few persons at rest, especially on upper floors of buildings. Delicately suspended objects may swing. (I to III Rossi-Forel Scale)
III.	Felt quite noticeably indoors, especially on upper floors of buildings, but many people do not recognize it as an earthquake. Standing motorcars may rock slightly. Vibration like passing truck. Duration estimated. (III Rossi-Forel Scale)
IV.	During the day, felt indoors by many; outdoors by few. At night, some awakened. Dishes, windows, and doors disturbed; walls make creaking sound. Sensation like heavy truck striking building. Standing motorcars rocked noticeably. (IV to V Rossi-Forel Scale)
V.	Felt by nearly everyone; many awakened. Some dishes, windows, etc. broken; a few instances of cracked plaster; unstable objects overturned. Disturbance of trees, poles, and other tall objects sometimes noticed. Pendulum clocks may stop. (V to VI Rossi-Forel Scale)
VI.	Felt by all; many frightened and run outdoors. Some heavy furniture moved; a few instances of fallen plaster or damaged chimneys. Damage slight. (VI to VI+ Rossi-Forel Scale)
VII.	Everybody runs outdoors. Damage negligible in buildings of good design and construction; slight to moderate in well-built ordinary structures; considerable in poorly-built or badly-designed structures. Some chimneys broken. Noticed by persons driving motorcars. (VIII Rossi-Forel Scale)
VIII.	Damage slight in specially-designed structures; considerable in ordinary substantial buildings, with partial collapse; great in poorly-built structures. Panel walls thrown out of frame structures. Fall of chimneys, factory stacks, columns, monuments, walls. Heavy furniture overturned. Sand and mud ejected in small amounts. Changes in well water. Persons driving motorcars disturbed. (VII+ to IX Rossi-Forel Scale)
IX.	Damage considerable in specially-designed structures; well-designed frame structures thrown out of plumb; great in substantial buildings, with partial collapse. Buildings shifted off foundations. Ground cracked conspicuously. Underground pipes broken. (IX+ Rossi-Forel Scale)
X.	Some well-built wooden structures destroyed; most masonry and frame structures destroyed with foundations; ground badly cracked. Rails bent. Landslides considerable from river banks and steep slopes. Shifted sand and mud. Water splashed (slopped) over banks. (X Rossi-Forel Scale)
XI.	Few, if any, structures (masonry) remain standing. Bridges destroyed. Broad fissures in ground. Underground pipelines completely out of service. Earth slumps and land slips in soft ground. Rails bent greatly.
XII.	Damage total. Waves seen on ground surfaces. Lines of sight and level distorted. Objects thrown upward into the air.

[a]Harry O. Wood and Frank Neuman, in Bulletin of the Seismological Society of America, Vol. 21, No. 4, December 1931.

$$I_{MM} = \log 14v / \log 2 \qquad (3\text{-}4)$$

$$\log a = 0.25\ I_{MM} + 0.25 \qquad (3\text{-}5)$$

where

a = peak particle acceleration in cm/sec^2 (except in Equation 3-5, it is the peak horizontal component)

v = peak particle velocity in cm/sec

I_{MM} = Modified Mercalli Scale values.

Based on Equations 3-3 through 3-5, earthquake-induced ground motion velocities of approximately 2 to 4 cm/sec and accelerations of 15 to 30 cm/sec^2 correspond to an I_{MM} value of V, the threshold of slight architectural damage.* One can be confident that ground motions of these magnitudes caused by chemical explosions will not cause significant damage because of their relatively short duration and higher frequency, compared to earthquakes.

INITIATION FROM EXPLOSIONS. There has been concern as to whether underground nuclear tests can initiate a natural earthquake that would have more energy and, thus, be more destructive than the ground motions from the explosion itself. In past underground nuclear tests at the Nevada Test Site (NTS), including explosions over 1,000 times larger than the largest HE tests, very few aftershocks have been found to originate beyond a distance of 20 kilometers (12.4 miles) from the explosion, according to the EIS for the NTS (Reference 66), which further states:

> The possibility of causing premature release of a large earthquake, with consequent destructive effects, cannot be absolutely ruled out, even though it appears very unlikely. A panel of scientists and engineers has recently examined this question and concluded, on the basis of test experience, that an explosion will not trigger a large earthquake (i.e., one releasing as much or more seismic energy than the explosion itself) unless the test is detonated near a fault on which an earthquake of this magnitude is imminent.

---

* Based on Reference 65, the ratio of a/v is approximately 5 to 11 for moderately strong earthquakes (magnitude 6.5) in soils. An average value of 8 is assumed to relate accelerations to velocity, i.e., a fundamental frequency of 1.3 Hz.

Based upon Reference 67, 600 tons of TNT buried and exploded in alluvium has a seismic magnitude of approximately 2.5. Experience with earthquakes in California indicates that a typical earthquake of this magnitude would be barely felt and would produce I_{MM} intensities of less than III at the epicenter (Reference 62), intensities that are not damaging to even the most sensitive manmade structures. Thus, initiation of a significant earthquake by a chemical explosion does not seem to be a credible possibility.

Effects on Buildings

Based on the results of a 10-year program to determine ground vibrations from blasting and their effects on structures, the U.S. Bureau of Mines established a criterion of 5 cm/sec for peak particle velocity ground motions to ensure no damage to residences (Reference 68). Vibrations from blasting cannot exceed a velocity vector magnitude of 5 cm/sec at any point in the ground near the foundation of a residence. As cited in Reference 68, earlier studies indicated that fine plaster cracks began to occur at ground motions from blasting of from 5 to 10 cm/sec.

Examination of Soviet Union blasting criteria in Table 3-4 indicates general agreement with the U.S. Bureau of Mines criterion for residences. In general, then, a safe blasting criterion to buildings and other structures is 3- to 5-cm/sec peak ground motion velocities, except perhaps for "large-panel buildings" where a criterion of 1.5 cm/sec is recommended based on Soviet experience. These criteria for transient ground motions from blasting are consistent with recommended limits to rotating machinery and machinery foundations of 2.5 cm/sec at steady-state frequencies below approximately 2,000 rpm (Reference 69).

These ground motion criteria of 1.5 to 5 cm/sec, or less, to assure no damage to buildings are met beyond relatively close distances from HE field tests, where damage from airblast predominates. For example, these criteria were met at distances beyond 700 to 1,500 meters from the 500-ton MIXED COMPANY III field test where the airblast peak overpressures of 14 to 5 kPa would have caused significant damage to buildings.

Initial experience with nuclear weapons testing seemed to indicate that a threshold for producing small cracks in plaster was approximately 20 cm/sec for newly-constructed residences and 10 cm/sec for older residences (References 70 and 71). The prevailing concept of a nuclear damage threshold between 5 and 10 cm/sec to structures, in conformance with experience from blasting with HE, was "rudely shattered" in 1964 by the SALMON nuclear test, a 5-KT underground test, when valid damage claims were received where it was certain that the ground motions were less than 5 cm/sec (Reference 72).

It now appears that there were at least three reasons why the SALMON nuclear test produced damage at considerably lower ground motion magnitudes than was expected, based on experience with HE and limited nuclear blast

Table 3-4. Soviet Union explosion-induced ground motion criteria.[a]

Structure	Maximum Permissible Ground Motion Velocities (cm/sec)
Brick buildings	5
Cinder-block buildings	3
Large-panel buildings	1.5
Large-block buildings	3
Brick buildings with suspended ceilings	3
Lightweight wooden buildings	5
Mine head work. with suspended panels	5
Reinforced concrete pipe	5
Brick pipe	3
Earthquake-proof buildings with a resistance of 7 on the S.V. Medvedev scale	10
Earthquake-proof buildings with a resistance of 8 on the S.V. Medvedev scale	15

[a]Mironov, P.S., Yu. P. Shchupletsov, and B.S. Pyatunin, "Seismic Vibrations During Explosions and Problems of Earthquake Safety of Buildings and Structures," a translation, Report FTD-HC-23-1571-77, Foreign Technology Division, Air Force Systems Command, U.S. Air Force, Wright-Patterson Air Force Base, Ohio, 20 June 1974.

experience. The SALMON ground shock motions were of long duration--on the order of 90 seconds (Reference 73); the longer a given magnitude of a ground motion persists, the greater will be the damage. Secondly, a given ground motion criterion level occurs at a greater distance from a typical nuclear explosion than would occur from a relatively small-yield chemical explosion. At greater distances, the higher frequency ground motions are more rapidly attenuated and lower frequencies predominate which are on the order of the fundamental frequencies of buildings and some other manmade structures. Thirdly, the SALMON test was conducted in the vicinity of several small towns where the relatively large number of structures provided a

sufficient data base to reveal that damage can occur at very small ground motion magnitudes, although with a low probability of occurrence. Due to settling and "ageing" of structures, some sensitive building members such as plaster or masonry walls become weakened and stressed to the point where an additional small stress is sufficient to cause failure.

Since the Bureau of Mines and Soviet Union criteria of 1.5 to 5 cm/sec are primarily based on HE charges that are very small compared to the multiton charges used in HE field tests, it is prudent to base damage predictions from such military field tests on experience with ground motions from nuclear explosions.

New damage criteria were developed from additional studies following the SALMON event and applied to structures in the vicinity of the 40-KT RULISON underground nuclear test. Table 3-5 summarizes the ground motion measurements in the towns near RULISON and Table 3-6 summarizes the resulting damage. Figures 3-8 and 3-9 are plots of the data in Tables 3-5 and 3-6 showing the frequency of credible complaints as a function of peak ground motion velocities and accelerations. Based on these data, 1 percent of the residences exposed to ground motions of approximately 20 cm/sec^2 peak acceleration will suffer slight architectural damage like fine cracks in plaster. Subsequent analysis has resulted in a criterion that ground motions from underground nuclear testing should not exceed a peak horizontal ground motion acceleration of 5 cm/sec^2 to preclude damage to unusually sensitive buildings and other structures (Reference 74). Assuming simple harmonic motion waves from large-yield HE charges (Reference 75), this criterion occurs at a horizontal peak particle velocity of approximately 0.13 cm/sec.

Based on Equations 3-3 through 3-5, 5 cm/sec^2 corresponds to an earthquake intensity of from approximately 1 to 3.5 on the Modified Mercalli Scale, which might be felt but which will not produce any physical damage to structures (see Table 3-3).

Effects on Other Structures and Natural Geologic Features

All other criteria for damage from ground motions are within the most conservative criteria of 5 cm/sec^2 or 0.13 cm/sec for "unusually sensitive structures," as given in Reference 74.

As shown in Table 3-4, Soviet Union blasting criteria for mine headworks with suspended panels and reinforced concrete pipe are 5 cm/sec, while the criterion for "brick pipe" is 3 cm/sec.

Based on surveys of structures in the vicinity of nuclear explosions, wells are relatively invulnerable to damage by ground shock. Reference 71 recommends a damage threshold of greater than 18 $W^{1/3}$ meters for cased holes in alluvium where the explosion is also in alluvium (W is the explosive yield in tons); e.g., for a 500-ton fully-contained explosion, cased wells in alluvium beyond 145 meters will not be damaged.

Table 3-5. Ground motion measurements near RULISON nuclear underground test. (Source: Reference 74)

Location	Slant Range (km)	Peak Vector Ground Motion		
		Acceleration (cm/sec^2)	Velocity (cm/sec)	Displacement (cm)
Grand Valley	10.6	540	8.27	0.236
Rifle				
Union Carbide	18.0	170	3.57	0.139
Church	20.2	94	3.13	0.106
Top of Hill	20.2	135	3.77	0.410
De Beque				
Station No. 1	22.8	100	2.20	0.099
Station No. 2	22.8	159	4.68	0.206
Collbran	18.8			
Silt (radial component	29.8	33	1.34	0.068

Table 3-6. Building count and damage data from RULISON ground motions (incomplete). (Source: Reference 74)

Location	Number of Buildings Exposed	Credible Damage Complaints	Percent of Buildings Damaged	Total Damage
Grand Valley	146	77	52.7	$15,044
Rifle	759	75	9.9	18,995
De Beque	102	6	5.9	1,320
Collbran	127	6	4.7	1,864
Silt	194	4	2.1	235

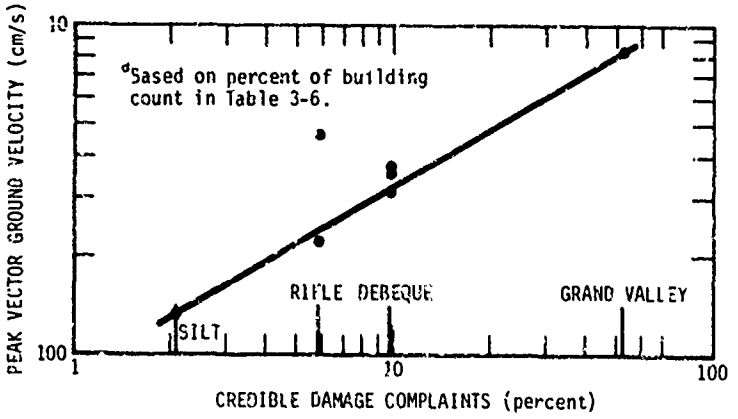

Figure 3-8. Credible damage complaints versus peak vector ground velocity.[a] (Source: Reference 74)

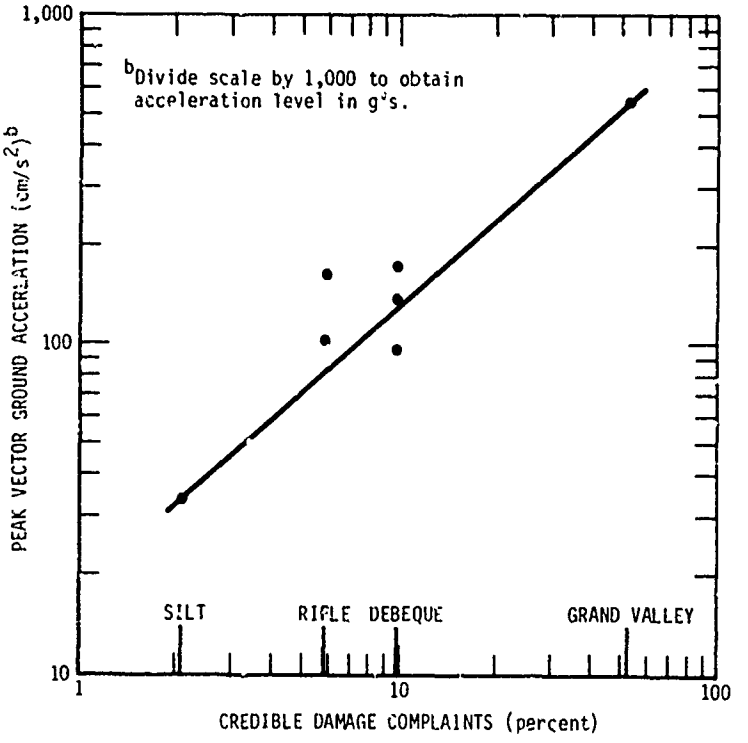

Figure 3-9. Credible damage complaints versus peak vector ground acceleration.[a] (Source: Reference 74)

Reference 71 does not give a threshold criterion for steel storage tanks but predicts severe damage to tanks of light construction at ground motions of 80 cm/sec. There was no damage to 10 small privately-owned water and fuel tanks located within 8 kilometers of the GNOME event, a 3-KT nuclear explosion fully contained in salt (Reference 71).

The threshold of structural damage to rigid-frame prefabricated buildings is in excess of 150 cm/sec, while the threshold of structural damage to small plywood buildings is 150 cm/sec (Reference 71). Instrumentated trailer vans on styrofoam pads have a damage threshold in excess of 300 cm/sec, while some types of light-wheeled heavily-loaded trailers suffer severe damage at 100 cm/sec. Other types are undamaged at greater ground motions (Reference 71). At 30 cm/sec, light objects can be thrown about (Reference 71).

A large number of 25-foot wooden utility poles erected in concrete bases at GZ of the GNOME event were undamaged (Reference 70). Two old 8-inch-diameter, guyed, 50-foot steel towers located approximately 300 meters from GZ of the BILBY event (a 200-KT fully-contained nuclear explosion) were undamaged although their foundations were cracked and the guy wires were slack (Reference 70). A light 200-foot, guyed communication antenna about 600 meters from GZ of the GNOME event was not damaged (Reference 70). A switching station 365 meters from the BILBY event suffered no significant damage to electrical equipment, the only damage being a slight twist to the angles on which the heavy equipment was mounted (Reference 70).

Reference 76 describes an HE test where a 1/4-scale model of a 24-inch-diameter pressurized pipeline was subjected to ground motions that should have been on the order of several g's. The pipeline was not significantly damaged.

Following the BILBY underground nuclear test, cracks in the 3-inch-thick asphalt paving on a 45-degree angle bunker slope were found to have opened up and the majority of the asphalt slid down 1 to 2 feet, where the ground motions were 735 cm/sec^2 and 70 cm/sec. Rock slides from RULISON were restricted to areas where the ground motion was in excess of 20 cm/sec^2. The few rock slides that did occur were small in size and were where rock slides occur several times a year (Reference 77).

Groundwater can be affected if the water table is confined by bedrock (either supported as in the case of a perched water table, or suppressed as in the case of an artesian head beneath a rock layer) and the bedrock is fractured to the extent that significant amounts of groundwater can flow through the fractured rock to a different elevation. For explosions on rock, Reference 10 suggests that the vertical limit for rupture is about 3 times the depth of the true crater, and the vertical limit for displacement (opening or closing of rock joints) is about 4 times the depth of the true crater. For a near-surface HE explosion on rock, the true crater

depth is typically not quite double the apparent crater depth; therefore, the vertical fracture zone for rock is approximately 6 times the apparent crater depth and the vertical displacement zone is approximately 8 times the apparent crater depth. Based on Equations 2-3 and 2-5 (see Section 2), the vertical limit for fracturing of rock (assuming a zero height-of-burst) would thus vary from about 8 meters for a 1-ton explosion to about 60 meters for a 500-ton explosion and the corresponding limits of displacement would be from about 10 and 75 meters, respectively. These values can be assumed as maximum limits for damage to bedrock beneath a layer of soil (unless the charge is significantly buried) because the soil layer will attenuate the shock to a greater extent than if the medium were entirely rock. In summary, if bedrock is at a lesser depth below the ground surface than indicated by the above approximate figures, the bedrock might possibly be damaged by a near-surface explosion. However, such damage has no environmental significance unless the bedrock is supporting or restraining a water table.

Effects on Animals and Humans

Reference 78 summarizes the observations of wildlife and domesticated animals exposed to ground motions from underground nuclear explosions. Physical damage to such animals has never been observed, even though the ground motions were several g's in some instances (1 g equals nearly 1,000 cm/sec^3). For example, cows and calves located near GZ of the CLEARWATER underground nuclear test suffered no physical damage at ground motions of from 2.5 to 4 g's and 140 to 230 cm/sec, although one cow was knocked to its knees. Other tests on cattle, horses, deer, and elk at lower ground motions had essentially negative results. The milk production of lactating cows was unchanged after exposure to ground shock. Studies specifically designed to determine the effect of ground shock on subsurface animals, plant roots, and microbes produced essentially negative results for blast-like pressure pulses (References 79 and 80).

The following ground motion criteria were established for the RULISON underground nuclear test: 0.3 g (300 cm/sec^2) as the level at which direct body hazard to humans might occur from falls; 0.05 g (50 cm/sec^2) for over-reaction from school children, etc. to perception of ground motion; and 0.005 g (5 cm/sec^2) for unexpected perception of ground motion by persons in vulnerable positions, such as on ladders (Reference 74). At the frequency of 6 Hz, human perception to ground motions ranges from "intolerable" at 3 cm/sec, to "very unpleasant, annoying" at 1 cm/sec, to "unpleasant" at 0.4 cm/sec, and "clearly perceptible" at 0.1 cm/sec, with the threshold of perception at approximately 0.03 cm/sec (Reference 81). These results are consistent with the summary in Table 3-7 where just perceptible, clearly perceptible, and annoying ground motions occur at velocities of approximately 0.03 to 0.08, 0.08 to 0.25, and over 0.25 cm/sec, respectively.

Table 3-7. Human response to ground motions. (Source: Reference 69)

Vibration From	Authority	Details	Observed		Reiher and Meister Classification	Derived	
			Amplitude (in.)	Frequency (cycles/sec)		Maximum Velocity (in./sec)	Acceleration (g)
Traffic	Hyde and Lintern (1929)	Single-deck motor bus, 18 mph, 30 feet away	0.00012	26	Just perceptible	19,700	0.0082
Traffic	Hyde and Lintern (1929)	Light truck, 13.6 mph, 20 feet away; rough road	0.00012	20	Just perceptible	15,700	0.0049
Traffic	BRS (1934)	General traffic at Brentford	0.00012	19	Just perceptible	14,300	0.0044
Traffic	Tillman (1933)	Measurements in house 30 to 50 feet from traffic	0.00025	24	Clearly perceptible	37,700	0.0145
Traffic	BRS (1950)	Vibrations from London; traffic as measured inside a building	0.00014	25	Just perceptible	22,000	0.009
Traffic	BRS (1950)	Traffic measurements in Queens Street, London	0.00031	14	Just perceptible	27,000	0.0062
Traffic	BRS (1950)	Traffic measurements in Farrington Street, London	0.00036	10	Just perceptible	22,600	0.003
Railways	US	Measurements of vibration in Times Building (NY), subway; floor vibrations	0.00078	15-20	Clearly perceptible	85,000	0.024
Railways	Mallock (1902)	Hyde Park area; building vibrations due to subway	0.001	10-15	Clearly perceptible	78,000	0.01
Railways	C.C. Williams	Freight train at 65 feet; passenger train at 25 to 30 feet	0.0009 0.0037				
Pile Driving	BRS	Close to occupied building	0.00053	30	Clearly perceptible--annoying	100,000	0.049

(Continued)

Table 3-7. (Continued)

Vibration From	Authority	Details	Observed		Reiher and Meister Classification	Derived	
			Amplitude (in.)	Frequency (cycles/sec)		Maximum Velocity (μin./sec)	Acceleration (g)
Blasting	BRS and RAE (1950)	Measurements in bomb-damaged tunnel; no damage caused by blasting vibration	0.0015 0.00007	6 80	Clearly perceptible Clearly perceptible	57,500 36,000	0.006 0.045
Blasting	G. Morris (1950)	Vibrations in villa 1,100 feet away; firing 2,000-pound explosive	0.0017	9.4	Clearly perceptible--annoying	100,000	0.015
Machinery	Tillman (1933)	Vibration from chocolate factory; measurements in nearby house	0.00056	42	Annoying	147,500	0.09
Machinery	Tillman (1933)	Vibration in houses (third story), 400 feet from 120-hp diesel	0.0008	3.5	Just perceptible	17,500	0.01
Machinery	BRS	Vibrating table; measurements on table	0.005	25	Painful	780,000	0.32
Machinery	Tillman (1933)	Vibration in 70-year-old house adjacent to six lithographic presses	0.00031	64	Annoying	125,000	0.133

Notes:

(1) From the foregoing results, it would appear that the maximum velocities involved at the various stages of perceptibility are (approximately) in μin./sec:

Just perceptible	10,000 to 30,000
Clearly perceptible	30,000 to 100,000
Annoying	Over 100,000

(2) Digby gives a nuisance-vibration velocity of 86,000 to 250,000 μin./sec and a faintly-perceptible-vibration of 25,000 to 63,000.

From Steffens (1962).

Damage Distances

In summary of the preceding discussion, it appears that a criterion of 20 cm/sec^2 (corresponding to a velocity of 0.5 cm/sec) for ground motions from large chemical explosions is a conservative criterion to ensure no significant damage. (For smaller contained explosions of a few tons, for example, the Bureau of Mines standard of 5 cm/sec for no damage is applicable.) This 20-cm/sec^2 level corresponds to a level that is annoying to humans but has only a 1-percent probability of damaging a residence, and below which rock slides have not been observed to occur. At a lower criterion of 5 cm/sec^2 (corresponding to a velocity of 0.13 cm/sec), the ground motion may be perceptible to humans but no damage to even the most sensitive structures will occur.

In Figure 3-10, these damage criteria levels are overlaid on the ground shock magnitudes versus distance from Section 2 to assess the potential for damage from ground shock. Comparing Figure 3-10 with Figure 3-6 for airblast, it can be seen that damage from ground shock will normally be within the range where airblast damage dominates. For example, at 4 kilometers from a near-surface 500-ton explosion, one residence in 100 is likely to be damaged from ground shock. A total of 100 residences corresponds to a small town with a population of about 300 people and roughly 5,700 windows. A 500-ton HE explosion above ground 4 kilometers away from such a small town could be expected to break about 450 windows under calm, nonrefracting meteorological conditions. Even a well buried explosion that would extend a given ground shock level a factor of 2.7 more distant (i.e., to 11 kilometers for damaging one residence out of 100) would still be at a distance where 10 to 20 windows could be expected to be broken from airblast for every residence damaged by ground shock.

EXPLOSIVE PRODUCTS AND DUST

The chemical products that are predicted to result from the detonation of explosives commonly used in field tests are shown in Table 2-4 (Section 2). For each of the explosives shown, over 90 percent by weight of the chemical products shown are either (1) solid carbon (for other than ANFO explosives), which may add to turbidity of surface water but that is otherwise biologically harmless except in large concentrations, or (2) water, nitrogen, oxygen, and carbon dioxide, which occur naturally in the air and are harmless in air, soil, or water. Nevertheless, some of the remaining less-than-10-percent of the chemical products are classified as pollutants in air or water.

The chemical species from ANFO, the type of explosive most widely used in large-scale field tests, that might affect soil or water are the nitrogenous and cyanide compounds. Nitrogenous compounds may beneficially increase soil fertility, but nitrates and cyanide are undesirable in water.

An extensive soil and water collection and analysis program was conducted as part of the environmental monitoring plan for the MISERS BLUFF

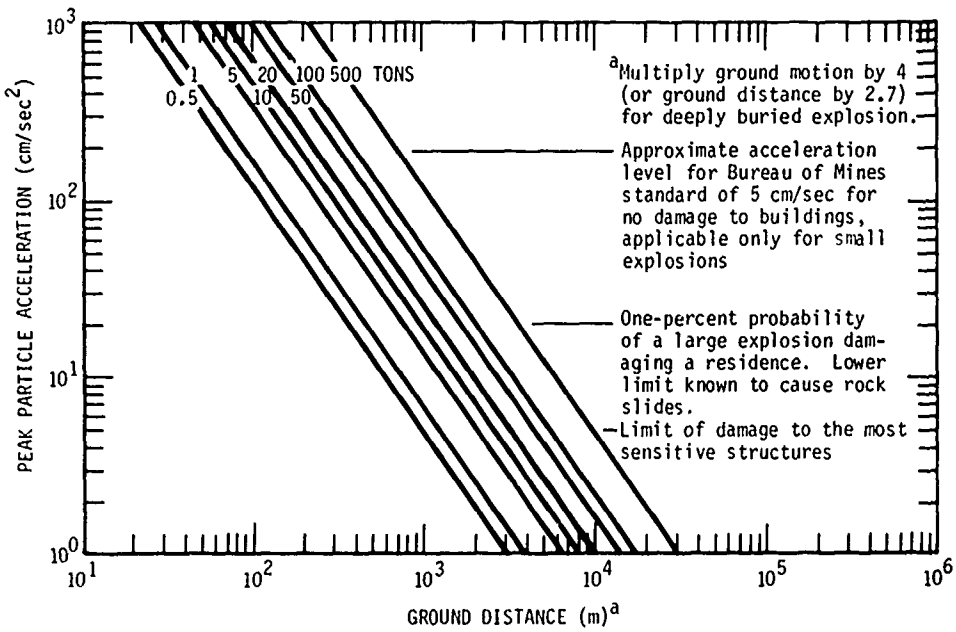

Figure 3-10. Damage-distance criteria for ground motions from near-surface explosions.

Phase II field test. The results of this program (Reference 16) indicate that ANFO explosions do not increase the salinity or cyanide concentration of soils and water. However, following the explosive tests, an increase in nitrate concentration was observed in one well that intersected the underwater flow from the crater area. The investigators concluded that the increase was probably caused by an increase in the nitrate levels in the ejecta used to fill the explosion craters; however, laboratory studies indicated that if this were the case, increased chloride levels should also have occurred and this was not observed. Regardless, any increase in the nitrate concentration in soil or water at a test site is of possible concern only if the water is used for drinking and the concentrations exceed the drinking water standards.

For the other types of explosives shown in Table 2-4, the only potential pollutants are ammonia and methane, and it is likely that the heat of the explosion and the availability of oxygen in the air would convert these compounds to oxides of carbon and nitrogen and water. TNT, and these other explosives, have been used for many years without noticeable effects on soils or groundwater; however, measurements are practically nonexistent.

Concern has been expressed as to whether some of the explosion products listed in Table 2-4 might produce nitrosamines. This question is of interest because nitrosamines (or, more broadly, N-nitroso compounds) are extremely potent carcinogens. Nitrosamines are produced when certain

nitrogen-containing compounds react with secondary amines, a group of organic compounds that can be considered as derived from ammonia with two of the hydrogen atoms replaced with organic radicals. The remaining nitrogen atom in the amine links with a nitroso group (i.e., a NO radical) to form the N-nitroso compound. Since Table 2-4 indicates that several nitrogen compounds are produced by the explosion of ANFO and since secondary amines are widely distributed in the environment, it would not be surprising if nitrosamines are produced. It does not appear that the question of nitrosamines has been addressed before in the context of explosive products. Ammonium nitrate is a common fertilizer and has been used as a blasting agent for many years.

Despite being potent carcinogens, it is known that nitrosamines are widely distributed in the environment--they are formed in soil and water by the reaction of nitrogen compounds with naturally occurring amines, they are present in tobacco smoke, they are formed in the human stomach when nitrites are ingested, and they occur in human saliva. Since the vicinity of most test sites is not used for human food crops or public water supply, it does not appear that any human hazard would result in most cases even if nitrosamines are produced.

The gaseous detonation products and the fine dust in the explosion cloud can be transported long distances downwind as the cloud diffuses. The maximum ground level exposures, predicted in Section 2 under worst-case assumptions, can be compared against air quality standards to assess the potential impact.

For a given geology and scaled depth-of-burst, it is shown in Section 2 that the crater volume is directly proportional to the size of the explosive charge. Since it is assumed that one-third of the crater volume is dust that is subject to distant air transport, the amount of dust in the explosion cloud is also directly proportional to the size of the explosive charge. For a given type of explosive, the amount of each chemical explosive product is obviously directly proportional to the size of the explosive charge. Therefore, all other factors being constant, the explosive products and dust in the explosion cloud that are subject to atmospheric diffusion are directly proportional to the weight of the explosive charge. Increasing the size of the explosive charge results in increasing the maximum downwind ground level exposure level, because the greater diffusion of the cloud from a large explosion is more than offset by the greater total amounts of chemical products and dust in the cloud from such a large explosion. For example, although Figure 2-20 shows that a given amount of material is 50 times more diffuse at ground level from a 500-ton explosion compared to a 1,000-pound explosion, the 500-ton explosion cloud contains approximately 1,000 times more materials than does the 1,000-pound explosion cloud; therefore, the maximum ground level exposure from the cloud from a 500-ton explosion is approximately 20 times greater than that from a 1,000-pound explosive. (Different meteorological conditions might change this conclusion, but Figure 2-20 is based on an unstable atmosphere which is a conservative assumption in that it produces the highest ground level

exposure levels.) Therefore, if a 500-ton explosive charge does not produce ground level exposures in excess of air pollution standards, neither should a smaller size charge.

A sample computation using conservative assumptions will show that dust from an explosion cloud transported long distances may exceed air quality standards. Assuming a site of dry clay, which has a high proportion of fine particles that are subject to distant transport, and a 500-ton explosion at a zero height-of-burst, the amount of dust subject to distant transport in the explosion cloud would be approximately 7×10^9 grams (i.e., the product of the unit weight of clay which is approximately 90 pounds/ft^3, the cratering efficiency of a charge at zero height-of-burst in a dry clay medium which is 1,000 ft^3/ton of explosive, the weight of the explosive which is 500 tons in this example, and the one-third of the crater volume that is assumed as dust in the explosion cloud based on the discussion in Section 2). From Figure 2-24, for a 500-ton explosion the normalized exposure is as follows:

$$E\,\bar{u}\,/Q = 2 \times 10^{-8} \,. \qquad (3\text{-}6)$$

Substituting the value of 7×10^9 grams for Q and assuming a relatively slow wind speed of 2 m/sec (a conservative assumption since slow winds result in a slower passing cloud that increases exposure), the maximum exposure downwind would be 70 g·sec/m^3. This value can be compared with the air quality standard that applies to the site in question. To compare it with the national secondary ambient air quality standard or the State of New Mexico standard, both of which are 150 µg/m^3 averaged over 24 hours, the 70 g·sec/m^3 is divided by the number of seconds in 24 hours to yield an average concentration of 810 µg/m^3. Thus in this example, the maximum ground level concentration of dust is about 5 times the maximum allowed by ambient air quality standards. With less conservative assumptions (e.g., a higher wind speed, a sandy soil, neutral or stable meteorological conditions, or a smaller charge size), the maximum concentration would be considerably less; however, it is possible that even more conservative assumptions might apply (e.g., a larger crater from a wet clay geology or a buried charge). For any particular field test, the specific characteristics of the test site and the explosive charge must be employed in the analysis to assess whether air quality standards are likely to be exceeded. The standards were designed for industrial operations, rather than single-event occurrences like HE field tests. The national standards can be exceeded no more than once per year.

Similar computations can be performed for each of the chemical constituents of the cloud by substituting the total amount of each pollutant given in Table 2-4 for the value of Q in Equation 3-6 and comparing the result with the air quality standards for the pollutant under question. The amounts of gaseous pollutants in the explosion cloud are so small compared to the amount of dust, however, that there is no possibility of exceeding air quality standards for explosive detonation products.

REFERENCES

1. Standard for Single Point Explosions in Air, American National Standards Institute; Committee on Mechanical Vibration and Shock, S-2; Working Group, Atmospheric Blast Effects, S-2-54; Reed, J.W., Chairman; 20 July 1976 draft report.

2. Event DIAL PACK Preliminary Report--Volume 1, DASA 2606-I (DASIAC SR-115), DASIAC, General Electric-TEMPO, Santa Barbara, California, May 1971.

3. Sadwin, L.D., and M.M. Swisdak, Jr., Performance of Multiton AN/FO Detonations, A Summary Report, NOLTR 73-105 (AD 912 525L), Naval Ordnance Laboratory, Silver Spring, Maryland, July 1973.

4. Anderson, J.H.B., Observations on the Blast Phenomenology of Unconfined Charges of Ammonium Nitrate/Fuel Oil Explosive (AN/FO IV and AN/FO V--October 1971), Suffield Technical Note No. 319 (AD 905 246), Defense Research Establishment Suffield, Alberta, Canada, June 1972.

5. Reisler, R.E., L. Giglio-Tos, and G.D. Teel, Air Blast Parameters from Pentolite Cylinders Detonated on the Ground, BRL Memorandum Report No. 2471, Army Ballistic Research Laboratories, Aberdeen Proving Ground, Maryland, April 1975.

6. Teel, G.D., "Free-Field Airblast Definition--Event DICE THROW," paper in the Proceedings of the DICE THROW Symposium, 21-23 June 1977, Volume 1, DNA 4377P-1, prepared for Defense Nuclear Agency by Ballistic Research Laboratory, July 1977.

7. Vortman, L.J., Explosive Cratering Experiments, Report SCR-406, Sandia Laboratories, Albuquerque, New Mexico, May 1961.

8. Personal conversation with J.W. Reed, Sandia Laboratories, Albuquerque, New Mexico, April 1977.

9. Cooper, H.S., Sr., Estimates of Crater Dimensions for Near-Surface Explosions of Nuclear and High-Explosive Sources, RDA-TR-2604-001, R&D Associates, Marina del Rey, California, September 1976.

10. Rooke, A.D., Sr., et al., Cratering by Explosives: A Compendium and an Analysis, N-74-1, U.S. Army Engineers Waterways Experiment Station, Vicksburg, Mississippi, January 1974.

11. Proceedings of the MIXED COMPANY/MIDDLE GUST Results Meeting 13-15 March 1973, DNA 3151P1, Volume II, Director, Defense Nuclear Agency, APTL, Washington, D.C., 1 May 1973.

12. Harvey, W.T., J.F. Dishon III, and T.M. Tami, Near-Surface Cratering Experiments, Fort Polk, Louisiana, AFWL-TR-74-351, Air Force Weapons Laboratory (DEV), Air Force Systems Command, Kirtland Air Force Base, New Mexico, November 1975.

13. Tami, T.M., ESSEX-DIAMOND ORE Research Program: Ground Motion in the Seismic Region--Project ESSEX I, Phase 2, DNA PR 0021, Director, Defense Nuclear Agency, Washington, D.C., July 1976.

14. Kurtz, M.K., Jr., Project PRE-GONDOLA I, Technical Director's Summary Report, PNE-1102 (AD 735 717), U.S. Army Engineer Nuclear Cratering Group, Livermore, California, May 1968.

15. Perret, W.R., et al, Project SCOOTER, SC-4602(RR), Sandia Laboratories, Albuquerque, New Mexico, October 1963.

16. Perry, G.L.E., et al., Environmental Monitoring--MISERS BLUFF Phase II Events, POR-7016, prepared by General Electric-TEMPO for Defense Nuclear Agency, Washington, D.C., 30 June 1979.

17. Turpening, R.M., and A.R. Liskow, Seismic Measurements for the PRE-DICE THROW II-1 (TNT Shot), PRE-DICE THROW II-2 (AN/FO Shot) and DICE THROW Events, AFOSR-TR-79-0028 (ERIM-120400-1-F), Environmental Research Institute of Michigan, Ann Arbor, Michigan, ADA064605, December 1978.

18. Cooper, H.F., Jr., and F.M. Sauer, "Crater-Related Ground Motions and Implications for Crater Scaling," Impact and Explosion Cratering, pp 1133-1163, Pergamon Press, New York, 1977.

19. Chaiken, R.F., E.B. Cook, and T.C. Ruhe, Toxic Fumes from Explosives: Ammonium Nitrate-Fuel Oil Mixtures, Bureau of Mines, U.S. Department of Interior, Report of Investigations 7867 (TN23.U7, No. 7867, 622.06173), 1974.

20. Mader, C.L., Detonation Properties of Condensed Explosives Computed Using the Becker-Kistiakowsky-Wilson Equation of State, LA-2900, UC-4 Chemistry, TID-4500 (20th edition), Los Alamos Scientific Laboratory, USC, Los Alamos, New Mexico, July 1963.

21. Computations furnished by C.L. Mader (author of Reference 20) to K.E. Gould, 14 November 1975.

22. Church, H.W., Cloud Rise from High-Explosives Detonations, SC-RR-68-903, Sandia Laboratories, Albuquerque, New Mexico, June 1969.

23. AFFDL-TR-66-155 (classified report).

24. Hyman, D.S., et al., Dust Cloud Analysis for Event DIAL PACK, DASA 2694, CR-1-219, prepared by General Research Corporation for Defense Atomic Support Agency (now DNA), May 1971.

25. Sprague, K.E., et al., MIDDLE COURSE II Cratering Series, Technical Report E-73-3, U.S. Army Waterways Experiment Station, Livermore, California, AD765436, July 1973.

26. Fitchett, Major D.J., MIDDLE COURSE I Cratering Series, NCG Technical Report Number 35, TID-4500, UC-35, U.S. Army Engineer Nuclear Cratering Group, Livermore, California, June 1971.

27. Boquist, W.P., "Optical Measurements of MISERS BLUFF Multiburst Cloud Phenomenology," Proceedings of the MISERS BLUFF Phase II Results Symposium, 27-29 March 1979, Volume III, DNA 5192, Defense Nuclear Agency, 26 September 1979.

28. Green, W.E., Airborne Sampling and Analysis of Particulates from the DIAL PACK Event, DASA 2600 (MR170 FR-948), Headquarters, Defense Atomic Support Agency, Washington, D.C., January 1971.

29. Thomas, C.R., and J.E. Cockayne, MISERS BLUFF Cloud Sampling Program, Data Summary and Dust Cloud Characterizations, DNA 5189F, Defense Nuclear Agency, 7 December 1979.

30. Slade, D.H., Ed, Meteorology and Atomic Energy 1968, U.S. Atomic Energy Commission, Air Resources Laboratories, Office of Information Services, July 1968.

31. Beals, Major G.A., USAF ETAC, Guide to Local Diffusion of Air Pollutants, Technical Report 214, Air Weather Service, USAF, available through DD2, AD726984, May 1971.

32. White, C.S., et al., The Biodynamics of Airblast, DNA 2738T, Lovelace Foundation for Medical Education and Research, Albuquerque, New Mexico, 1 July 1971.

33. Damon, E.G., et al., The Tolerance of Birds to Airblast, DNA 3314F, Director, Defense Nuclear Agency, Washington, D.C., July 1974.

34. Gesswein, J., and P. Carrao, The Position of Eardrum Rupture and Hearing Loss in the Scale of Injuries from Nuclear Blast, NSCDC 3789, Naval Ship Research and Development Center, Bethesda, Maryland, February 1972.

35. Richmond, D.R., et al., The Relationship between Selected Blast-Wave Parameters and the Response of Mammals Exposed to Air Blast, DASA 1860, Lovelace Foundation for Medical Education and Research, Albuquerque, New Mexico, November 1966.

36. Richmond, D.R., et al., Tertiary Blast Effects: The Effects of Impact on Mice, Rats, Guinea Pigs and Rabbits, DASA 1245, Lovelace Foundation for Medical Education and Research, Albuquerque, New Mexico, 28 February 1961.

37. TTCP Panel N-5 Meeting--21-23 March 1972, DASIAC SR-139, DASIAC, General Electric-TEMPO, Santa Barbara, California, July 1972.

38. Bowen, I.G., et al., Translational Effects of Air Blast from High Explosives, DASA 1336, Lovelace Foundation for Medical Education and Research, Albuquerque, New Mexico, 7 November 1962.

39. Fletcher, E.R., et al., Determinations of Aerodynamic-Drag Parameters of Small Irregular Objects by Means of Drop Tests, CEX-59.14, Lovelace Foundation for Medical Education and Research, Albuquerque, New Mexico, June 1960.

40. Bowen, I.G., et al., Translational Effects of Blast Waves, DA-49-146-XZ-055, Lovelace Foundation for Medical Education and Research, Albuquerque, New Mexico, 11 March 1963.

41. Richmond, D.R., et al, "Blast Biophysics; Past, Present and Future," Proceedings of the MISERS BLUFF Phase II Results Symposium, 27-29 March 1979, Volume III, POR 7013-3, Defense Nuclear Agency, 29 September 1979.

42. Morris, P.J., Forest Blowdown from Nuclear Airblast, DNA 3054F (URS 7049-10, Rev. I), URS Research Company, San Mateo, California, July 1973.

43. Glasstone, S., and P.J. Dolan, The Effects of Nuclear Weapons, U.S. Government Printing Office, Washington, D.C., 1977.

44. Pickering, E.E., and J.L. Bockholt, Probabilistic Air Blast Failure Criteria for Urban Structures, SRI Project 6300, Stanford Research Institute, Menlo Park, California, November 1971.

45. Wilton, C., and B. Gabrielsen, Summary Report: House Damage Assessment, DNA 2906F, Headquarters, Defense Nuclear Agency, Washington, D.C., January 1973.

46. Reed, J.W., Simplified Blast Nuisance Predictions for Small Explosions, Sandia Laboratories, Albuquerque, New Mexico, 9 July 1974.

47. Nicholls, H.R., C.F. Johnson, and W.I. Duvall, Blasting Vibrations and Their Effects on Structures, Bureau of Mines Bulletin 656, U.S. Department of the Interior, Washington, D.C., 1971.

48. Wiggins, J.H., Jr., "Sonic Boom Damage to Structures," Institute of Environmental Sciences, 1969 Proceedings, 15th Annual Technical Meeting--Man in His Environment, 20-24 April 1969, Anaheim, California, Institute of Environmental Sciences, Mt. Prospect, Illinois, pp 189-197.

49. Reed, J.W., Acoustic Wave Effects Project: Airblast Prediction Techniques, SC-M-69-332, Sandia Laboratories, Albuquerque, New Mexico, 1969.

50. Maglieri, D.J., V. Huckle, and T.L. Parrott, Ground Measurements of Shock-Wave Pressure for Fighter Airplanes Flying at Very Low Altitudes and Comments on Associated Response Phenomena, NASA TN-E-3443, Langley Research Center, Langley Station, Hampton, Virginia, July 1966.

51. Warren, C.H.E., "Recent Sonic-Bang Studies in the United Kingdom," Journal of the Acoustical Society of America, Vol. 51, No. 2 (Part 3): 783-788, February 1972.

52. Weber, G., "Sonic Boom Effects 11.1: Structures and Terrain," Journal of Sound and Vibration, Vol. 20, No. 4:531-534, 1972.

53. Wiggins, J.H., Jr., Effects of Sonic Boom, J.H. Wiggins Company, Palos Verdes Estates, California, 1969.

54. The Effects of Sonic Boom and Similar Impulsive Noise on Structures, NTID300.12, U.S. Environmental Protection Agency, Washington, D.C., December 31, 1971.

55. Nixon, C.W., Proceedings of Noise as a Public Hazard, ASHA #4, February 1969.

56. Cotterau, P., "Sonic Boom Exposure Effects 11.5: Effects on Animals," Journal of Sound and Vibration, Vol. 20, No. 4:531-534, 1972.

57. Civil Aircraft Sonic Boom Regulation (Final EIS), EIS-AA-73-0115-F, Federal Aviation Administration, Washington, D.C., January 1973.

58. Bell, W.B., "Animal Response to Sonic Booms," The Journal of the Acoustical Society of America, Vol. 51, No. 2 (Part 3):758-765, February 1972.

59. Nixon, E.W., H.K. Hille, H.C. Sommer, and E. Guild, Sonic Booms Resulting from Extremely Low-Altitude Supersonic Flight: Measurements and Observations on Houses, Livestock and People, AMRL-TR-68-52, Aerospace Medical Research Laboratories, Aerospace Medical Division, Air Force Systems Command, Wright-Patterson Air Force Base, Ohio, October 1968.

60. Information on Levels of Environmental Noise Requisite to Protect Public Health and Welfare with an Adequate Margin of Safety, 550/9-74-004, U.S. Environmental Protection Agency, Office of Noise Abatement and Control, U.S. Government Printing Office, Washington, D.C., March 1974.

61. "Occupational Noise Exposure," Code of Federal Regulations, Title 29, Paragraph 1910-95, pp 220-221, Rev. January 1, 1972.

62. Richter, C.F., Elementary Seismology, W.H. Freeman and Company, San Francisco, California, 1958.

63. Orphal, D.L., and J.A. Lahoud, "Prediction of Peak Ground Motion from Earthquakes," Bulletin of the Seismological Society of America, Vol. 64, No. 5:1563-1574, October 1974.

64. O'Brien, L.J., J.R. Murphy, and J.A. Lahoud, The Correlation of Peak Ground Acceleration Amplitude with Seismic Intensity and Other Physical Parameters, Final Technical Report (Draft), Computer Sciences Corporation, Falls Church, Virginia, March 1976.

65. Seed, H.G., et al, "Relationships of Maximum Velocity, Distance from Source, and Local Site Conditions for Moderately Strong Earthquakes," Bulletin of the Seismological Society of America, Vol. 66, No. 4:1323-1342, August 1976.

66. Environmental Statement Underground Nuclear Test Programs, Nevada Test Site (Tests of One Megaton or Less), United States Atomic Energy Commission, September 1971.

67. Bolt, B.A., Nuclear Explosions and Earthquakes, The Parted Veil, W.H. Freeman and Company, San Francisco, California, 1976.

68. Nicholls, H.R., C.F. Johnson, and W.I. Duvall, Blasting Vibrations and Their Effects on Structures, U.S. Department of the Interior, Bureau of Mines Bulletin 656, 1971. Available from Superintendent of Documents, U.S. Government Printing Office, Washington, D.C. 20402 ($1.00).

69. Richart, F.E., Jr , J.R. Hall, Jr., and R.D. Woods, Vibrations of Soils and Foundations, Prentice-Hall, Inc., Englewood Cliffs, New Jersey, 1970.

70. Cauthen, L.J., Jr., "The Effects of Seismic Waves on Structures and Other Facilities," Third Plowshare Symposium--Engineering with Nuclear Explosives, 21-23 April 1964, University of California, Davis, California, UCRL-7773, U.S. Army Corps of Engineers, Lawrence Radiation Laboratory, University of California, Livermore, California, 1964.

71. Cauthen, L.J., Jr., Survey of Shock Damage to Surface Facilities and Drilled Holes Resulting from Underground Nuclear Detonations, UCRL-7964, Lawrence Radiation Laboratory, University of California, Livermore, California, July 1964.

72. Holzer, F., Ground Motion Effects from Nuclear Explosions: A Review of Damage Experience and Prediction Methods, UCRL-51062 (TID-4500, UC-35), Lawrence Radiation Laboratory, University of California, Livermore, California, June 2, 1971.

73. Shamin, V.M., "Seismic Effect of Powerful Explosions," Doklady of the Academy of Sciences U.S.S.R., Earth Science Sections, Volume 135, March-April 1969, published by the American Geological Institute.

74. Structural Response Studies for Project RULISON, Report JAB-99-78, John A. Blume & Associates Research Division, San Francisco, California, February 1971.

75. Proceedings of the MIXED COMPANY/MIDDLE GUST Results Meeting 13-15 March 1973; Vol. II, Sessions 2B and 2C, DNA 3151P2, Director, Defense Nuclear Agency, Washington, D.C., 1 May 1973.

76. Letter to LCDR J.D. Strode of DNA Field Command from L.K. Davis of the Waterways Experiment Station, 5 May 1977.

77. Structural Effects of the RULISON Event, Report JAB-99-76, John A. Blume & Associates Research Division, San Francisco, California, December 1969.

78. Smith, D.D., Observations on Wildlife and Domestic Animals Exposed to the Ground Motion Effects of Underground Nuclear Detonations, Report NERC-LV-539-24, Farm and Animal Investigation Branch, Monitoring Systems Research and Development Laboratory, National Environmental Research Center, U.S. Environmental Protection Agency, Las Vegas, Nevada, October 1973.

79. Newcombe, C.L., Studies of Shock Effects on Selected Organisms, Report FBFRC-TR-4 (USNRDL-TRC-71) (AD 803 769), Department of Biology, San Francisco State College, San Francisco, California, 12 October 1966.

80. Newcombe, C.L., Experimental and Field Studies of Effects of Underground Shock on Terrestrial Organisms, USNRDL-TR-9, San Francisco State College, San Francisco, California, December 1965.

81. Effects Prediction Guidelines for Structures Subjected to Ground Motion, Report JAB-99-115, John A. Blume & Associates, Engineers, San Francisco, California, July 1975.

DISTRIBUTION LIST

DEPARTMENT OF DEFENSE

Armed Forces Radiobiology Rsch Institute
ATTN: Director

Assistant to the Secy of Defense
Atomic Energy
ATTN: Executive Assistant

Defense Advanced Rsch Proj Agency
ATTN: Dir, Strat Tech Off
ATTN: NMRO
ATTN: Col A. Lowery

Defense Communications Agency
ATTN: Code 510
ATTN: C670

Defense Intelligence Agency
ATTN: DT-1C
ATTN: DI-7D
ATTN: DT-2
ATTN: DB-4C, P. Johnson

Defense Nuclear Agency
ATTN: SPSS
ATTN: SPTD
ATTN: NAFD
ATTN: NATD
ATTN: STNA
ATTN: RAEE
ATTN: NASD
ATTN: STSP
ATTN: STRA
ATTN: NATA
ATTN: RAEV
ATTN: SPAS
ATTN: RAAE
4 cy ATTN: TITL

Defense Technical Info Center
12 cy ATTN: DD

Department of Defense Explo Safety Brd
ATTN: Chairman

Field Command
DNA Det 1
Lawrence Livermore
ATTN: FC-1

Field Command
Defense Nuclear Agency
ATTN: FCTXE
ATTN: FCTT, G. Ganong
ATTN: FCTT, W. Summa
ATTN: FCTX
ATTN: FCTT
ATTN: FCPR
ATTN: FCT

Joint Chiefs of Staff
ATTN: SAGA
ATTN: GD50, J-5 Force Plng & Prog Div
ATTN: GD10, J-5 Nuc & Chem Div

Under Secy of Def for Rsch & Engrg
ATTN: Strat & Space Sys, OS
ATTN: Engrg Tech, J. Persh

DEPARTMENT OF DEFENSE (Continued)

Joint Strat Tgt Planning Staff
ATTN: JPTP
ATTN: JLTW-2
ATTN: JPTM
ATTN: JLA, Threat Applications Div

National Security Agency
ATTN: Director
ATTN: P. Deboy
ATTN: E. Butala

DEPARTMENT OF THE ARMY

Army Logistics Management Ctr
ATTN: Commandant

US Army Electronics R&D Command
ATTN: DELAS-EO, F. Niles
ATTN: DELAS-EO

BMD Advanced Tech Ctr
ATTN: ATC-T
ATTN: ATC-T, M. Capps

BMD Program Office
ATTN: DACS-BMZ
ATTN: Program Manager
ATTN: DACS-BMT

BMD Systems Command
ATTN: BMDSC-HW, R. Dekalb
ATTN: BMDSC-NW
ATTN: BMDSC-HUL, E. Martz
ATTN: BMDATC-R, W. Dickerson
ATTN: BMDSC-H

Chemical Systems Lab
ATTN: J. Andrea

Chief of Engineers
ATTN: DAEN-ZCM
ATTN: DAEN-MPE-T, D. Reynolds
ATTN: DAEN-ZCM, Bernard

Dep Ch of Staff for Ops & Plans
ATTN: DAMO-NCZ

Dep Ch of Staff for Rsch Dev & Acq
ATTN: DAMA-CSS-N, Spt Sys Div, Nuc Tm
ATTN: DAMA-CSM-N

Deputy Ch of Staff for Logistics
ATTN: DALO-ZA

Harry Diamond Labs
ATTN: DELHD-TA-L
ATTN: DELHD-NW-P, J. Gwaltney
ATTN: DELHD-DTSO
ATTN: DELHD-NW-P
ATTN: DELHD-NW-P, F. Balicki

Research & Dev Ctr
ATTN: Commander

US Army Armament Material Readiness Cmd
ATTN: Commander

DEPARTMENT OF THE ARMY (Continued)

US Army Armament Rsch Dev & Cmd
ATTN: Commander
ATTN: DRDAR-LCW
ATTN: DRDAR-LCE
ATTN: DRDAR-LCN
ATTN: DRDAR-LC
ATTN: DRDAR-LCS-W

US Army Aviation R&D Cmd
ATTN: Project Manager

US Army Aviation R&D Cmd
ATTN: Commander

US Army Ballistic Research Labs
ATTN: DRDAR-BLE
ATTN: DRDAR-BLT, Dr Celmins
ATTN: DRDAR-BLT
ATTN: DRDAR-BLT, J. Keefer
ATTN: DRDAR-TSB-S
ATTN: DRDAR-BLT, Schuman

US Army Chem School
ATTN: ATZN-CM-CS

US Army Combat Surv & Target Acq Lab
ATTN: DELCS-R, Mr Robbiani

US Army Comm Cmd
ATTN: Commander
ATTN: CC-OPS-PD

US Army Communications Cmd
ATTN: Commander

US Army Construction Engrg Res Lab
ATTN: Director

US Army Elct Warfare Lab
ATTN: Director

US Army Electronics R&D Command
ATTN: DELET-ER
ATTN: DELET-R, S. Kronenberg

US Army Engr Waterways Exper Station
ATTN: WESGH
ATTN: WESSA
ATTN: WESSE
ATTN: WESNV, J. Fiathau
ATTN: WESGR
ATTN: WESSD
ATTN: WESSS

US Army Foreign Science & Tech Ctr
ATTN: DRXST-SD

US Army Health Services Cmd
ATTN: Plans & Operations Div
ATTN: Commander

US Army Material & Mechanics Rsch Ctr
ATTN: DRXMR-HH
ATTN: Commander

US Army Materiel Dev & Readiness Cmd
ATTN: Ofc of Project Management
ATTN: Commander
ATTN: DRXAM-TL
ATTN: DRCDE-D

DEPARTMENT OF THE ARMY (Continued)

US Army Materiel Sys Analysis Actvy
ATTN: Commander

US Army Mobility Equip R&D Cmd
ATTN: Commander

US Army Natick Rsch & Dev Cmd
ATTN: DRDNA-UST

US Army Nuc & Chem Agency
ATTN: MONA-OPS
ATTN: MONA-WE, J. Berberet
ATTN: MONA-WE

US Army Operational Test & Eval Agy
ATTN: Commander

US Army Satellite Comm Agency
ATTN: Commander
ATTN: Tech Library

US Army Signal Warfare Lab, VHFS
ATTN: DELSW-OS

US Army Test & Evaluation Cmd
ATTN: DRSTE-CM-F, R. Galasso

US Army Training & Doctrine Cmd
ATTN: ATCD-Z
ATTN: ATORI-OP
ATTN: ATCD-T

US Army Troop Support Cmd
ATTN: Commander

US Tank Command
ATTN: Commander

US Army White Sands Missile Range
ATTN: STEWS-FE-R

USA Missile Command
ATTN: DRSMI-RH
ATTN: Document Sec
ATTN: DRCPM-PE, Pershing Proj Mgr
ATTN: DRCPM-PE-EG, W. Johnson
ATTN: Commander

USA Night Vision & Electro-Optics Lab
ATTN: Director

DEPARTMENT OF THE NAVY

Ch of Naval Ops
ATTN: OP-981-N1

12th Naval District
ATTN: S. Gianodo

David Taylor Naval Ship P&D Ctr
ATTN: Structures Dept
ATTN: Code 17
ATTN: Commander

David Taylor Naval Ship R&D Ctr
ATTN Code 770
ATTN: Commander

Joint Cruise Missiles Project Ofc
ATTN: Director

DEPARTMENT OF THE NAVY (Continued)

Marine Corps
ATTN: Code POG-31

Naval Civil Engineering Lab
ATTN: Mr. Keenan
ATTN: Naval Construction Bn Ctr
ATTN: Mr. Tancreto

Naval Coastal Systems Lab
ATTN: D. Sheppard
ATTN: Commander

Naval Facilities Engrg Cmd
ATTN: Commander

Naval Material Cmd
ATTN: Commander
ATTN: MAT-0323

Naval Ocean Systems Ctr
ATTN: W. Shaw
ATTN: Code 8122, W. Flanigan
ATTN: Commander

Naval Research Lab
ATTN: Code 7780
ATTN: Code 6770
ATTN: Commander
ATTN. Code 2627

Naval Sea Systems Cmd
ATTN: SEA-3221
ATTN: SEA-0352

Naval Ship Engrg Ctr
ATTN: NAVSEC 105

Naval Surface Weapons Ctr
ATTN: Code F31
ATTN: Code R15
ATTN: F31, J. Downs
ATTN: Code E21
ATTN: Code K06

Naval Surface Weapons Ctr
ATTN: Commander

Naval Weapons Ctr
ATTN: Commander
ATTN: Code 32607

Naval Weapons Evaluation Facility
ATTN: Director

Ofc of the Deputy Chief of Naval Ops
ATTN: NOP 931
ATTN: NOP 654, Strat Eval & Anal Br
ATTN: OP 62

Office of Naval Research
ATTN: Commander

Strat Systems Project Office
ATTN: Director
ATTN: NSP-272

DEPARTMENT OF THE AIR FORCE

Aeronautical Systems Division,
ATTN: ASD/ENFTV
ATTN: ASD/ENFTV, D. Ward
ATTN: ASD/ENSG, Capt J. Greneczho

Aerospace Medical Division
ATTN: Commander

Air Force Armament Lab
ATTN: Commander

Air Force Engineering & Svcs Ctr
ATTN: Commander

Air Force Flight Test Ctr
ATTN: Commander

Air Force Geophysics Lab
ATTN: LY
ATTN: Commander

Air Force Inspection & Safety Ctr
ATTN: Commander

Air Force Institute of Technology
ATTN: Library

Air Force Logistics Cmd
ATTN: Commander

Air Force Rocket Propulsion Lab
ATTN: Commandant
ATTN: LKCP

Air Force Systems Cmd
ATTN: XRTO
ATTN: SDM
ATTN: DLWM, Maj Waltham

Air Force Test & Evaluation Ctr
ATTN: Commander

Air Force Weapons Lab
ATTN: NTYV
ATTN: SAB
ATTN: NTE
ATTN: SUL
ATTN: NTO
ATTN: NT, Col S. Tyler

Air Force Wright Aeronautical Lab
ATTN: FIMG
ATTN: Commandant

Air Force Wright Aeronautical Lab
ATTN: MAS
ATTN: LPH
ATTN: Commandant
ATTN: MBE
ATTN: MBC

Air University Library
ATTN: AUL-LSE

Arnold Engrg Dev Ctr
ATTN: AEDC, DOFOV

DEPARTMENT OF THE AIR FORCE (Continued)

Ballistic Missile Office
ATTN: ENSN
ATTN: SYDT
ATTN: ENSN, Lt Col Baran
ATTN: Hq Space Div, RST
ATTN: Hq Space Div, RSS
ATTN: ENMR

Deputy Ch of Staff, Rsch, Dev & Acq
ATTN: AFRD

Deputy Chief of Staff
Research, Dev & Acq
ATTN: AFRDQI
ATTN: AFRDS, Space Sys & C3 Dir

Electronic Security Cmd
ATTN: Commander

Electronic Sys Div, OCRS
ATTN: Maj Sugg

Foreign Tech Div
ATTN: Commander
ATTN: PDBG
ATTN: IOPTN
ATTN: IDFBD

Headquarters, US Air Force
ATTN: AFXOOTS

Military Airlift Cmd
ATTN: Commander

Rome Air Development Ctr
ATTN: Commander

Space & Missile Test Center
ATTN: Commander

Strat Air Cmd
ATTN: XPFS, Maj Skluzacek
ATTN: XOBM
ATTN: XPQM
ATTN: DOXT
ATTN: XPFS

Tactical Air Command
ATTN: Commander

1035 Tech Operations Group
ATTN: Dr Kneidlen

DEPARTMENT OF ENERGY

Department of Energy
ATTN: R. Fletcher
ATTN: D. Richmond

Department of Energy
ATTN: OMA, RD&T

Department of Energy
ATTN: G. Bennett

OTHER GOVERNMENT AGENCIES

Federal Emergency Management Agency
ATTN: Ofc of Rsch, NP, D. Bensen

OTHER GOVERNMENT AGENCIES (Continued)

US Coast Guard
ATTN: Commandant

DEPARTMENT OF ENERGY CONTRACTORS

University of California
Lawrence Livermore National Lab
ATTN: Director
ATTN: L-262, J. Knox
ATTN: L-8, R. Andrews
ATTN: L-125, J. Keller

Los Alamos National Lab
ATTN: MS 670/T&V
ATTN: J. Hopkins

Oak Ridge National Lab
ATTN: Civ Def Res Proj, Mr Kearny

Sandia National Lab
ATTN: Dept 1100, T. Dowler

DEPARTMENT OF DEFENSE CONTRACTORS

Aerospace Corp
ATTN: R. Crolius

Analytic Services, Inc, ANSER
ATTN: J. Selig

AVCO Systems Div
ATTN: Doc Con

Boeing Aerospace Co
ATTN: M/S 13-13, R. Dyrdahl

Boeing Co
ATTN: M/S 85/20, E. York
ATTN: R. Holmes

California Research & Technology, Inc
ATTN: K. Kreyenhagen

Calspar Corp
ATTN: M. Holden

University of Denver
ATTN: Sec Officer for L. Brown
ATTN: Sec Officer for J. Wisotski

EG&G, Inc
ATTN: R. Ward

Electro-Mech Sys, Inc
ATTN: R. Shunk

Ford Aerospace & Communications Corp
ATTN: P. Spangler

General Research Corp
ATTN: J. Mate

General Rsch Corp
ATTN: T. Stathacopoulos

Institute for Defense Analyses
ATTN: Classified Library

Kaman Sciences Corp
ATTN: F. Shelton

DEPARTMENT OF DEFENSE CONTRACTORS (Continued)

Kaman AviDyne
ATTN: N. Hobbs
ATTN: S. Criscione

Kaman Sciences Corp
ATTN: D. Sachs

Kaman Tempo
ATTN: DASIAC
4 cy ATTN: K. Gould

Kaman Tempo
ATTN: G. Perry

Kaman Tempo
ATTN: E. Bryant

Lockheed Missiles & Space Co, Inc
ATTN: F. Borgardt

Lockheed Missiles & Space Co, Inc
ATTN: R. Walz

Lockheed Missiles & Space Co, Inc
ATTN: T. Fortune

Martin Marietta Corp
ATTN: G. Aiello

McDonnell Douglas Corp
ATTN: E. Fitzgerald

National Academy of Sciences
ATTN: National Materials Advisory Brd
ATTN: D. Groves

University of New Mexico
ATTN: G. Lane

Northrop Corp
ATTN: D. Hicks

TRW Electronics & Defense Sector
ATTN: R. Mortensen
ATTN: P. Dai

DEPARTMENT OF DEFENSE CONTRACTORS (Continued)

Pacific-Sierra Research Corp
ATTN: H. Brode, Chairman SAGE

Physics International Co
ATTN: Tech Library

R&D Associates
ATTN: F. Field
ATTN: J. Carpenter
ATTN: P. Haas

S-CUBED
ATTN: R. Duff

Science Applications, Inc
ATTN: J. Manship
ATTN: W. Plows

Science Applications, Inc
ATTN: C. Swain

Science Applications, Inc
ATTN: W. Layson

Southern Research Institute
ATTN: C. Pears

SRI International
ATTN: H. Lindberg
ATTN: A. Burns
ATTN: G. Abrahamson

Teledyne Brown Engineering
ATTN: R. Patrick

Terra Tek, Inc
ATTN: S. Green

TRW Electronics & Defense Sector
ATTN: N. Lipner

Pan Am World Svc, Inc
ATTN: AEDC, Library Doc, TRF

PDA Engineering
ATTN: J. McDonald